

THE COMBINATION OF SMART HYDROGELS AND FIBRE OPTIC SENSOR  
TECHNOLOGY FOR ANALYTE DETECTION

DANIEL PETER HARVEY

Doctor of Philosophy

ASTON UNIVERSITY

April 2011

This copy of this thesis has been supplied on the condition that anyone who consults it is understood to recognise that its copyright rests with its author and that no quotation from the thesis and no information derived from it may be published without proper acknowledgement.

ASTON UNIVERSITY

THE COMBINATION OF SMART HYDROGELS AND FIBRE OPTIC SENSOR  
TECHNOLOGY FOR ANALYTE DETECTION

DANIEL PETER HARVEY

Doctor of Philosophy

April 2011

SUMMARY

The subject of investigation of the present research is the use of smart hydrogels with fibre optic sensor technology. The aim was to develop a cost-effective sensor platform for the detection of water in hydrocarbon media, and of dissolved inorganic analytes, namely potassium, calcium and aluminium.

The fibre optic sensors in this work depend upon the use of hydrogels to either entrap chemotropic agents or to respond to external environmental changes, by changing their inherent properties, such as refractive index (RI).

A review of current fibre optic technology for sensing outlined that the main principles utilised are either the measurement of signal loss or a change in wavelength of the light transmitted through the system. The signal loss principle relies on changing the conditions required for total internal reflection to occur.

Hydrogels are cross-linked polymer networks that swell but do not dissolve in aqueous environments. Smart hydrogels are synthetic materials that exhibit additional properties to those inherent in their structure. In order to control the non-inherent properties, the hydrogels were fabricated with the addition of chemotropic agents.

For the detection of water, hydrogels of low refractive index were synthesized using fluorinated monomers. Sulfonated monomers were used for their extreme hydrophilicity as a means of water sensing through an RI change. To enhance the sensing capability of the hydrogel, chemotropic agents, such as pH indicators and cobalt salts, were used.

The system comprises of the smart hydrogel coated onto an exposed section of the fibre optic core, connected to the interrogation system measuring the difference in the signal. Information obtained was analysed using a purpose designed software.

The developed sensor platform showed that an increase in the target species caused an increase in the signal lost from the sensor system, allowing for a detection of the target species. The system has potential applications in areas such as clinical point of care, water detection in fuels and the detection of dissolved ions in the water industry.

**Keywords: hydrogel, polymer, fibre optic, sensor, water detection, inorganic analyte detection.**

## Acknowledgements

I would like to thank Professor Brian Tighe for giving me the opportunity and facilities to complete my PhD.

I am grateful to Dr Neil Hayes and his colleagues at EvanesCo Ltd. for their technical support throughout my PhD.

I am indebted to thank my family and friends, especially Anna, Antzela, and James. You have each given me support in your own ways, you helped to keep my sanity from deteriorating further.

I owe my deepest gratitude to thank Sofia Topakas who has supported me throughout the whole process. Without her by my side it would have been very difficult, if not impossible, to successfully reach that famous light at the end of the PhD tunnel. The reduction ad absurdum was not completely necessary, I must add. To quote Dr Sheldon Cooper “[S]he’s engaging in reduction ad absurdum. It’s the logical fallacy of extending someone’s argument to ridiculous proportions and then criticizing the result. And I do not appreciate it!”.

## List of Contents

SUMMARY .....	2
Acknowledgements .....	3
List of Contents .....	4
List of Tables .....	8
List of Figures.....	9
List of Abbreviations .....	15
Chapter 1- Introduction .....	17
1.1 Fibre optic sensing .....	18
1.2 Refraction, reflection and total internal reflection .....	21
1.3 Polymer fibre optic cable fabrication.....	25
1.4 Fibre optic technology for sensing .....	28
1.5 Existing fibre optic sensor systems.....	29
1.6 The rationale for selecting the proposed technique .....	35
1.7 Polymer-based sensor coating and hydrogels as a signal loss control mechanism .....	36
1.8 Hydrogels – nature and properties.....	38
1.8.1 <i>The properties of hydrogels and their suitability for tissue replacement</i> .....	39
1.8.2 <i>Smart Hydrogels</i> .....	41
1.9 Hydrogel Preparation - principles and practicalities.....	44
1.9.1 <i>Free radical polymerisation</i> .....	45
1.10 Example of the uses of smart hydrogels .....	49
1.10.1 <i>Biosensitive hydrogels</i> .....	49
1.10.2 <i>pH-sensitive hydrogels</i> .....	50
1.10.3 <i>Temperature-sensitive hydrogels</i> .....	52
1.10.4 <i>Drug Delivery</i> .....	52
1.10.5 <i>Prosthetic Biomaterials</i> .....	53
1.10.6 <i>Extraction and Separation</i> .....	53
1.10.7 <i>Applications of Smart Hydrogels</i> .....	54
1.11 Considerations for the applications of smart hydrogels.....	54
1.12 Scope & object of present work – analytes and applications.....	57

Chapter 2. Materials and Equipment .....	59
2.1 Materials – monomers and sensing agents .....	60
2.2 Equipment.....	63
PMMA fibre optic cable – (product code SH4001) Super Eska™ Polyethylene Jacketed Optical fibre Cord supplied by LasIRvis. ....	63
End stop splitter/coupler 50:50 supplied by EvanesCo (EV). ....	63
2.3 The sensing system: hardware and software .....	64
Chapter 3. Polymers and Coatings: The Development of Experimental Methodologies.....	67
3.1 Introduction .....	68
3.2 Preparation and synthesis of the hydrogel membrane .....	68
3.2.1 <i>Polymerisation rig for the synthesis of a linear macromer</i> .....	68
3.2.2 <i>Free radical polymerisation, the synthesis of the macromer</i> .....	70
3.2.3 <i>Extraction of the polymer via precipitation</i> .....	71
3.2.4 <i>Infrared Spectroscopy as a quick intermediate analysis</i> .....	71
3.2.5 <i>Functionalisation of linear macromers</i> .....	74
3.2.6 <i>Functionalisation of the macromer: Experimental Procedure</i> .....	76
3.2.7 <i>Final cross-linking reaction to form a cross-linked hydrogel sensor coating</i> .....	76
3.2.8 <i>Final cross-linking reaction: Experimental Procedure</i> .....	80
3.3 Nafion®.....	80
3.4 Fibre preparation and coating techniques.....	81
3.4.1. <i>“U” bend fibre preparation</i> .....	81
3.4.2 <i>“End stop” bend fibre preparation</i> .....	82
3.5 Coating of the membrane .....	83
Chapter 4. The design and selection of hydrogel-sensing membranes.....	86
4.1 Introduction .....	87
4.2 Refractive index change as a sensing mechanism – principles and practicalities .....	89
4.3 Design and synthesis of membranes to control and exploit refractive index changes.....	90
4.4 Chemotropic membranes – the use of entrapped colourimetric agents...	97

4.5 Design and synthesis of membranes to control and exploit colourimetric changes.....	98
Chapter 5. The design and development of a sensing platform. ....	102
5.1 introduction .....	103
5.2 The fibre optic probe: materials and configurations .....	105
5.3 Hardware of the sensor system.....	108
5.3.1 The hydrogel membrane.....	108
5.3.2 <i>The fibre optic probe</i> .....	110
5.3.3 <i>The user interface</i> .....	112
5.4 Calibration and use of the system – coating and configuration issues ..	114
5.5 The rationale for the sensor system selection. ....	116
Chapter 6. Hydrogels for the detection of water: Results and Discussion.....	119
6.1 Introduction .....	120
6.2 Hydrogels used for the detection of water.....	122
6.2.1 <i>Hydrogels using refractive index change for the detection of water</i>	123
6.2.2 <i>Hydrogels containing cobalt salts for the detection of water</i> .....	139
6.2.3 <i>Sulfonated hydrogels containing organic dyes for the detection of water- methyl orange</i> .....	146
6.2.4 <i>Sulfonated hydrogels containing organic dyes for the detection of water- crystal violet</i> .....	149
6.3 Applications in the fuel industry.....	152
6.4 Applications in humidity detection.....	154
Chapter 7. Hydrogel coatings for the detection of inorganic analytes: Results and Discussion.....	155
7.1 Introduction.....	156
7.2 Point of care assays: Tear Electrolytes.....	158
7.3 Potassium as a target analyte .....	160
7.4 Calcium as a target analyte .....	166
7.5 Aluminium as a target analyte .....	171
7.6 Possible applications of the sensor system.....	174
7.6.1 <i>Applications in ophthalmic diagnosis</i> .....	174
7.6.2 <i>Applications in the water industry</i> .....	177
7.6.3 <i>Applications in wound healing monitoring</i> .....	178

7.7 Issues of result reproducibility .....	178
Chapter 8. Summary and Conclusions.....	183
8.1 Development of the system: experimental aspects .....	184
8.1.1 Refractive index changes and water sensing.....	184
8.1.2 Inorganic analytes and chemotropic sensing.....	186
8.2 Future Work .....	187
Chapter 9. References .....	189

## List of Tables

Table 1. Monomers, initiators and cross-linking agents used.....	60
Table 2. List of chemotropic agents used.....	62
Table 3. Table of monomers, initiators and solvent system used in the synthesis of the macromers for the creation of hydrogels.....	70
<b>Table 4.</b> The compositions of hydrogels used for sensing water in jet fuel. ....	129
Table 5. The composition of DH2.....	163
<b>Table 6.</b> The radii of several cations and three crown ether cavities <sup>125</sup> . ....	167



## List of Figures

Figure 1. An illustration of Daniel Colladons recreation of John Tyndall's light guiding experiment which he published as "La Fontaine Colladon" in La Nature 2nd half year 1884, p.325. Demonstrating a waveguide <sup>1</sup> .....	18
Figure 2. A SEM micrograph of a 1.2 $\mu\text{m}$ core pure-silica photonic-crystal fibre <sup>5</sup> . .....	19
Figure 3. A diagram representing light launched into a block of glass showing the principle of refraction and reflection. ....	22
Figure 4. Reflection: ray of light from point P travels in a line to hit the mirror at point O, at an angle of $\theta_i$ ; the light is then reflected from point O to point Q at an angle of $\theta_r$ , where $\theta_i = \theta_r$ . ....	22
Figure 5. Light launched down a block of PMMA showing the phenomenon of total internal reflection <sup>15</sup> . ....	23
Figure 6. Internal reflection: the black line represents the boundary of the two media; the grey area is glass, and the white area represents air. The red line represents the light that hits the boundary at an angle larger than the critical angle, the blue line represents light that hits the boundary at an angle less than the critical angle and is completely reflected <sup>14</sup> . ....	23
Figure 7. A schematic of the structure of a generic fibre optic cable. The fibre core (white) is surrounded by a cladding layer (blue), which has a lower RI than the fibre core. ....	25
Figure 8. Schematic representation of the preform and drawing fibre optic cable fabrication process <sup>18</sup> . ....	26
Figure 9. Schematic of the extrusion fibre optic cable fabrication process <sup>17</sup> . ....	27
Figure 10. Fibre optic cable between two corrugated plates in a strain sensor <sup>21</sup> . .....	29
Figure 11. A schematic of the fibre optic sensor system for kerosene detection in diesel or petrol <sup>23</sup> . ....	30
Figure 12. The percentage of normalised power of the light source vs kerosene <sup>24</sup> . .....	30
Figure 13. A graph of temperature and strain calibration data of the fluorescence intensity ratio R, for various applied temperatures and strains <sup>28</sup> . ....	32
Figure 14. A graph of temperature and strain calibration data of the Bragg wavelength for various applied temperatures and strains <sup>29</sup> . ....	32

Figure 15. Time response curve of mode-filtered light fibre optic sensor with and without bromocresol green subject to various pH solutions: (a) 2.0, (b) 3.0, (c) 4.0, (d) 5.0, (e) 6.0, (f) 7.0, and (g) 8.0. (A) With bromocresol green and (B) without bromocresol green <sup>31</sup> .	34
Figure 16. Experimental set-up scheme <sup>33</sup> .	35
Figure 17. A graph of equilibrium water content of a HEMA-MMA copolymer hydrogel (circles) and of a HEMA-NVP copolymer hydrogel (squares) <sup>50</sup> .	39
Figure 18. A graph of Dk vs EWC for conventional hydrogels. Quotes manufacturers data (solid diamonds); reference materials at 25°C (open squares); reference materials at 34°C (open circles) <sup>52</sup> .	40
Figure 19. A representation of a 3D hydrogel network. The red, green and black lines represent polymer chains. Blue lines represent cross-links between the polymer chains <sup>57</sup> .	42
Figure 20. Cartoon schematics of the polymer chains in (A) a high cross-link density hydrogel unhydrated, (B) a high cross-link density hydrogel hydrated, (C) a lower cross-link density hydrogel unhydrated, and (D) a lower cross-link density hydrogel hydrated. .	43
Figure 21. Initiation by a) AIBN, and b) potassium persulfate, using heat as the energy source to reach the required dissociation energy. .	45
Figure 22. Free radical propagation step with AIBN (initiator) and NaAMPs (monomer). .	46
Figure 23. Methods of termination in free radical polymerisation. a) Combination, two active chain ends interact. b) An active chain end and initiator radical interact. c) Two radical initiator molecules reacting to reform the initiator molecule. .	47
Figure 24. Disproportionation of two active chain ends during termination. ....	48
Figure 25. The effect of single oxygen radicals on polymerisation. .	49
Figure 26. A graph of swell vs pH to exemplify the relationship between swell and pH for an imaginary polyacid and polybase. .	51
Figure 27. The EV5000 interrogation unit connected to a laptop with an end stop probe connected via a splitter/coupler. .	64
Figure 28. An example graph of the data plotted as signal loss vs time for a period of ten minutes. .	65
Figure 29. Polymerisation rig, used for the synthesis of the linear polymer. ....	69

Figure 30. An example of using IR spectroscopy to identify monomers incorporated into DH8, and the structure of the monomers incorporated in DH8. .....	73
Figure 31. The condensation reaction of NMA with an alcohol functional group in a macromer backbone <sup>96</sup> .....	74
Figure 32. Condensation reaction mechanism of NMA with a hydroxy group in a macromer backbone. ....	75
Figure 33. The initiation of Irgacure 184.....	77
Figure 34. Propagation of a Irgacure 184 radical centre ( represented as I) with the cross-linking agent Ebacryl 11. ....	78
Figure 35. Propagation of the linear macromer cross-linking site (where R represents the linear macromer backbone), with an Irgacure 184 radical (represented as I).....	78
Figure 36. Termination of the free radical cross-linking reaction by a propagating cross-linking agent, with a propagating cross-linking site on the macromer. ....	79
Figure 37. Schematic representation of the coupler used with end stop probes. .....	83
Figure 38. A schematic representation of a possible fibre optic cable and interrogation system setup. ....	90
Figure 39. A molecular diagram of a sulfonate functional group, a carboxyl functional group and an alcohol group. ....	92
Figure 40. A sulfonate functional group and a carboxyl functional group with the negative charge delocalised.....	92
Figure 41. Graph showing the effect of salt concentration in solution on EWC of three hydrogel compositions <sup>110</sup> . ....	94
Figure 42. Graph of pH vs swelling ratio of five polymer blends of poly(acrylic acid) (PAA) : poly(vinyl alcohol) (PVA) : <sup>112</sup> .....	95
Figure 43. A carboxylic acid group reacting with a sodium hydroxide molecule. .....	97
Figure 44. The four steps of creating a Grignard reagent by protecting the alcohol group, forming the Grignard reagent, Grignard reaction, and the removal of the protecting group from the alcohol <sup>114</sup> . ....	99

Figure 45. A representation of the entrapment of chemotropic agents within a hydrogel network. The red dots represent hydrophobic groups. The large green circles represent the chemotropic agent trapped by the hydrophobic groups within the hydrogel network.....	100
Figure 46. Light emitted from an LED represented as waves that are not in phase with each other. ....	105
Figure 47. The light from a laser represented as waves, all in phase with each other.....	105
Figure 48. A Schematic representation of two cleaved fibres. A, shows a fibre that has been cleaved with an angle of 0°. B, shows a fibre that has been cleaved with a 7°, angle at the end of the fibre.....	107
Figure 49. Schematic overview of the four sensor system components.....	108
Figure 50. A. “U” bend fibre optic cable with cladding layer. B. Cladding layer removed to expose the fibre core. C. The core of the fibre coated with a hydrogel coating (red area). ....	109
Figure 51. A PMMA fibre optic cable that has a “U” bend in it to encourage signal loss, coated with a smart hydrogel, to attain sensitivity to a particular stimulus.....	110
Figure 52. A straight fibre optic probe coated with a smart hydrogel being used to perform a direct assay of the lower tear meniscus. ....	111
Figure 53. Hardware user interface.....	112
Figure 54. A) Signal loss vs time of three concentrations of aluminium (Al) in water. B) The average signal loss vs concentration of three samples of aluminium solution. ....	113
Figure 55. A Colourimetric probe of methyl orange, in a coating of NBNMA, NVNMA and MMA (crosslink density 0.8%). The probe was dipped into a solution of HCl, and sodium hydroxide (NaOH) alternatively three times.....	115
Figure 56. A probe coated in a PVA/sulfonated macromer (crosslink density 1%) in ambient air then placed over a beaker of water at room temperature. The light source used was a white LED, the red, green and blue lines represent the data collected from each channel, i.e. red, green and blue wavelengths. ....	115
<b>Figure 57.</b> Morin chelating with aluminium. ....	120
Figure 58. Sodium tetraphenylborate undergoing a displacement reaction with potassium to form potassium tetra phenyl borate.....	121

Figure 59. Variation of refractive index (RI) with EWC for various methacrylate hydrogels at 20°C (filled dots) and at 34°C (empty squares) <sup>127</sup> .....	124
Figure 60. Variation in refractive index (RI) with composition for polymers of styrene:HEMA, in both hydrated (triangles) and dehydrated (diamond) state <sup>128</sup> . .....	125
Figure 61 A) An uncoated PMMA “U” bend fibre subjected to jet fuel samples containing 0, 3 and 5% water. B) Average signal loss values for 0, 3 and 5% water in jet fuel obtained from an uncoated “U” bend PMMA fibre.....	128
Figure 62. A) A plot of signal loss vs time for a PMMA “U” bend probe coated with the hydrogel DH5 exposed to samples of jet fuel containing from left to right, 0, 1, 3 and 5% water. B) A plot of the average signal loss vs the % water in jet fuel. ....	132
Figure 63. A) A plot of signal loss vs time for a “U” bend probe coated with the hydrogel DH8 exposed to samples of jet fuel containing from left to right, 0, 1, 3 and 5% water. B) The average signal loss vs % water in jet fuel for a U” bend probe coated with the hydrogel DH8.....	134
Figure 64. A) A plot of signal loss vs time for a “U” bend PMMA probe coated with the hydrogel DH9 exposed to samples of jet fuel containing from left to right, 0, 1, 3 and 5% water. B) a plot of average signal loss vs % water in jet fuel for a “U” bend PMMA probe coated with the hydrogel DH9.....	136
Figure 65. A comparison of the average signal loss values generated by an uncoated, and DH5, DH8 and DH9 coated “U” bend PMMA fibres optic probe for a range of jet fuel containing water. ....	137
Figure 66. Example of a coordinated complex. Cobalt (II) being coordinated by 6 ammonia ligands.....	140
Figure 67. A) Signal loss data collected for a “U” bend PMMA fibre probe coated in hydrogel DH5 containing cobalt (II) chloride, for a range of water in jet fuel. B) The average signal loss values obtained for each sample of jet fuel containing water.....	141
Figure 68. A) Signal loss data collected for a “U” bend PMMA fibre probe coated in hydrogel DH5 containing cobalt (II) acetyl acetonate, for a range of water in jet fuel. B) The average signal loss values obtained for each sample of jet fuel containing water. ....	143
Figure 69. The average signal loss values obtained for a “U” bend fibre optic probe coated in DH7 exposed to 0, 1, 3 and 5% water in jet fuel.....	144
Figure 70. A comparison of the average signal loss values generated by the coatings DH5 containing cobalt (II) chloride, DH9 cobalt (II) acetyl acetate,	

and DH7 coated onto a “U” bend PMMA fibre optic probe for a range of jet fuel containing water.....	145
Figure 71. Methyl orange being protonated by H <sup>+</sup> , undergoing a colour change from orange to yellow.....	147
Figure 72. A) Signal loss data collected for a “U” bend PMMA fibre probe coated in hydrogel DH9 containing methyl orange, for a range of water in jet fuel. B) The average signal loss values obtained for each sample of jet fuel containing water.....	148
Figure 73. The dissociation of a sulfonate group in the presence of water. ...	149
Figure 74. The protonation of crystal violet. ....	150
Figure 75. The average signal loss obtained from a PMMA “U” bend probe coated with Nafion® containing crystal violet when exposed to jet fuel containing water.....	152
Figure 76. DH2 coated “end stop” glass probe with sodium tetra phenyl borate entrapped in the hydrogel, subjected to samples of potassium in water. ....	165
Figure 77. The log of the stability constant for complexes of three crown ethers plotted against the size of several cations <sup>125</sup> .....	167
Figure 78. The average signal loss of a PMMA “U” bend coated with DH2 containing benzo 18 crown 6, exposed to three samples of water containing varying levels of calcium ions.....	170
Figure 79. Morin complexing with aluminium to form the aluminium salt of Morin.....	171
Figure 80. Time vs Signal loss for a probe coated with smart hydrogel DH2 containing the chemotropic agent Morin. The probe is subjected to three samples of water containing increasing levels of aluminium.....	173
Figure 81. The average signal loss for a probe subjected to three samples of water containing 0, 499 and 998 µg/ml Al. ....	173
Figure 82. Three “U” bend PMMA probes coated with hydrogel DH9 exposed to jet fuel containing various levels of water to show the difference in signal loss between fibres.....	179
Figure 83. Three “end stop” glass probes exposed to air, and dry jet fuel to show the difference in signal loss between fibres. ....	181

## List of Abbreviations

**ACMO** – Acryloyl morpholine

**AGA** – Acrylamidoglycolic acid monohydrate

**AIBN** – 2,2'-azobis(2-methylpropionitrile)

**Al** – Aluminium

**B-18-C-6** – Benzo 18 crown 6

**CoSPA** – 3-sulfopropyl ester acrylate cobalt (II) salt

**EWC** – Equilibrium water content

**EV** – EvanesCo

**FT-IR** – Fourier transform infrared

**H<sub>2</sub>O** – Water

**HCl** – Hydrogen chloride

**HEA** – 2-hydroxyethyl acrylamide

**HEMA** – 2-hydroxyethyl methacrylate

**IR** – Infrared

**LCST** – Lower critical solution temperature

**LED** – Light emitting diode

**MeCN** – Acetonitrile

**MMA** – Methyl methacrylate

**NaAMPs** – Sodium salt of 2-acrylamido-2-methylpropane sulfonic acid

**NaCl** – Sodium chloride

**NaOH** – Sodium hydroxide

**NBNMA** – *N*-benzyl-*N*-methylacrylamide

**NMA** – *N*-methylol acrylamide

**NMR** – Nuclear magnetic resonance

**NVNMA** – *N*-vinyl-*N*-methyl acetamide

**NVP** – *N*-vinyl pyrrolidone

**PAA** – Poly (acrylic acid)

**PDEAEMA** – Poly (2-(diethylamino)ethyl methacrylate)

**PEG** – Poly (ethylene glycol)

**PMMA** – Poly (methyl methacrylate)

**PVA** – Poly (vinyl alcohol)

**RI** – Refractive index

**SPA** – 3-sulfopropyl ester acrylate potassium salt

**UV** – Ultraviolet



## **Chapter 1- Introduction**

## 1.1 Fibre optic sensing

Fibre optics is a term associated with television, broadband internet and telephone communication networks. In the following, a broad overview of the principles of fibre optic technology, advances in the materials used for fibre optic cables and the main applications of this technology will be discussed.

Fibre optics date back to the mid 1800's when a wave-guide was first used to guide light using refraction, as a simple demonstration of a scientific phenomenon called total internal reflection<sup>1</sup>. Figure 1 is a picture from Daniel Colladons recreation of this demonstration.



**Figure 1.** An illustration of Daniel Colladons recreation of John Tyndall's light guiding experiment which he published as "La Fontaine Colladon" in La Nature 2nd half year 1884, p.325. Demonstrating a waveguide<sup>1</sup>.

The potential of this simple phenomenon has been realised and turned into a vast array of applications, all based on the simple fact that light can be passed through the length of a fibre optic cable (or launched down the fibre, as frequently referred to in the fibre optic industry) and the light that reaches the other end of the cable measured. This has spawned the fibre optic communications industry, whereby light is sent down fibres to transmit information almost instantaneously, which is then interpreted by a detector unit

and appropriate computer software. Communications companies increasingly choose fibre optic cabling over traditional copper wire because the interference and the signal loss experienced with fibre optic cables are less than with its copper counterpart<sup>2</sup>. More recent applications have included the use of fibre optics in the sensor field.

Fibre optic cables have seen an increasing range of uses from simple decorative lighting, to use in medical surgery as a means of “seeing” inside the patient without the need for making very large incisions<sup>2</sup>. The range of uses of fibre optic cables has increased because of the advances in the materials used to produce fibre optic cables<sup>2</sup>. Historically fibre optic cables were made from glass, as the attenuation properties of glass were vastly superior to those of polymers at the time, and as such, glass fibres have formed the backbone of modern optical communication<sup>2</sup>.

One advancement in the glass fibre optic cable is the photonic crystal fibre, otherwise known as the holey fibre<sup>3</sup>. This type of fibre has channels that run along the length of the fibre, as shown in figure 2, in a periodic arrangement that gives these air clad optical fibres the appearance of a crystal<sup>4</sup>. Photonic crystal fibres are based on the properties of photonic crystals, which give the fibre the ability to confine light in hollow cores, giving it characteristics that are not matched in conventional optical fibres<sup>4</sup>.



**Figure 2.** A SEM micrograph of a 1.2  $\mu\text{m}$  core pure-silica photonic-crystal fibre<sup>5</sup>.

Advances in the composition of polymers have led to the development of low loss polymer fibre optic cables<sup>2</sup>. One of the advances is the replacement of H atoms on polymer backbones with heavier deuterated atoms, resulting in the reduction of the attenuation in the polymer fibre optic cable<sup>2</sup>. An additional advancement in polymer composition is the replacement of H atoms with heavier F atoms that again reduces the attenuation in polymer fibre optic cables<sup>2</sup>. The progression in polymer fibre optic cable composition has led to the replacement of glass fibre optic cables with polymer fibre optic cables in order to reduce costs<sup>2</sup>.

In fibre optical communication systems the most important parameter is the attenuation characteristic of the fibre, as loss of signal is undesired<sup>2</sup>. Silica fibres have an attenuation of 0.2 dB/km at 1.55  $\mu\text{m}^2$ , which is far lower than that of a polymer optical fibre and it is this property that makes polymer-based fibres suitable in applications where only a short length of fibre is needed<sup>2</sup>. Consequently, three types of polymer optical fibres have received interest due to their attenuation characteristics, namely poly (methyl methacrylate) (PMMA) fibres, deuterated PMMA fibres, and perfluorinated fibres<sup>2</sup>.

PMMA fibres have a theoretical minimum attenuation of 100 dB/km at 0.65  $\mu\text{m}^2$ . However, the actual figure is closer to 200dB/km, which limits the use of PMMA fibres to several hundred meters<sup>6</sup>. In deuterated PMMA, there are no 'normal' carbon-hydrogen bonds, which cause the large attenuation that is observed in normal PMMA fibres<sup>2</sup>. By replacing the normal carbon-hydrogen bond with a carbon-deuterated bond the attenuation can be reduced to 25dB/km at 650 $\mu\text{m}^2$ . Whilst this improves the attenuation characteristics of the polymer optical fibre, this type of fibre absorbs water readily, creating other problems<sup>2</sup>. Also deuterated monomers are more expensive, making them a less attractive alternative for the replacement of glass fibre optic communication systems. An alternative method of reducing attenuation in polymer optical fibres is to replace the hydrogen atoms with a heavier atom like fluorine<sup>7</sup>. Perfluorinated polymer optical fibres have a resonant absorption wavelength in the range of 7.7-10 $\mu\text{m}$ , which is far from the visible light range<sup>7</sup>. To date, the best-recorded attenuation

of a perfluorinated polymer optical fibre is 10dB/km<sup>7</sup>, which is a vast improvement of a normal PMMA optical fibre.

Single-mode and multi-mode optical fibres differ in their diameter<sup>8</sup>. Multi-mode fibres allow more modes (rays of light) to travel through the fibre due to their diameter being larger than that of a single-mode fibre, which only allows one mode<sup>8</sup>. In terms of practicality, the multi-mode fibre allows for simpler connections<sup>9</sup>, and the use of cheaper light sources, such as light emitting diodes (LEDs)<sup>9</sup>. The properties of multi mode fibres have made their use possible in communication networks within buildings. Single-mode fibres have more delicate connections due to their size<sup>10</sup>, and require a more expensive light source, such as a laser. Lasers produce coherent light of a narrow wavelength spectrum<sup>11</sup>, as opposed to other light sources that produce light that is less coherent and has a phase that varies randomly<sup>12</sup>.

Cladding in optical fibres is important. The cladding layer surrounds the core of the fibre, and is a material that has a lower refractive index (RI) than that of the core, thus stopping light from escaping from the core of the fibre. The choice of material will depend upon the RI of the core<sup>2</sup>. For example, PMMA fibres have a refractive index of 1.48<sup>13</sup> and therefore can be cladded with fluoropolymers, because of their lower refractive index (1.35-1.42)<sup>13</sup>.

## **1.2 Refraction, reflection and total internal reflection**

The first step in understanding the phenomenon of total internal reflection is to look at what happens when light passes from one optically transparent medium to another of a different density. If light from a slit lamp were to hit a block of glass at an angle of 90 degrees, it would seem that the light continues to travel unaffected<sup>14</sup>. However, the actual observation is that the light travels slower through the glass than in the air without changing direction. If the angle at which the light hits the glass, the angle of incidence, were to be changed from 90, then the light from the slit lamp would still travel slower through the glass, but would change direction<sup>14</sup>. This phenomenon is referred to as refraction<sup>14</sup>. The

angle at which the light changes direction in the new medium will depend on the RI of the medium.

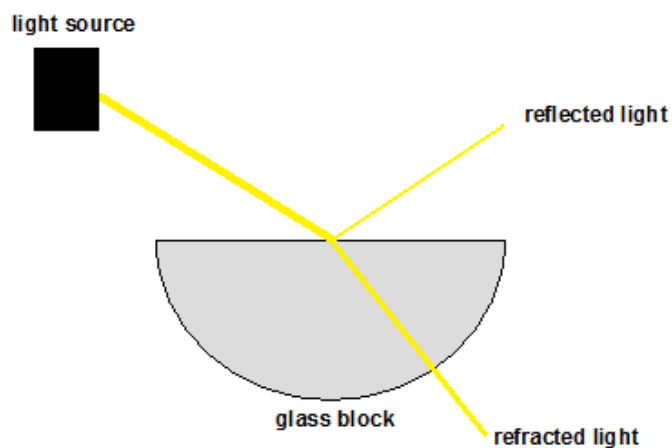


**Figure 3.** A diagram representing light launched into a block of glass showing the principle of refraction and reflection.

Another important optical occurrence is that of reflection. If the angle of incidence at which the light hits a medium is changed, it could result in the light being reflected<sup>14</sup>. In this instance light is thought of as a wave rather than as a discrete particle. Reflection of light is the change in the direction of a wavefront when it hits a new medium and reflects back into the original medium, in a new direction<sup>14</sup>. The new direction is governed by the angle at which the wave hits the new medium. The angle of incidence ( $\theta_i$ ) is equal to the angle of reflection ( $\theta_r$ ), as shown in figure 4.

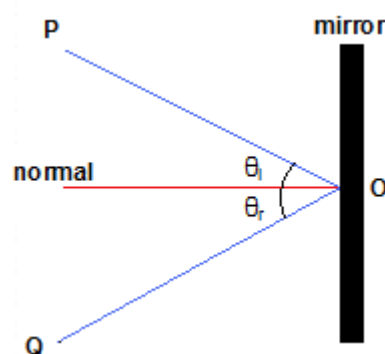


**Figure 4.** Reflection: ray of light from point P travels in a line to hit the mirror at point O, at an angle of  $\theta_i$ ; the light is then reflected from point O to point Q at an angle of  $\theta_r$ , where  $\theta_i = \theta_r$ .

Reflection can occur when a light wave hits a surface of a different RI. In certain circumstances it is possible to use reflection to contain light within a medium, so that it can be directed from one point to another, as demonstrated in figures 5 and 6.



**Figure 5.** Light launched down a block of PMMA showing the phenomenon of total internal reflection<sup>15</sup>.

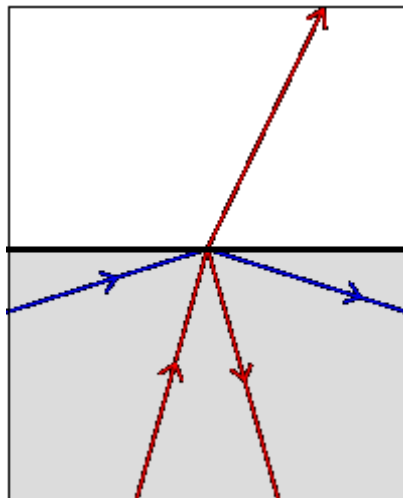


**Figure 6.** Internal reflection: the black line represents the boundary of the two media; the grey area is glass, and the white area represents air. The red line represents the light that hits the boundary at an angle larger than the critical angle, the blue line represents light that hits the boundary at an angle less than the critical angle and is completely reflected<sup>14</sup>.

Figure 5 represents the phenomenon of total internal reflection, i.e. light shone into a medium is completely reflected so that none of the light escapes the medium. There are two conditions that must be met for total internal reflection to occur. Firstly, the RI of the second medium must be lower than that of the first medium. Secondly, the angle of incidence at which the light hits the boundary of the two media is less than that of the critical angle of incidence<sup>14</sup>, as represented in figure 6. When both conditions are met, the light is reflected back into the first medium.

The phenomenon of total internal reflection is the main principle of fibre optics technology. This allows the fibre optics industry to exploit this phenomenon using waveguides referred to as fibre optic cables<sup>14</sup>. Waveguide is the term used to describe optically clear materials that can transmit and direct light<sup>14</sup>. Fibre optic cables rely upon total internal reflection for transmitting light along the length of the cable<sup>14</sup>. When applied in the context of fibre optic cables, the phenomenon of total internal reflection occurs when the angle of incidence at which the light hits the boundary of the core of the fibre is less than that of the critical angle of incidence, and the RI of the medium outside the fibre core is lower than that of the core of the fibre, which means that the light will not pass out of the core of the fibre, but will be reflected back into the fibre<sup>16</sup>. Fibre optic cables are constructed in a way that allows total internal reflection to occur. Figure 7 shows a schematic of a fibre optic cable with a cladding layer. The cladding layer, which coats the whole surface of the fibre core, has a lower RI than that of the fibre core RI. This prevents light from escaping the fibre core, given that the angle at which light hits the boundary between the cladding layer and the core is lower than the critical angle of incidence<sup>16</sup>.



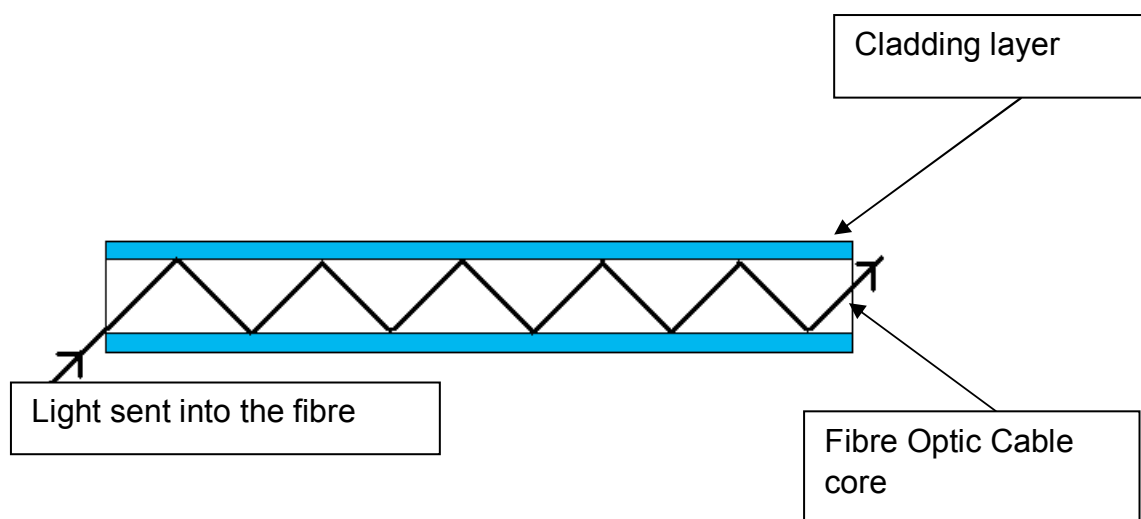


**Figure 7.** A schematic of the structure of a generic fibre optic cable. The fibre core (white) is surrounded by a cladding layer (blue), which has a lower RI than the fibre core.

### 1.3 Polymer fibre optic cable fabrication

PMMA fibres are manufactured from the monomer methyl methacrylate (MMA) by using the preform and drawing method<sup>2</sup>, or from pre-synthesized PMMA with the extrusion method<sup>2</sup>. When using the preform and drawing method, the inhibitor in MMA is removed by distillation or chromatography, and the monomer is degassed to remove any bubbles in the MMA<sup>2</sup>. It is also important to remove any impurities from the monomer to prevent any scattering in the resulting fibre<sup>2</sup>. An initiator, such as peroxide or AIBN, is added to the monomer, along with a chain transfer reagent usually containing an S-H group, which controls the molecular weight of the resulting polymer<sup>2</sup>. MMA monomer has a RI of approximately 1.402<sup>2</sup>, which is polymerised and used as the cladding material for the core of the fibre. For the fibre to support total internal reflection the core must have a RI of more than 1.402, which can be achieved by the addition of a dopant<sup>2</sup>. The relationship between increasing the level of dopant and increasing the RI is linear<sup>2</sup>. There are many dopants that can be used, many contain benzene groups, and just as dopants can increase the RI,

dopants such as trifluoroethyl methacrylate can be used to lower the RI of the fibre's core<sup>2</sup>.

There are two methods for the fabrication of polymer fibre optic cables, preform and drawing, and the extrusion method. For the preform and draw method as shown in figure 8 the preform is fabricated by pouring a mixture of MMA monomer, initiator, and a transfer reagent into a glass tube that is spun at 3000rpm in an oven at 70°C for 1-2 days<sup>2</sup>. The high-speed rotation causes the mixture to polymerise, leaving a space in the centre, where the core of the fibre will be polymerised<sup>2</sup>. Once the cladding is polymerised, the core is made by pouring a mixture of index raising dopant, initiator, monomer, and chain transfer reagent into the space created for the core, and is spun at 50 rpm, at 95°C for 24 hours<sup>2</sup>. Now the preform is ready to be drawn into fibres<sup>2</sup>. The glass transition temperature of the resulting preform will determine the drawability of the polymer optical fibre<sup>2</sup>. This temperature is approximately 110°C, with an average molecular weight of less than 80,000 u<sup>2</sup>. To draw the fibre, the preform is slowly fed under computer control into a 280-290°C furnace, and drawn into a polymer optical fibre<sup>2</sup>. This method of making polymer optical fibres allows many different varieties of fibre to be made, such as single mode, multi-mode, and dye-doped fibres<sup>2</sup>. However, because there is only a finite length of preform made for drawing, only a finite length of fibre can be made each time, making it not very commercially attractive route of production<sup>2</sup>.



**Figure 8.** Schematic representation of the preform and drawing fibre optic cable fabrication process<sup>18</sup>.

The extrusion method shown in figure 9 uses solid polymer pebbles or powder, in contrast to liquid monomers which are used in the preform and drawing method<sup>2</sup>. First the powder for the core of the fibre is fed into the extruder from one feeder, and then for the cladding layer powder is fed from another feeder<sup>2</sup>. Then a set of feed screws pushes the powder to the output die at the end of the diffusion zone<sup>2</sup>. Through the diffusion zone (about 6.5 cm long) there is a gradient of temperature that reaches a maximum of 280°C approximately<sup>2</sup>, which helps to create graded-index fibres. The extrusion rate will vary between 93-245g/hr. The die has two concentric nozzles which create the core and the cladding of the fibre<sup>2</sup>. The diameter of the core and thickness of the cladding is controlled by the size of the nozzles used<sup>2</sup>. Extrusion allows for a long length of fibre to be made, making it a commercially attractive process<sup>2</sup>.



**Figure 9.** Schematic of the extrusion fibre optic cable fabrication process<sup>17</sup>.

Multi-mode optical fibres have a larger diameter than single mode fibres<sup>10</sup>, allowing more modes (rays of light) to be transmitted along the length of the fibre. In terms of practicality, the multi mode fibre allows for simpler connections<sup>10</sup>, and the use of cheaper light sources such as LEDs<sup>10</sup>. Such properties of multi-mode fibres have led to their use in communication networks within buildings<sup>2</sup>. The single mode fibres have more delicate connections due to

their size, and require a more expensive light source, such as lasers<sup>6</sup>. Lasers produce coherent light of a narrower wavelength spectrum<sup>11</sup>, compared to other light sources that produce less coherent light with a phase that varies randomly<sup>11</sup>.

The cladding layer surrounds the core of the fibre, and its importance lies in the fact that it is a material with a lower RI than that of the core, stopping light escaping from the core of the fibre<sup>16</sup>. Selection of a suitable material will depend upon the RI of the core. For example, fluoropolymers have a RI of 1.35-1.42<sup>13</sup> and can therefore be used to coat PMMA fibres, as their RI is 1.48<sup>13</sup>. If, however, the core was made from polystyrene with a RI of 1.59-1.60<sup>13</sup>, then PMMA could be used for the cladding layer.

Signal loss in optical fibres can be controlled by changing the RI of the medium that is in contact with the optical fibre core. In order to amplify this effect a bend can be put into the fibre, so that the signal loss is more significant<sup>19</sup>. One possible way to control signal loss is to coat the surface of the fibre with a medium that has a RI that can be altered by the presence of certain stimuli. One such medium is a hydrogel, which can be responsive to a stimulus that is present in the system that the fibre is in contact with. The stimulus will change the RI of the hydrogel coating and therefore affect the signal loss through the fibre. This behaviour makes hydrogels an ideal subject of research for use in combination with fibre optic sensing.

#### **1.4 Fibre optic technology for sensing**

The use of fibre optic technology is not limited to communication applications. Fibre optic technology has been exploited in the field of sensor technology; there are many variations on how fibre optic technology is exploited. However there is one underlying principle for the application of fibre optic technology in a sensor paradigm. In all systems utilising fibre optic technology for sensors, the difference in intensity of light is measured between the source of light transmitted along a cable and the end of the fibre optic cable. There are a

variety of methods for controlling the loss of light from the fibre optic cable, dependent on what is being measured. In the next section several methods of generating a signal loss are presented, as well as the advantages and disadvantages of using such methods in terms of cost and accuracy, as well as other practical issues.

### 1.5 Existing fibre optic sensor systems

An example of a simple fibre optic sensor system is that for the measurement of structural strain monitoring. Luo *et al*<sup>20</sup> built a microbend system to measure strain in a structure. A fibre optic cable is placed between two corrugated plates. This results in a loss of light from the fibre when strain is applied, which causes the fibre to bend<sup>20</sup>, as shown in figure 10. The amount of strain applied to the plates will influence the extent of the bend in the fibre, and therefore larger or smaller amount of light that is lost from the system. Loss occurs because the bend in the fibre causes the angle of incidence at which the light hits the cladding layer to change<sup>20</sup>.



**Figure 10.** Fibre optic cable between two corrugated plates in a strain sensor<sup>21</sup>.

This type of sensor could have applications in online monitoring of large engineering structures for security purposes or for damage diagnosis.

Another example of a fibre optic sensor system is one constructed by Roy<sup>22</sup>, which relies solely on the RI change of liquids. This sensor system has been developed for the determination of adulteration of petrol and diesel by kerosene<sup>22</sup>. The RI of a liquid substance changes when a new substance is added to it<sup>22</sup>.



**Figure 11.** A schematic of the fibre optic sensor system for kerosene detection in diesel or petrol<sup>23</sup>.

In this system the cladding layer of the fibre optic cable is removed, so that the fuel solution makes contact with the fibre core. This allows the fuel solution to be the second medium, whose RI affects whether the conditions for total internal reflection are met<sup>22</sup>. If the RI of the fuel solution is lower than the core of the fibre then total internal reflection occurs. As the RI of the solution increases above that of the core of the fibre, the light escapes the fibre. Figure 12 shows that as the kerosene levels increase in the fuel solution, the power of the signal that reaches the end of the fibre decreases

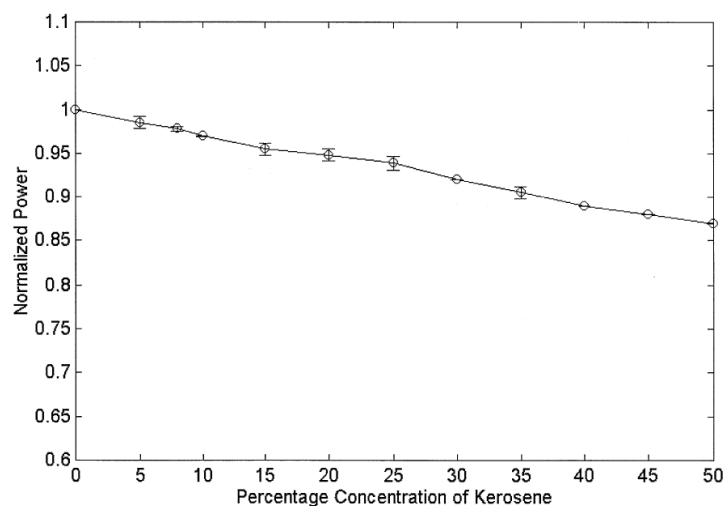


**Figure 12.** The percentage of normalised power of the light source vs kerosene

24

Whilst this system utilises the theory of changing the RI of the medium surrounding the core of the fibre optic cable to generate a change in the normalised power and shows positive results, its limitation lies in the fact that kerosene was tested as the only variable causing a RI change in a known fuel sample. The system is adequate for detecting whether or not the fuel has been adulterated when the RI of the fuel is a known variable. However, fuels from different sources have different RIs due to the presence of different additives, making it possible for a positive reading to be obtained when no adulteration has occurred.

Another type of fibre optic sensor is the fibre Bragg grating sensor<sup>25</sup>. A fibre Bragg grating is a short length of fibre where the RI of the fibre core has been altered, this can be achieved by using a laser to alter the RI of the fibre, or materials of varying RI can be incorporated into the fibre<sup>26</sup>. This means that the fibre will only transmit light of certain wavelengths, while blocking other wavelengths<sup>26</sup>. Fibre Bragg gratings are used in temperature and strain sensors, as changes in strain and temperature result in the path length of the grating altering which changes the transmission properties of the grating<sup>26</sup>. In other words, a change in strain or temperature in the fibre causes a shift in the wavelength of the light transmitted<sup>26</sup>. Trpkovski *et al*<sup>27</sup> designed a dual temperature and strain sensor, using a fiber Bragg grating. The fiber Bragg grating reacts to the strain, and the Er<sup>3+</sup> doped part of the fiber is sensitive to temperature changes<sup>27</sup>. When strain is applied to the grating, this causes the transmittance properties of the grating to alter, allowing light of different wavelengths to pass through the grating whilst blocking other wavelengths.

The temperature change causes the doped part of the fibre to fluoresce<sup>27</sup>, with the extent of the temperature change affecting the intensity of the fluorescence. This work showed that the fluorescence of the doped fiber was dependent only on the temperature change and not on the strain<sup>27</sup>, as shown in figure 13.

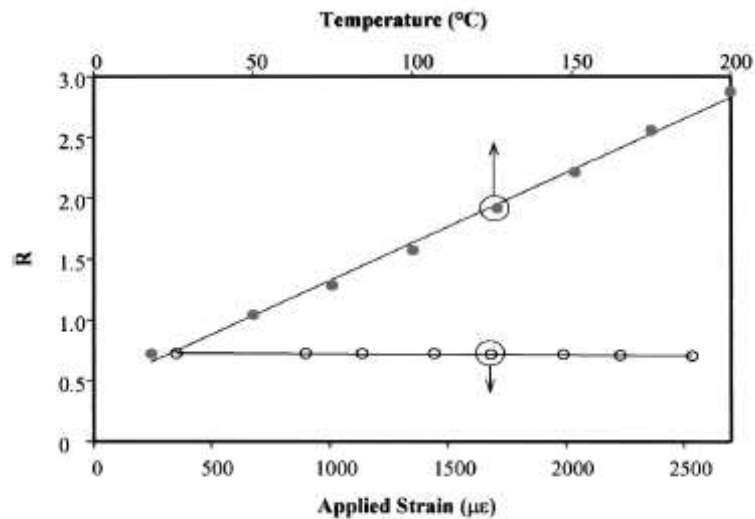


**Figure 13.** A graph of temperature and strain calibration data of the fluorescence intensity ratio  $R$ , for various applied temperatures and strains<sup>28</sup>.

The fiber Bragg grating, however, shows cross-sensitivity to strain and temperature<sup>27</sup>, as shown in figure 14.

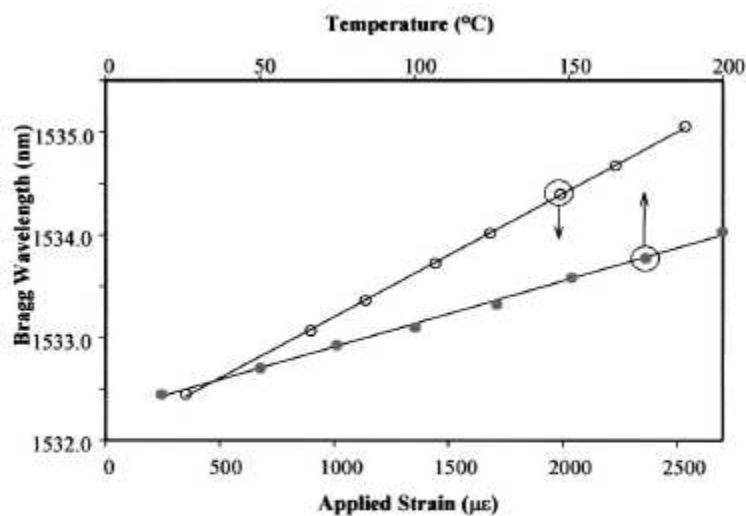


**Figure 14.** A graph of temperature and strain calibration data of the Bragg wavelength for various applied temperatures and strains<sup>29</sup>.

The above examples of fibre optic sensor systems detect different targets, using different methods to create a change of signal within the system. Each system has its own advantages and disadvantages. The main advantage of these systems is their accuracy, which is due to the high-powered lasers that



they use, and comes hand in hand with the disadvantage of cost. Other disadvantages of these three examples include complex analysis of the generated data, cross-sensitivity, and the lack of specificity to the target species. More specifically, in the case of Roy's<sup>22</sup> fibre optic sensor system for kerosene detection, the RI change may be due to kerosene or due to other additives that may be present in different fuels.

Unlike the previous examples of fibre optic sensor systems, the two types of sensor systems that follow utilise a sensing element that is stimulus-specific with little or no interference from other variables in the sample. The first system, developed by Wu *et al*<sup>30</sup>, is more stimulus-specific and it utilises a sol-gel to immobilise bromocresol green and cresol red onto a fibre optic cable, in order to detect pH<sup>30</sup>. This system uses the sol-gel as the cladding layer. Any change in pH causes a colour change in the sol-gel due to the interaction of either bromocresol green or cresol red with the hydronium ion<sup>30</sup>. The associated colour change causes signal intensity to reduce as pH changes from 1 to 8, in the case of bromocresol green. Figure 15 shows the response of the sensor system to pH of varying concentrations with and without bromocresol green. This system utilises pH detectors to give a response specifically due to pH change.

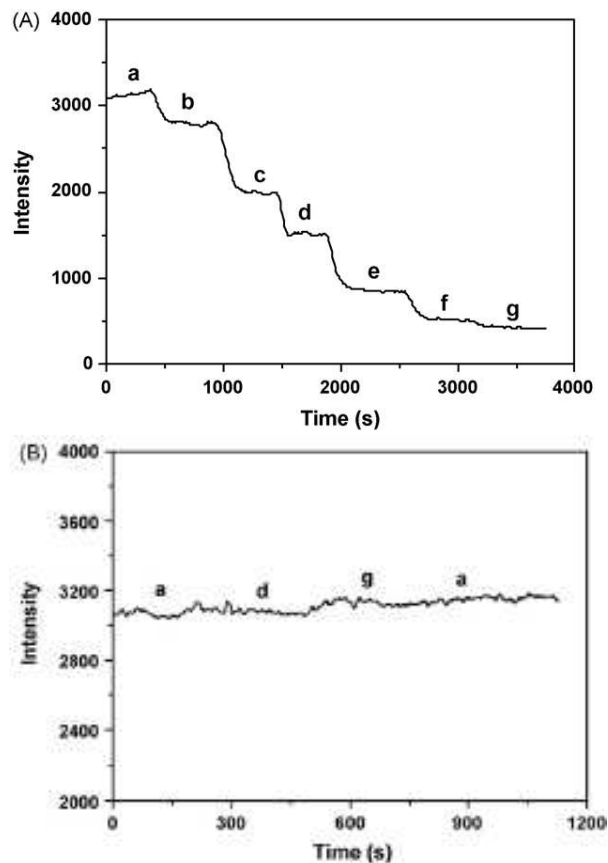


**Figure 15.** Time response curve of mode-filtered light fibre optic sensor with and without bromocresol green subject to various pH solutions: (a) 2.0, (b) 3.0, (c) 4.0, (d) 5.0, (e) 6.0, (f) 7.0, and (g) 8.0. (A) With bromocresol green and (B) without bromocresol green<sup>31</sup>.

The system developed by Estella *et al.*<sup>32</sup> was designed so that the sensing element has a specificity only to humidity. It utilises a porous xerogel as the sensing element to detect humidity with a fibre optic sensor system<sup>32</sup>. It uses changes in reflected optical power, due to the absorption of water molecules into the xerogel<sup>32</sup>. The absorption of water into the xerogel deposited on the end of the fibre causes the RI of the gel to change, which affects how much light is reflected back along the fibre<sup>32</sup>.



**Figure 16.** Experimental set-up scheme<sup>33</sup>.

This system allows for the measurement of relative humidity, as the RI of the xerogel sensing element changes in accordance to the level of humidity the system is exposed to. In consequence this causes light to be lost from the system, as a result of the RI changes that occurred<sup>32</sup>.

### **1.6 The rationale for selecting the proposed technique**

The sensor systems discussed in the last section all require a laser light source. Whilst this makes the sensor systems highly accurate for their intended purpose, it increases their cost and reduces their portability. In the case of the dual strain and temperature sensor, the fibre Bragg grating showed cross-sensitivity to temperature and strain. The cross-sensitivity was dealt with by the application of a quadratic to the obtained data. This meant that the analysis of the obtained results becomes more complicated.

The sensor system developed by Roy<sup>22</sup> relies on the RI change of the sample. This means that any change to any of the components of the fuel leads to a RI change. The result is that the addition of any compound that affects the RI of a

solution will cause a change in the measured normalised power. In other words, this system lacks specificity to the target species. This means that this sensor system can only be calibrated for use in the case of a sample with a known origin and composition. The system developed by Estella *et al.*<sup>32</sup> and Wu *et al.*<sup>30</sup> uses a xerogel to give the sensor system a specificity to changes in humidity, and no other external stimulus. This means that the sensor system in this instance could be used to measure humidity anywhere.

For the design of a simple cost-effective fibre optic sensor system, the most straightforward approach is to exploit the conditions required for total internal reflection, namely the RI of the medium surrounding the core of a fibre optic cable. An alternative approach is to use chemical agents that cause a change in the light reflected back into the fibre optic cable core due to a colour change, fluorescence or the formation of a precipitate (which scatters light). The use of a carefully chosen compound that causes reflection will give the sensor system specificity to the target species without interference from other variables within the sample. Utilising a laser will give higher accuracy in a fibre optic sensor system as the light produced has more power, which helps with the issue of attenuation of fibre optic cables. However, the use of a chemotropic agent that fluoresces in the presence of the target analyte increases the amount of light reflected into the fibre. This means that a light source of lower power, such as an LED, coupled with the use of short lengths of fibre optic cable for the probe element of the system would result in a reduction of the attenuation problem, making the proposed system more cost effective for use in fibre optic sensing.

### **1.7 Polymer-based sensor coating and hydrogels as a signal loss control mechanism**

In fibre-optic based sensor systems there are two possible routes that can be followed in the creation of a signal loss-based sensor system<sup>34</sup>. One way would be to use gratings that are inserted into, or fabricated as part of, the fibre. This type of system requires laser light sources, which are expensive<sup>35</sup>, and the resulting analysis of the generated data can be complex. Another way would be

to either expose the fibre core in order to rely on the RI change of the sample solution<sup>34</sup>, or to coat the fibre core with a material that has an associated RI change<sup>34</sup>. In the first instance, the RI change of a solution can be due to the target species or any component of the solution that affects the RI<sup>34</sup>. Consequently, the method is not ideal when there is a possibility that the variables which affect RI of a solution cannot be controlled, i.e. an unknown sample. In the second instance, the use of a coating material that has an associated RI change can be designed, so that the RI properties of the coating material change according to the presence and concentration of the target species.

Unlike the method of incorporating or fabricating a grating as part of the fibre, the use of a coating material with an associated RI change does not necessarily require a laser light source, provided that short lengths of fibre optic cable are used. The data obtained via this method, may result in less complicated data analysis, provided that the system measures the light loss.

Polymer-based coatings as a means of controlling the signal loss from a fibre optic sensor system have been used in previous research. One such example is the system used by Estella *et al.*<sup>32</sup> where a xerogel is used as the mechanism to control the signal loss, as discussed earlier. This system meets its design criteria of being able to sense humidity. However, due to the size of the apparatus, it is only appropriate for static use in a laboratory-based environment or for installation on location.

The system proposed in this research utilises hydrogels as the mechanism for the generation of a signal loss produced by the presence of a target species, whether it be a soluble analyte or water. Hydrogels are used to replace a section of the cladding layer of the fibre optic cable. Associated changes in the RI of the hydrogel due to the presence or absence of the target species exploits the second condition of the phenomenon of total internal reflection, which states that the RI of the medium outside the core of a fibre optic cable must have a lower RI than the core of the fibre.

For the work discussed in this thesis, the sensor system that was developed was based on the use of a hydrogel with a RI that changes in the presence of moisture. Hydrogels are well-established materials whose properties in aqueous environments are well documented<sup>36-42</sup>. Furthermore, the incorporation of materials such as dyes and drugs into hydrogel membranes<sup>37</sup> is the basis for the incorporation of chemotropic agents, which give the hydrogel sensitivity not only to water, but also to atoms or molecules that react with the chemotropic agent<sup>43-45</sup>. The hydrogel network is an ideal matrix into which a chemotropic sensing agent can be entrapped hydrophobically<sup>46, 47</sup>, giving the sensor system specificity to the target molecule and address the problems such as those discussed in the previous section. For these reasons, hydrogels were deemed to be the most suitable material for the coating of fibre optic cables.

In the case of moisture sensing, the hydrogel coating will change RI dependent on its level of hydration<sup>48</sup>, causing the light to be retained or lost from the fibre. If the RI of the coating is lower than that of the core of the fibre then the light will be retained<sup>19</sup>, but as it increases above the RI of the core, the light lost from the system will increase<sup>19</sup>. Inclusion of a chemotropic agent enables the sensor system to detect dissolved species, such as aluminium, in a solution<sup>49</sup>. This system relies on the chemotropic agent trapped in the hydrogel network fluorescing in the presence of the target species. The intensity of the fluorescence is proportional to the level of the target species, which can be detected by the sensor system. Using two or more chemotropic agents that change colour or fluoresce at different wavelengths allows for detection of two or more analytes, provided that a light source of multiple wavelengths is used, such as white light. When a suitable detection unit is incorporated into the system, it can measure the intensity of different wavelengths of light, and therefore several target species can be sensed at once.

## **1.8 Hydrogels – nature and properties**

Hydrogels are networks of lightly cross-linked hydrophilic polymer chains that when placed in an aqueous solution swell, but do not dissolve. Water which is

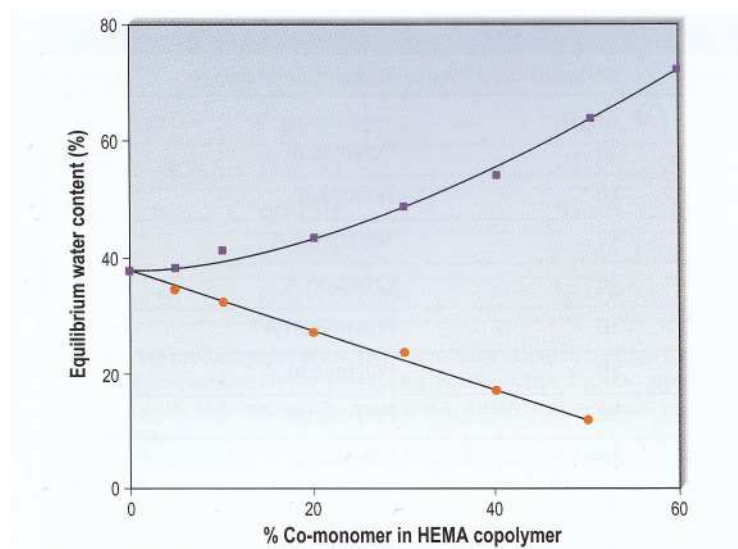
present in a hydrogel controls three main properties of the hydrogel namely the mechanical, surface, and transport properties<sup>39</sup>. The amount of water present in a hydrated hydrogel matrix is defined as the equilibrium water content (EWC). This is defined as the ratio of the water in the hydrogel to the total weight of the hydrogel expressed as a percentage.

$$\text{EWC (\%)} = \frac{\text{Weight of water in hydrogel membrane}}{\text{Total weight of hydrated hydrogel membrane}} \times 100$$

Equation 1.

### 1.8.1 The properties of hydrogels and their suitability for tissue replacement

The EWC of a hydrogel at a given temperature is determined by the monomers used in its synthesis, and the cross-link density of the hydrogel network<sup>40</sup>.



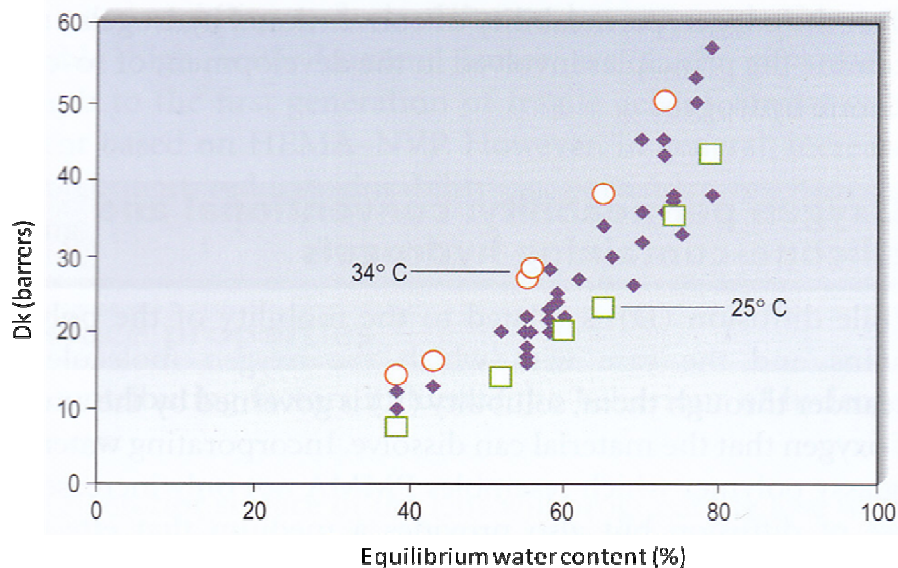
**Figure 17.** A graph of equilibrium water content of a HEMA-MMA copolymer hydrogel (circles) and of a HEMA-NVP copolymer hydrogel (squares)<sup>50</sup>.

Figure 17 shows that an increase of the *N*-vinyl pyrrolidone (NVP) comonomer in a 2-hydroxyethyl methacrylate (HEMA) hydrogel causes the EWC of the hydrogel to increase. Conversely, increasing the MMA comonomer in a HEMA hydrogel causes the EWC of the hydrogel to decrease. The increase in the ratio of the comonomer NVP to HEMA increases the EWC of the resulting hydrogel

as the number of hydrophilic groups present in the membrane increases pulling more water molecules into the hydrogel membrane. MMA is a hydrophobic monomer, therefore increasing the percentage of the MMA in a HEMA-MMA copolymer hydrogel decreases the EWC of the hydrogel. This is because the hydrophilicity of the hydrogel is reduced, and therefore its ability to entrap water within the membrane diminishes.

The EWC affects the hydrogels' properties. Water in an hydrogel affects the transport of water soluble species, surface and mechanical properties of the hydrogels<sup>39</sup>. Water in a hydrogel acts not only as a transport medium for water-soluble species, but also as a surface energy bridge between the hydrogel and the body for in vivo applications<sup>39</sup>. In addition, water acts as a plasticiser, modifying the flexibility of the hydrogel, and as a lubricant for the hydrogel, lowering its coefficient of friction<sup>51</sup>.

The EWC of a hydrogel controls the transport properties of a hydrogel. Water transports water-soluble species and therefore if a hydrogel has a high EWC then more dissolved species can move through a membrane than a hydrogel with a lower EWC.



**Figure 18.** A graph of Dk vs EWC for conventional hydrogels. Quotes manufacturers data (solid diamonds); reference materials at 25°C (open squares); reference materials at 34°C (open circles)<sup>52</sup>.



The permeability of a hydrogel can be characterised by measuring the transport of gases through the hydrogel. Permeability is a product of diffusion (D) and solubility (K) and is expressed as DK in Barrers<sup>53</sup>. Many gases are water-soluble, meaning that this measurement can be expressed as a function of EWC. As can be seen from figure 18, the amount of water that is present in a hydrogel determines its permeability to oxygen. This property allows for the application of hydrogels not only in applications involving water-soluble species, such as metal ions and sugars, but also where gas permeation is required. A contact lens is again useful example to illustrate this point. The cornea is a non-vascular tissue, which means that it does not receive the oxygen required from the blood stream<sup>54</sup>. Instead, the cornea relies upon atmospheric oxygen that it absorbs<sup>54</sup>. If a contact lens material did not have sufficient oxygen permeability, the normal metabolic processes which occur in the eye would be impaired. Lack of oxygen to the cornea can lead to corneal oedema, a condition whereby the cornea retains fluid and swells<sup>55</sup>. The fact that hydrogels are permeable to oxygen, coupled with the ability to manipulate and measure this permeability allows for the creation of hydrogels that are suitable for use as tissue replacements for the cornea, while ensuring the delivery of oxygen from the atmosphere.

### **1.8.2 Smart Hydrogels**

Smart hydrogels are defined as “synthetic materials that have multiple functions in addition to inherent structural properties”<sup>56</sup>. A hydrogel is a 3-D network which swells in aqueous environments, whilst maintaining structural integrity<sup>41</sup>. The normal response of a hydrogel is to swell in an aqueous environment, a smart hydrogel however can respond to a stimulus by expanding, shrinking, bending, or the degradation of its structure. Also smart hydrogels respond not only to aqueous environments (i.e. water) but also may respond to temperature, pH, ionic strength, salt type, electric field, external stress, solvent, light, specific ligand molecules, enzymes or any combination of these<sup>41</sup>.

Due to its nature a hydrogel will often have more than one response to a stimulus. For example, if a hydrogel was designed to change colour in the

presence of a stimulus which is dissolved in water, the hydrogel would change colour, but also expand as it becomes saturated with water<sup>41</sup>.

The functional groups that are present within a hydrogel network will determine the type of response, and which stimuli the hydrogel will respond to<sup>41</sup>. One of the most common responses of a hydrogel is a volume change<sup>41</sup>. This is usually measured as a swell ratio of either the weight or volume of the swollen hydrogel to those of the dried hydrogel<sup>41</sup>. These two measurements are referred to respectively as either the weight or volume degree of swelling<sup>58</sup>.

It is relevant to consider the network structure of the hydrogel in a little more detail. The conventional model is that of a non-crystalline 3D network of polymer chains linked together, as shown in figure 19<sup>57</sup>.



**Figure 19.** A representation of a 3D hydrogel network. The red, green and black lines represent polymer chains. Blue lines represent cross-links between the polymer chains<sup>57</sup>.

Within this non-crystalline network, the cross-links provide the retractive forces that hold the polymer chains together, but do not prevent rotation around the bonds of the monomer units. They do not impede the hydration but may restrict it, thus enabling the functional groups to interact with the stimulus or stimuli present in the aqueous medium that hydrates the network<sup>55</sup>. Due to the rotational freedom of the bonds in the polymer chains, when the matrix is hydrated by an aqueous environment, the tangled structure of the hydrogel can begin to untangle in order to accommodate the aqueous environment within the matrix. The level of cross-linking within the network will determine the flexibility

of the network and its ability to swell (untangle)<sup>54</sup>. Higher levels of cross-linking within the network limit the ability of the bonds in the polymer chains to rotate, and stretch apart reducing its ability to swell, as illustrated in figure 20.



**Figure 20.** Cartoon schematics of the polymer chains in (A) a high cross-link density hydrogel unhydrated, (B) a high cross-link density hydrogel hydrated, (C) a lower cross-link density hydrogel unhydrated, and (D) a lower cross-link density hydrogel hydrated.

Figure 20 demonstrates how the level of cross-link density in a hydrogel affects how the hydrogel expands, and therefore the amount of water that can become imbibed into the hydrogel network. A higher cross-link density reduces the amount of rotation that can occur in the polymer chains within the network. This means that the tangled network of polymer chains has a limited ability to untangle, creating a smaller volume within the hydrogel to accommodate water within the network<sup>42</sup>. Conversely, the hydrogel with the lower cross-link density allows for a greater amount of rotation of the polymer chains within the network,

allowing the chains to untangle to a greater extent. This creates a larger volume within the hydrogel, accommodating more water within the hydrogel, which also means that it has a larger EWC<sup>42</sup>.

### **1.9 Hydrogel Preparation - principles and practicalities**

There are many methods for preparing a hydrogel. The most common route is to polymerise monomers with cross-linking agents, forming covalently linked hydrogels<sup>56</sup>. This method enables the synthesis of a hydrogel membrane which, through careful consideration of the ratio of the monomers included, exhibits the desired properties.

This way, the hydrogel can be designed to respond to a particular stimulus, and the level of response that the hydrogel exhibits is controlled by the percentage of the functional groups present<sup>56</sup>. Incorporation of an inert monomer (a monomer with an unsaturated C=C bond, and no other functional group such as a hydroxyl group) can be used to control the percentage of functional groups. The inert monomer is used in combination with the other monomers in forming the polymer backbone. Free radical polymerisation will be discussed in more detail in the next sections.

Free radical polymerisation is one of the most common routes of polymerisation used in the formation of hydrogels<sup>56</sup>. This method of polymerisation allows for the incorporation of various functional groups into the polymer backbone<sup>56</sup>. The incorporation of an inert monomer allows for the control of the percentage of functional groups present in the hydrogel. This approach determines the type and level of response the resulting hydrogel will have<sup>56</sup>.

Free radical reactions occur in three steps, namely initiation, propagation and termination.

### 1.9.1 Free radical polymerisation

The first step of a free radical polymerisation is initiation. For the initiation of a free radical polymerisation, an initiator molecule is required. Initiator molecules generally have a weak bond with low bond dissociation energy<sup>59</sup>. When the bond dissociation energy is reached, the bond breaks down homolytically to form two “half” molecules, both with an unpaired electron<sup>59</sup>. The unpaired electron on a free radical molecule is very reactive<sup>59</sup>. Radical molecules attack molecules with an unsaturated carbon to carbon double bond, where there are electrons to form a new bond with<sup>59</sup>. Once the free radical molecule has bonded, with the molecule with an unsaturated carbon to carbon double bond, the unpaired electron is transferred onto the attacked molecule<sup>59</sup>. The dissociation energy requirements of an initiator differ from molecule to molecule<sup>59</sup>. Different free radical initiators have different dissociation energies, therefore requiring different amounts and different sources of energy<sup>59</sup>. Below are two examples of initiator molecules homolytically breaking down to form free radical molecules.

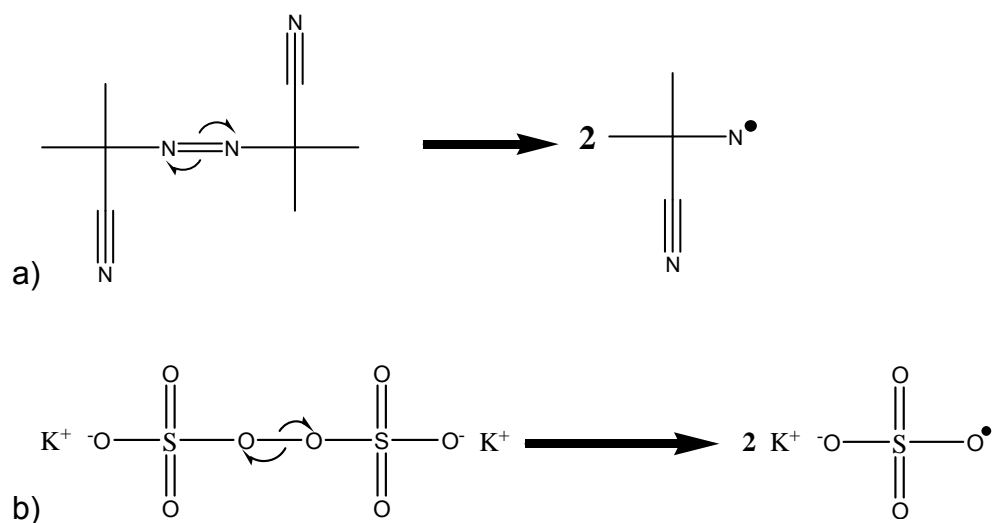


**Figure 21.** Initiation by a) AIBN, and b) potassium persulfate, using heat as the energy source to reach the required dissociation energy.

Once the initiator molecule has homolytically broken down, the next step in a free radical polymerisation is the propagation<sup>59</sup>. During the propagation step, the free radical molecule attacks an unsaturated double bond<sup>59</sup>, typically a C=C bond, and forms a new bond with the molecule, as shown in figure 22.

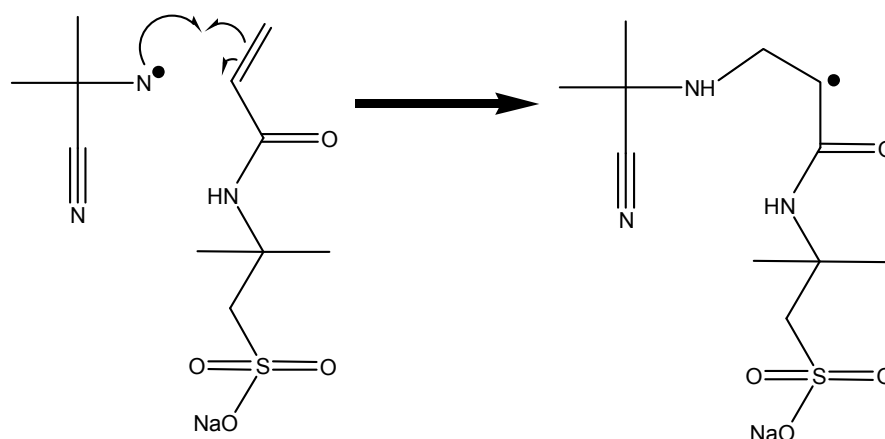


**Figure 22.** Free radical propagation step with AIBN (initiator) and NaAMPs (monomer).

In this example the C=C double bond in the sodium salt of 2-acrylamido-2-methylpropane sulfonic acid (NaAMPs) donates an electron to form a new covalent bond with the AIBN radical. The other electron forms a new radical on the other carbon of the C=C double bond<sup>59</sup>. This new radical in turn reacts with another unsaturated C=C bond to obtain the electron it needs to make a bond. The reaction results in the formation of a growing polymer chain<sup>59</sup>. Propagation of the growing polymer chain continues until two radical centres react with each other, resulting in no new radical centres being formed<sup>59</sup>. This is called termination, which will be discussed next. Alternatively, propagation will cease, when there is no more monomer left to react<sup>60</sup>. If more monomer with unsaturated bonds were added into the system, propagation would resume until either the monomer is used up or termination occurs<sup>60</sup>.

The termination of a free radical polymerisation refers to the radical centres in the reaction, in the ideal case reacting together, so that no new radical centre is formed<sup>60</sup>. However, there are several ways in which free radical polymerisation can terminate. Theoretically, the propagation stage of a free radical reaction

could continue indefinitely if there was an unlimited supply of monomer with an unsaturated double bond. First is combination, when two active chain ends both react to pair their unpaired electron to form a new bond; this would eliminate the two radical centres, without creating a new one<sup>60</sup>, as shown in figure 23a. The second way is similar to the first in that two radical centres react together to eliminate each other, without forming a new radical centre<sup>60</sup>. Instead of two active chain ends meeting, this time an active chain end and an initiator radical react to pair their unpaired electrons in order to form a new covalent bond<sup>60</sup>, as shown in figure 23b. The third way that termination occurs is through the transfer of the active centre to another molecule, like an initiator molecule. Again, the radical centres are eliminated by the unpaired electron that reacts with another unpaired electron in order to form a new covalent bond<sup>60</sup>. In figure 23c two initiator radicals react to form a new bond, reforming the initiator molecule.

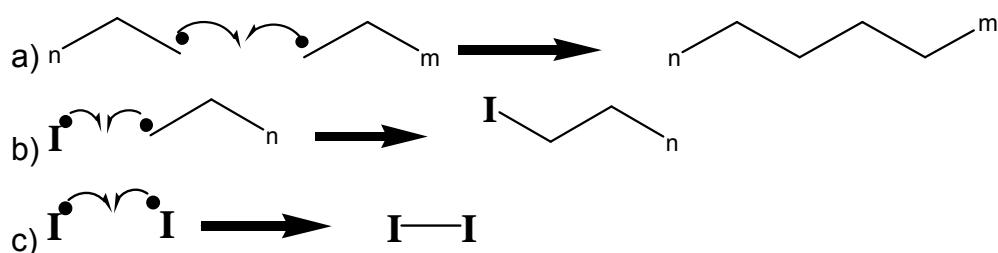


**Figure 23.** Methods of termination in free radical polymerisation. a) Combination, two active chain ends interact. b) An active chain end and initiator radical interact. c) Two radical initiator molecules reacting to reform the initiator molecule.

The most common route of termination is the first route where the two radical centres on a chain end react to form a new covalent bond. Another route to termination of the propagation of a free radical reaction is disproportionation. Similar to combination, disproportionation of free radical reaction involves two active chain ends but instead of reacting to form a new covalent bond, the one active chain abstracts a hydrogen molecule from the other active chain end<sup>60</sup>, as shown in figure 24.

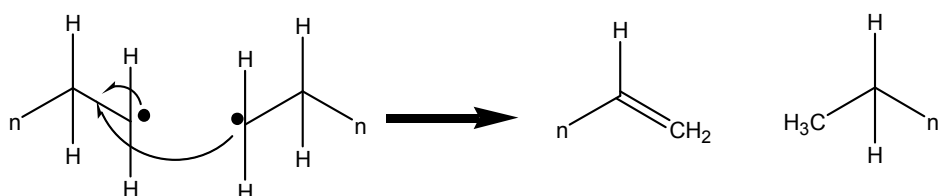


**Figure 24.** Disproportionation of two active chain ends during termination.

In free radical reactions inhibition of the reaction may occur. Inhibition occurs when something competes with the free radical centre, stopping the free radical from reacting with the monomer. As AIBN has been used as the initiator for the free radical polymerisations carried out in this project, the discussion that follows will focus on the inhibition of AIBN.

When utilising AIBN as the initiator for the reaction in free radical polymerisations, it is normal to carry the reaction out under an inert atmosphere, usually nitrogen. This is done to remove all the oxygen that could be present in the system as oxygen is an inhibitor of AIBN.

Oxygen is one constituent of air and as such, in order to remove the oxygen from the reaction vessel, it is required to actually remove all air. Oxygen is often used as the term to refer to the molecule dioxygen ( $O_2$ ). Dioxygen is a stable radical molecule, due to the parallel spins of the electrons. Oxygen in its ground state is an unreactive spin unpaired diradical<sup>61</sup>. However, if the energy barrier between the spins can be overcome with high temperature, a more reactive unpaired spin diradical oxygen becomes available, or the extremely reactive spin-unpaired diradical can be achieved. Heat can be provided by the exothermic reaction that occurs with the formation of free radicals, such as in the formation of radical centres from AIBN. The extremely reactive spin unpaired oxygen radical can then react with the highly reactive AIBN radical or propagating centre, to terminate any further propagation stopping the reaction<sup>61</sup>, as seen in figure 25.



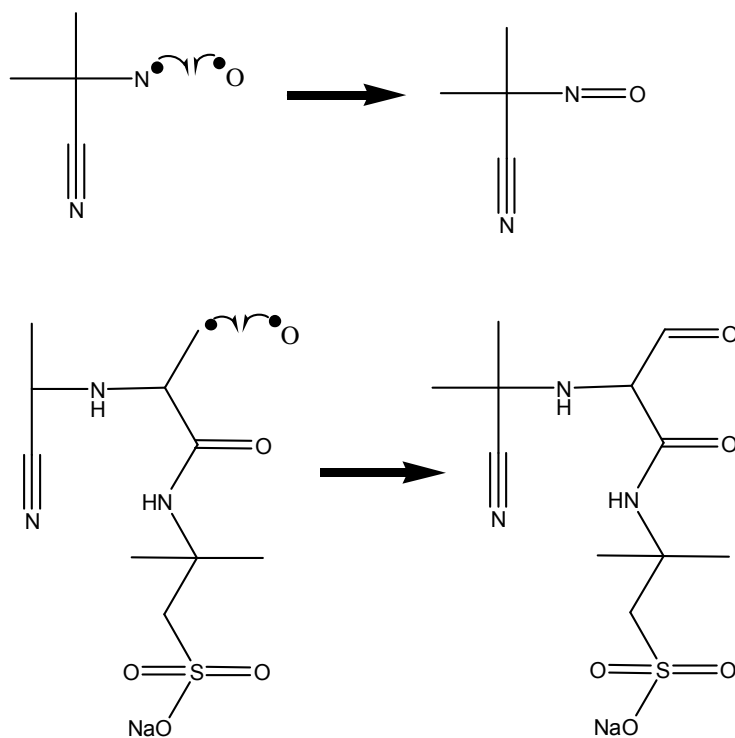


**Figure 25.** The effect of single oxygen radicals on polymerisation.

### 1.10 Example of the uses of smart hydrogels

In the following sections, several uses of hydrogels will be discussed; particularly pH-, temperature- and bio-sensitive hydrogels, the use of hydrogels for drug delivery and the creation of prosthetic biomaterials, as well as the use of hydrogels in extraction and separation.

#### 1.10.1 Biosensitive hydrogels

Biosensitive hydrogel is a term used to describe a smart hydrogel responsive to molecules found in an environment such as the body. Biosensitive hydrogels have received great interest as they find use in areas such as drug delivery<sup>41</sup>, tissue replacement<sup>41</sup>, and as an indicator of the presence of certain molecules that are important in the functioning of the body<sup>41</sup>. One example is the ability of a hydrogel to detect the levels of glucose in the body<sup>41</sup>. Glucose is an important molecule for the functioning of the body and the potential application of glucose

detection is the development of a self-regulating insulin delivery system for patients with diabetes<sup>41</sup>. This glucose sensitive hydrogel was prepared by taking a quaternary copolymer, which contained a phenylboronic acid group<sup>62</sup>. The boronate and the PVAs hydroxyl groups interact to form a complex gel. Hydroxyl groups on the PVA can be displaced by free glucose, which then interact with the phenylboronic acid group and the hydrogel becomes a sol<sup>62</sup>. This is just one of many examples of a biosensitive hydrogel, as there are many biomolecule-specific interaction systems found in nature. Antigen-antibody, ligand-receptor and avidinbiotin interactions are a few additional examples of systems that can be used to make hydrogels sensitive to specific biomolecules<sup>63</sup>.

### ***1.10.2 pH-sensitive hydrogels***

The presence of weak acid or base functional groups in the polymer backbone of a hydrogel causes pH sensitivity in hydrogels<sup>41</sup>. Styrene sulfonate is one of the commonly used weak acids, and 2-(dimethylamino)ethyl methacrylate is one of the more commonly used weak bases<sup>41</sup>. The range of sensitivity where the volume of a pH-responsive hydrogel increases or decreases considerably will depend upon the types of weak acids or bases used<sup>41</sup>. If the functionality of the hydrogel is a weak acid then the volume of the hydrogel will increase as the pH of the medium increases, and the reverse is observed if the functionality is that of a weak base<sup>41</sup>.

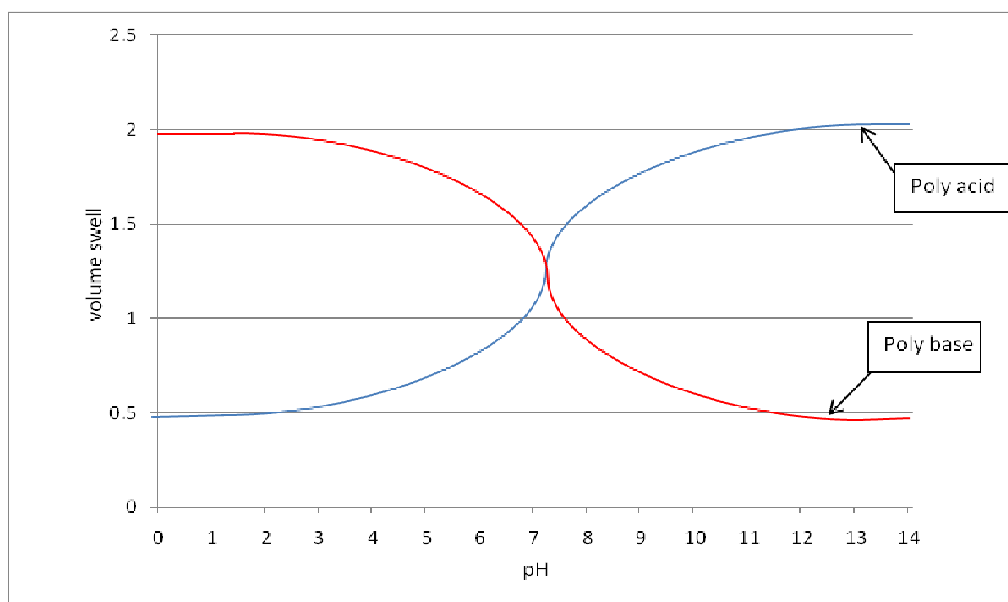


**Figure 26.** A graph of swell vs pH to exemplify the relationship between swell and pH for an imaginary polyacid and polybase.

If a hydrogel composition for example included charged acid or base groups then there is a specific pH value at which there will be maximum swelling of the hydrogel. The maximum swelling is about the midpoint of the helix-to-coil transition of the polypeptide backbone<sup>65</sup>, which makes hydrogels of this nature very useful when a system is required to respond at a specific pH.

Polyelectrolyte hydrogels swell due to the charge repulsion among the charged pendent groups. If the salt concentration (ionic strength) is increased then the swelling at a given pH is reduced<sup>64</sup>. Polyampholyte hydrogels contain both weak acid and weak base functionality<sup>66</sup>. This type of hydrogel is synthesized by copolymerising both anionic and cationic monomers. Simple polyelectrolyte hydrogels differ in that these ampholyte hydrogels have increasing swelling with increasing ionic strengths, because the electrostatic attraction between the different charges is reduced<sup>41</sup>.

Simple polyelectrolyte hydrogels grafted with neutral polymers are also pH responsive. At low pH, polymers which contain weak acid monomers such as poly(methacrylic acid) will form a strong complex with neutral polymers like poly ethylene glycol (PEG) via hydrogen bonding. When the pH of the medium is low

then these types of hydrogel contract, but the hydrogen bonding breaks down as the acid is ionised, which in turn leads to large volume changes over small pH changes<sup>41</sup>.

### **1.10.3 Temperature-sensitive hydrogels**

The characteristic change seen in a thermo-responsive (or temperature, sensitive) hydrogel is a decrease in the volume of the hydrogel when it is heated above a specific temperature<sup>67</sup>. This volume decrease is due to the monomers used in the hydrogel, which exhibit the lower critical solution temperature (LCST) phenomenon<sup>68</sup>. *N*-substituted acrylamide derivatives are the most common LCST monomers because of the ease of their preparation or obtainability<sup>41</sup>. The main interactions are hydrophobic due to the breaking of hydrogen bonds, which is enhanced by temperature increase due to the energy release during the breaking of hydrogen bonds of water molecules surrounding hydrophobic moieties<sup>69</sup>. Temperature-sensitive hydrogels made from LCST monomers volume decreases at a temperature that is higher than that of its monomers, and swells again at a temperature below that of the LCST. The re-association of the excluded water with the hydrogel's matrix when the temperature is reversed, is the cause of the hydrogels thermoreversibility<sup>68</sup>.

### **1.10.4 Drug Delivery**

Smart hydrogels have a wide range of possible applications in various areas. One such example is that of drug delivery<sup>41</sup>. Advances in technology have made it possible to deliver drugs into the body at a constant rate for long periods of time, which is useful in the treatment of certain injuries and many diseases, but not all that require constant medication<sup>41</sup>. In some diseases, like diabetes, the delivery of drugs is required at varying intervals; this is where hydrogels can be utilised to control the delivery of insulin to the body<sup>41</sup>.

In general, most hydrogels that are glucose-sensitive use pH-sensitive polymers like poly [2-(diethylamino)ethyl methacrylate] (PDEAEMA)<sup>70,71</sup>.

Glucose oxidase is often immobilised in a pH-sensitive hydrogel where it converts glucose into gluconic acid, lowering the pH of the hydrogel, whilst protonating the amino moieties in the PDEAEMA hydrogel<sup>41</sup>. These moieties, which are now charged, repel each other, causing the hydrogel membrane to swell, which causes insulin to be released from the hydrogel membrane<sup>41</sup>. In addition, glucose sensitive sol-gel phase reversible hydrogels also have the ability to control the pulsate release of insulin<sup>62</sup>.

### **1.10.5 Prosthetic Biomaterials**

The transformation of electrochemical stimuli into mechanical work is best exemplified by human muscle tissue<sup>41</sup>. Demand from advanced robotics for electrically driven muscle-like actuators made from hydrogels has motivated the study of polymeric gels that can reversibly contract and expand due to physicochemical stimuli<sup>72</sup>. This idea of smart materials which can mimic the function of organs that can release secretions or contract due to natural stimuli such as those found in the body (like pH, electrochemical, temperature, or electric field) could lead to the future creation of smart hydrogels being used in medical implants, prosthetic muscles or organs<sup>41</sup>.

### **1.10.6 Extraction and Separation**

Due to the ability of hydrogels to reversibly swell and shrink with minor changes to their surroundings, they are useful for purification devices<sup>73</sup>. Smart hydrogels, thermo and pH in particular, are ideal for concentrating dilute aqueous solutions of macromolecular solutes, including proteins and enzymes, without affecting the function of the enzymes<sup>73</sup>. Macromolecules are extracted by the smart hydrogel absorbing the water, excluding the macromolecules from the hydrogel network by size and net charge<sup>75</sup>. Altering the temperature or pH of the hydrogel causes the release of the absorbed water from the hydrogel, allowing the same hydrogel to be recycled again and again<sup>41</sup>. Reactions of immobilised enzymes and substrates can be controlled by smart hydrogels which control the diffusion of the substrate by swelling changes<sup>41</sup>. In one example, Park and

Hoffman immobilised *Arthrobacter simplex* in a thermally reversible hydrogel, and investigated temperature cycling on the conversion of steroid<sup>76</sup>. Steroid conversion was found to be higher in hydrogels of higher hydrophobicity due to the high partitioning of water-insoluble steroids into the hydrophobic areas of the hydrogel, and reduced product inhibition within the hydrophobic gel matrices<sup>76</sup>.

### **1.10.7 Applications of Smart Hydrogels**

The fact that smart hydrogels can be designed to suit a purpose lends them many possible applications within the biomaterial area. Each smart hydrogel can be tailored to each application, not only by its function, but also by its sensitivity to the particular target molecule that it is to interact with. This sensitivity can be achieved by altering the amount of functional groups present in the hydrogel and by using inert monomers to replace monomers with functional groups sensitive to the target molecule.

### **1.11 Considerations for the applications of smart hydrogels**

The required application of smart hydrogels will determine its particular functionality. However, there are several factors regarding the application that will determine the final decision to use the smart hydrogel with or without modification, or not at all.

One of the first considerations for the application of a smart hydrogel will be the required response time. For example, artificial muscles and microswitches require a fast response time to carry out the function properly<sup>41</sup>. Regarding smart hydrogels used for drug delivery, fast and slow response times may be required dependent upon the rate at which the drug needs to be released into the site<sup>41</sup>. For a hydrogel that is to be used as artificial muscle, or a micro switch, a volume change of 50% in a few seconds is required<sup>41</sup>. Another factor that also affects the response time of a hydrogel is the size, a large hydrogel

requires more water to swell and therefore will take longer to reach its EWC than a smaller hydrogel<sup>41</sup>.

The response time of a hydrogel can be manipulated to the desired conditions by controlling the ratio of the monomers used, and the percentage of the functional groups in the hydrogel<sup>77</sup>. For example, if a hydrogel that responds to moisture were required to be less sensitive, the hydrophilic monomers in the hydrogel would need to be reduced, and the hydrophobic monomers increased.

In the case of a membrane for a sensor application, the response time is very important. If there is a need to record real time environmental changes, then a rapid response time is required. The response time of a hydrogel is measured using swelling ratios, which are recorded when the hydrogel has reached equilibrium<sup>41</sup>. Not only is the response time to the stimulus important, but also the time it takes for the hydrogel to return to its original state when recording real time environmental changes<sup>78,79</sup>. This is because the sensor system will give a reading that is in between the actual level of stimulus and what “was” present due to a too slow response time.

There are many factors affecting the response times of a hydrogel. However, the factor that ultimately affects the response time, i.e. the time it takes for the hydrogel to reach equilibrium water content or the time for the hydrogel to respond to a change in the environment, depends upon the structure of the hydrogel and the structure and nature of the environment the hydrogel is situated, as well as the size of the hydrogel<sup>80</sup>.

When looking at the environment where the hydrogel is situated is the temperature is the first factor which must be considered. The temperature of the aqueous environment controls the rate at which molecules move within that environment, and therefore into the hydrogel<sup>81</sup>. Temperature also affects the hydrogel's ability to expand and allow the entry of molecules within the structure, due to the energy required for the bonds within the polymer chains to rotate and untangle, allowing the hydrogel to expand<sup>81</sup>. At lower temperatures,

it takes longer for enough energy to be obtained that is required for the bonds to rotate.

Diffusion describes the movement of solutes from an area of high concentration to that of an area of lower concentration<sup>82</sup>. The path that the molecules take in the solvent as they diffuse is a random pattern governed only by the speed at which the molecules are moving, and the fact that they will inevitably crash into each other, prompting each particle in the collision to take a new course<sup>82</sup>. In a solution this concentration is defined as osmoles per litre, or osmolarity<sup>83</sup>. Where a membrane such as a hydrogel is involved, this membrane becomes a new variable in the process of diffusion. This process is now defined as osmosis, the movement of water solutes through a selectively permeable membrane from a high concentration to a low concentration<sup>83</sup>. A difference in concentrations is referred to as the concentration gradient<sup>83</sup>. The rate at which molecules move in and out of the hydrogel membrane is controlled by the rate at which the solvent molecules move<sup>84</sup>. As mentioned before, this is directly to the temperature; the higher the temperature the faster the molecules move<sup>84</sup>. In this case it will always be considered that there is no solute present in the membrane. If the concentration of the solute in the solvent outside the membrane is high, then the rate of diffusion is quicker, as there are more solute molecules moving around and bumping into each other<sup>84</sup>. This increases the probability that the solute molecules will spread out quicker than if there was a lower concentration of solute molecules in the solvent. Resulting in the solute molecules reaching the hydrogel membrane quicker in a solution of higher concentration of solute. The membrane of the hydrogel is a selective membrane, as it is a macroporous membrane<sup>80</sup>. Since the pore size of the membrane is controlled by the length and the number of cross-links within the network<sup>80</sup>, if the pores are not particularly large then large molecules (such as proteins) cannot enter the network. Conversely, small molecules, such as dissolved metal ions, can pass easily through the small pores of the membrane.

By its nature, a hydrogel is weak and susceptible to structural degradation, making it suitable for short-term applications only<sup>41</sup>. However, there may be applications where the soft and flexible nature of the hydrogel is needed if



delicate materials are not to be damaged by the hydrogel<sup>85</sup>, such as a healing wound. In order to be suitable for a long term application, a hydrogel would need to have more structural resilience to maintain its expansion/contraction properties.

It becomes clear that by design, the properties of a hydrogel can be manipulated to suit a purpose. Nevertheless, the design of a hydrogel is not as straight forward as just adding a monomer to exhibit a desired property without affecting any of the other hydrogel properties. For example, to improve the structural integrity of a hydrogel, the cross-link density needs to be increased. However, increasing the level of cross-linking in a hydrogel past a certain level increases the opaqueness of the hydrogel<sup>86</sup>. Therefore to design a hydrogel with the required properties for a particular application, careful consideration must be given to which monomers, and the quantity of the monomers used.

With the use of hydrogels in the body, the issue of biocompatibility arises. The hydrogel used should not affect the body site adversely, while at the same time preserving its functionality<sup>41</sup>.

Cost is also another important factor. If hydrogels are not cost-effective and there is a cheaper alternative available, this would hinder the future development of smart hydrogels<sup>41</sup>.

### **1.12 Scope & object of present work – analytes and applications**

The work discussed in this thesis is concerned with the combination of fibre optic sensor technology with smart hydrogels to produce a sensor system for analytes in aqueous environments. Some possible applications of such a system will be discussed in this section. For example, there is room for improvement of the diagnosis techniques at the clinical point of care<sup>87</sup>. One such case is in the field of optometry. Optometric practitioners rely upon visible symptoms that patients display for diagnosis. These symptoms are normally the result of tear abnormalities. One such abnormality is the increased levels of

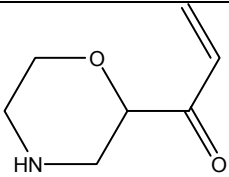
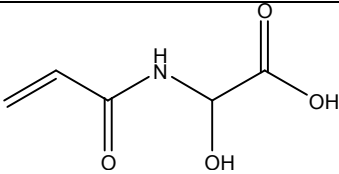
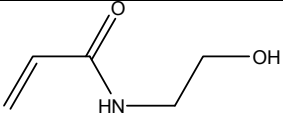
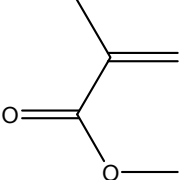
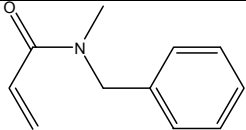
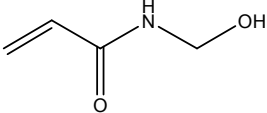
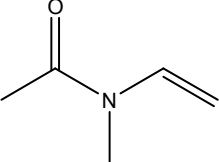
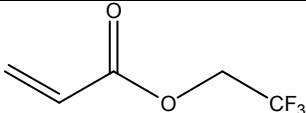
potassium, one of the causes of dry eye<sup>88</sup>. Such a method of diagnosis is not always reliable, as it relies upon experience of the practitioner and the interpretation of written symptoms. Sensor technology can be used as a tool to assist with routine point of care diagnosis of conditions that arise from tear abnormalities. Other possible applications of the proposed sensor system can include a wide variety of cases where an aqueous environment is present. An example is in the quality control in processes where a liquid feed is used, such as refuelling an aircraft with jet fuel, where water levels in the fuel<sup>89</sup> or aluminium levels in the water need to be closely monitored<sup>90</sup>. In these environments a fibre optic sensor system could provide real time information of levels of the target analyte present. The technology could even be used for remote sensing, such as water feeds from remote reservoir locations.

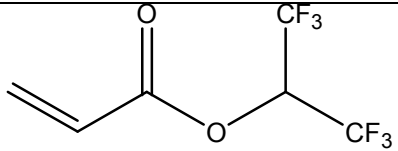
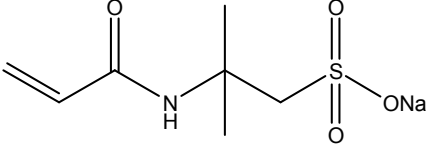
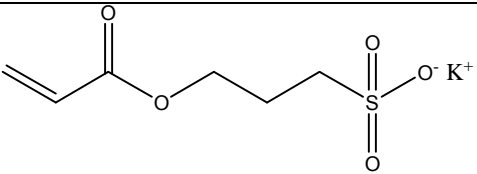
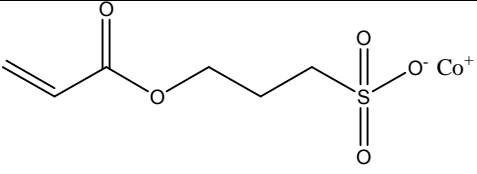
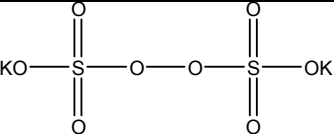
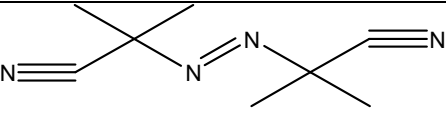
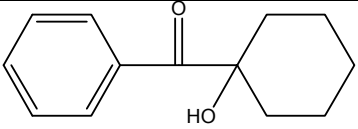
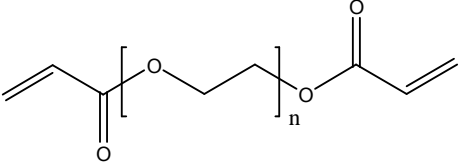
## **Chapter 2. Materials and Equipment**

## 2.1 Materials – monomers and sensing agents

All the reagents used in this work were used as supplied without further purification.

**Table 1.** Monomers, initiators and cross-linking agents used.

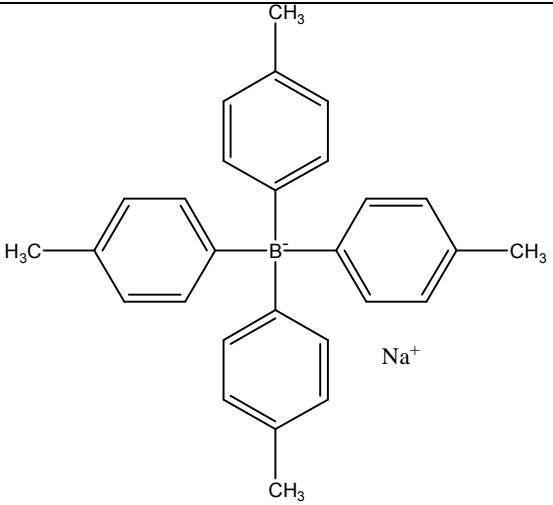
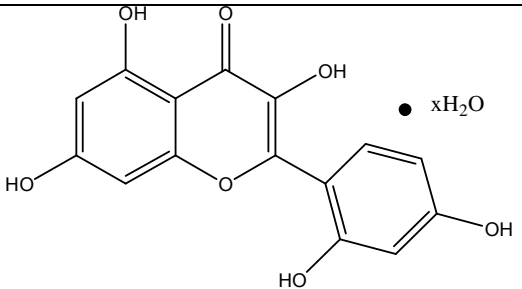
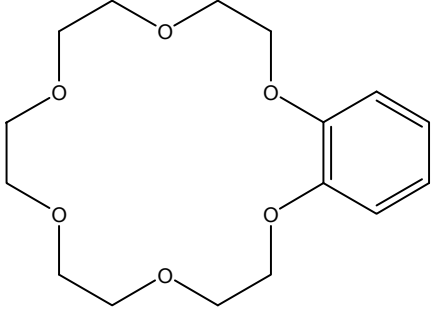
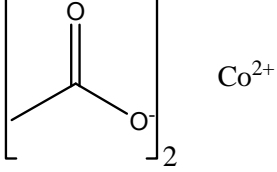
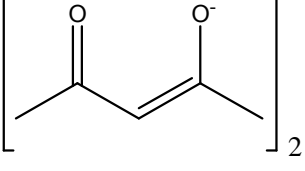
Material	Structure	Supplier	RI
acryloyl morpholine (ACMO)		KOHJIN Co Ltd Tokyo Japan	1.4723*
2- acrylamidoglycolic acid monohydrate – (AGA)		Sigma- Aldrich	N/A
2-hydroxyethyl acrylamide (HEA)		Aldrich	1.505*
methyl methacrylate – (MMA)		Aldrich	1.414*
<i>N</i> -benzyl – <i>N</i> - methylacrylamide – (NBNMA)		Aldrich	1.585 <sup>a</sup>
<i>N</i> -methylol acrylamide (NMA)		Sigma	1.413*
<i>N</i> -vinyl – <i>N</i> - methyl acetamide – (NVNMA)		Sigma	1.484*
2,2,2 – trifluoro ethyl acrylate		Sigma	1.35*

1,1,1,3,3,3, hexafluoroisopropyl acrylate		Aldrich	1.319*
2-Acrylamido-2- methylpropane sulfonic acid -  (NaAMPs)		Sigma	1.4220*
3-sulphopropyl ester acrylate potassium salt (SPA)		Sigma	N/A
3-sulphopropyl ester acrylate cobalt salt (CoSPA)		Synthesized in the laboratory	N/A
potassium persulfate		Sigma	N/A
2,2'-azobis(2- methylpropionitrile) (AIBN)		Sigma	N/A
Irgacure 184		Ciba	N/A
Ebacryl 11- Poly (ethylene glycol) diacrylate  M <sub>n</sub> 575		First Water	1.467*

\*Value supplied by manufacturer

<sup>a</sup>RI of a homopolymer of this monomer reported in reference 98.

**Table 2.** List of chemotropic agents used.

Chemotropic agent	Structure	Supplier
sodium tetra phenyl borate		Sigma
Morin		Sigma
cobalt (II) chloride	CoCl <sub>2</sub>	BDH laboratories
Benzo-18-crown-6 (B-18-C-6)		Sigma
cobalt (II) acetate		Sigma
cobalt (II) acetyl acetonate		Sigma

## 2.2 Equipment

FT-IR Spectrometer – Thermo Scientific Nicolet 380 FT-IR, Smart Orbit Platform configuration, with the diamond 30,000-200cm<sup>-1</sup> plate.

Light source and detection unit – EV5000 light source and detection unit.

Software – EvanesCo Fibre Detection Unit software.

Glass fibre optic cable – (product code BFL48-400) Multimode Fibre, 0.48 NA, Low OH, 400 µm Core supplied by Thor laboratories.

Glass fibre optic cable cleaving tool – (product code S90W) Diamond Wedge Scribe, 90°. Supplied by Thor laboratories.

PMMA fibre optic cable – (product code SH4001) Super Eska™ Polyethylene Jacketed Optical fibre Cord supplied by LasIRvis.

Fibre end polishing disc – (product code D50-SMA) SMA Connector Polishing Disc.

Fibre end polishing paper – (product code LFG03P) 13" x 9" Aluminium Oxide Lapping (Polishing) Sheet, 0.3 µm, and (product code LFG5P) 13" x 9" Silicon Carbide Lapping (Polishing) Sheet, 5 µm (10 Sheets).

End stop splitter/coupler 50:50 supplied by EvanesCo (EV).

### 2.3 The sensing system: hardware and software



**Figure 27.** The EV5000 interrogation unit connected to a laptop with an end stop probe connected via a splitter/coupler.

Upon setting up the sensor rig, a calibration “dark” reading is taken. This is done by screwing the cover cap onto the signal return port, where the intensity of the returning light is measured. Using the EV software, a sample reading of 2-3 seconds is taken to obtain the signal loss of a light free environment. This is done to establish a reading of zero light and only needs to be done once at the beginning of testing on a given day.

The EV software for the sensor system measures the signal loss from the fibre optic cable as it travels from the light source along the fibre, which is connected to a photo diode in the EV5000 interrogation unit. Signal loss is measured over time intervals that can be set using the EV software. Time intervals can be set from a tenth of a second per measurement and up to several hours between measurements. For the purpose of the project at hand, the time interval was set to one measurement per second. Due to the nature of the software which measures signal loss over time, it was necessary to take a note of the times that a sample was introduced and removed from the fibre optic cable probe attached to the sensor rig.



Once the samples were prepared and the fibre optic cable probe attached to the system – and after a calibration reading was taken – the system was set to record. In all instances, the sensor rig was left recording the signal loss of the probe in air, before and after each sample was introduced to the probe. This was done so that later when data manipulation was carried out, there is a reference reading before and after each sample. Each sample was introduced to the probe for the same length of time, and the probe was left in air for the same length of time between each sample. For example, if the set of samples are to be in contact with the probe for five minutes, then between each sample the probe is left recording in air for five minutes.

Data collected by the interrogation system are in turn recorded by the EV software and exported to an Excel spreadsheet for further analysis. The exported data and the calibration readings are copied into a separate Excel spreadsheet provided by EvanesCo, the company that provided the hardware and the software for the research. A formula in the spreadsheet calculates the signal loss recorded at each measurement in decibels (dB), and plots the results into a graph of signal loss vs time.

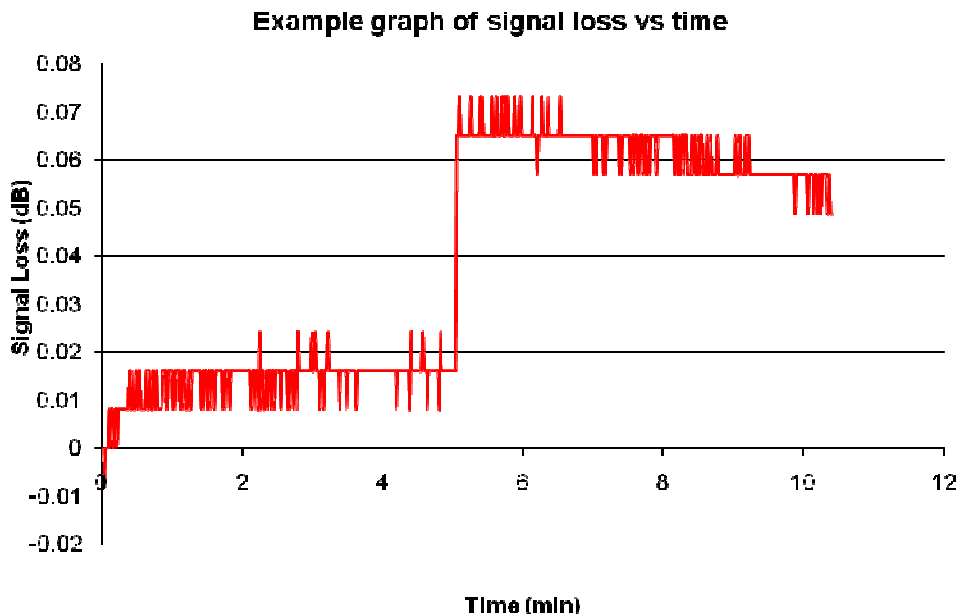


**Figure 28.** An example graph of the data plotted as signal loss vs time for a period of ten minutes.

As the data are collected in an Excel spreadsheet, it can be manipulated easily by the user to different formats. One such example would be to create a table of average signal loss recorded for a particular sample.

## **Chapter 3. Polymers and Coatings: The Development of Experimental Methodologies**

### **3.1 Introduction**

In the main introduction of this work (chapter 1) the principles of synthesis and cross linking of hydrogels were discussed. Here in this section, the focus is given to the reaction specifics, fibre optic probe fabrication, and the coating of the hydrogel membranes onto the fibre optic probes.

### **3.2 Preparation and synthesis of the hydrogel membrane**

The preparation and synthesis of the hydrogel coatings for fibre optic probes comprises three parts. 1. Synthesis of a linear macromer via free radical polymerisation. 2. Functionalisation of the linear macromer, ready for cross-linking via condensation reactions. 3. Cross-linking the functionalised macromer and the chemotropic agent to form a smart hydrogel coating on the fibre optic probes. The above steps are discussed in more detail in the following sections.

#### ***3.2.1 Polymerisation rig for the synthesis of a linear macromer***

Free radical polymerisation for the production of the linear polymer was carried out in solution, under agitation, heat, and an inert atmosphere, in order to prevent an inhibition of the free radical initiator. The reaction rig used is shown in figure 29.

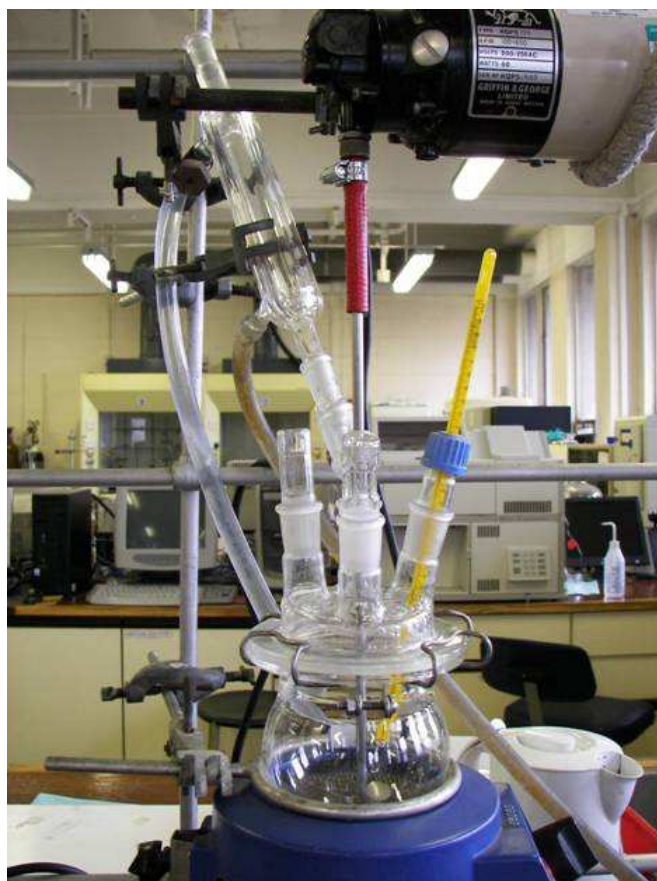


**Figure 29.** Polymerisation rig, used for the synthesis of the linear polymer.

In this setup, a reaction vessel with a sealable lid that has 5 side arms was used to allow for the mechanical agitation of the solution, an inflow of nitrogen, a thermometer for temperature control, and a condenser to be fitted. A condenser was used to prevent the solution from evaporating, and to allow for the excess nitrogen to escape the system. The fifth side arm is used for the addition of the initiator solution and other solutions as needed. Sealing the polymerisation vessel is important to ensure that no air gets into the system. The whole rig is clamped to an upright stand, allowing for the isomantle that is used to heat the system to be lowered easily if needed, without having to move the reaction rig. After the polymerisation was completed the reaction vessel can be dismantled easily, to allow the easy removal of the solution containing the linear polymer from the reaction vessel, ready for the next step, which is the precipitation of the polymer.

### 3.2.2 Free radical polymerisation, the synthesis of the macromer

Using free radical polymerisation reaction, the following macromers were synthesized according to the compositions, the solvent system and the initiator, as described in table 3.

**Table 3.** Table of monomers, initiators and solvent system used in the synthesis of the macromers for the creation of hydrogels.

<i>Macromer</i> <b>Monomer</b>	<i>DH2</i>	<i>DH4</i>	<i>DH6</i>	<i>DH7</i>	<i>DH8</i>	<i>DH9</i>
NBNMA	38.1ml	0.8ml				
NVNMA	20.7ml	0.4ml	5.6g	5.6g	10.94g	7.88g
MMA 48%sol	38.1ml					
2,2,2, Trifluoro-ethylacrylate					6.25g	
Hexa-Isopropyl-acrylate		0.8ml				
HEA 45% sol			2.25g	2.25g	1.5g	4.5g
SPA			4.5g		6.25g	1.13g
ACMO			5.6g	5.6g		7.88g
AGA			4.5g			1.13g
CoSPA				4.5g		
NaAMPs 50% sol				4.5g		
<b>Initiator</b>						
AIBN	0.88g	0.017g				
K <sub>2</sub> S <sub>2</sub> O <sub>8</sub>			0.4g	0.4g	0.4g	0.4g
<b>Solvent system</b>						
Toluene : MeOH (1:1)	103.5ml					
MeOH		2ml				
MeCN : H <sub>2</sub> O (4:6)			100ml	100ml		100ml
MeOH : Toluene (3:1)					100ml	

The monomers were weighed and put into the polymerisation rig, to which 95% of the solvent system was added. To dissolve the monomers, the stirring propeller and the isomantle were turned on at 60°C for 30 minutes. Nitrogen was fed into the system to create an inert atmosphere. The other 5% of the solvent system was used to dissolve the initiator in a sample vial, which was

placed onto a shaker bed for 30 minutes to dissolve. Initiator solution was added to the monomer solution via one of the side arms using a syringe. The reaction solution was left to polymerise for 2 hours at 60°C under a nitrogen atmosphere. After 2 hours the resulting polymer is precipitated in acetone, and dried in a vacuum oven. In the case of DH3 and DH4, due to the amount of macromer to be prepared, the use of the polymerisation rig was not practical. Instead, the macromer is synthesized in a sample vial in a hot water bath at 60°C under nitrogen. The initiator solution is introduced to the system via a syringe.

### ***3.2.3 Extraction of the polymer via precipitation***

When the polymerisation of the linear polymer was complete, the linear polymer remained in solution in the solvent system used for the polymerisation. The linear polymer has to be precipitated using a non-solvent for the polymer. The solvent to be used can be determined from the dielectric constant of the solvents used in the reaction system. Non-polar solvents generally have a dielectric constant of 15 or less, while the dielectric constant of polar solvents is higher than 15. So if the solvent used for the reaction system was acetonitrile ( $\epsilon_r$  36.04 at 25°C)<sup>93</sup> and water ( $\epsilon_r$  78.36 at 25°C)<sup>93</sup> (50:50) then the dielectric constant would be 54.2. Therefore, a solvent of a lower dielectric constant like acetone ( $\epsilon_r = 20.82$  at 25°C)<sup>93</sup> could be employed to precipitate the polymer<sup>94</sup>.

### ***3.2.4 Infrared Spectroscopy as a quick intermediate analysis***

After the polymerisation has been carried out, a quick qualitative test to see if polymerisation had occurred would be to visually observe if the viscosity of the solution has increased. Whilst this is useful to see if polymerisation has occurred, it does not reveal if the polymerisation has gone to completion. A quick and simple method can be used to check that all the monomer has reacted into the macromer. This is done by using infrared (IR) spectroscopy to look at the functional groups (and their relative amounts), giving an indication of

the amount of the monomer used in the reaction. In IR spectroscopy a beam of infrared radiation impinges on the sample<sup>93</sup>. A sample, depending upon its structure, will absorb infrared light of certain wavelengths causing the bonds in the sample to bend, stretch, or twist<sup>93</sup>. The wavelength of light absorbed corresponds to the energy that a particular bond needs to bend, stretch or twist, making it a useful technique to look at the presence of particular bonds and therefore functional groups<sup>93</sup>. In addition to this, the areas under each peak can be measured, and used to calculate the reactivity ratios of the monomers used<sup>94</sup>. An example of this, the IR spectra for the macromer DH8, is shown in figure 30. The bonds we would expect to see in this spectrum would be C=O, C-F, and C-N, which all appear in the spectrum, and we would expect that if a successful polymerisation has been carried for there to be no peak at 1640-1680 of medium intensity for a C=C bond<sup>59</sup> indicating a successful polymerisation.





**Figure 30.** An example of using IR spectroscopy to identify monomers incorporated into DH8, and the structure of the monomers incorporated in DH8.

Once the macromer backbone has been extracted via precipitation and dried, it needs to be functionalised so that it can be readily cross-linked in the final step. Whilst IR spectroscopy is useful as a quick test, for a more accurate method of testing monomer conversion Nuclear Magnetic Resonance (NMR)

spectroscopy could be employed to calculate exact monomer conversions. This spectroscopic technique, whilst more accurate than IR spectroscopy, is more time intensive.

### **3.2.5 Functionalisation of linear macromers**

The functionalisation of a macromer describes the reacting of a specific molecule containing a functional group onto the linear macromer<sup>95</sup>. This molecule will give the macromer a functionality that it did not possess before. One example is the addition of a carbon-carbon double bond to allow the linear macromer to be cross-linked. The functionality could be quantum dots, which could be used to colour code the linear macromer. For the purpose of the project at hand, the functionalisation step was used to add C=C double bonds for cross-linking sites into the linear polymer backbone. The reason for this is the fact that the C=C double bonds could not be inserted at the polymerisation stage because the free radical centres would have attacked these bonds and incorporated them into the backbone, rather than leaving them free for the subsequent cross-linking reaction. Cross-linking sites on the linear polymer are necessary for the final cross-linking of the linear polymer chains in the final reaction. Once cross linked into a cross-linked polymer network, the polymer is no longer soluble, but still flexible enough to allow the polymer to hydrate in the presence of water. This particular functionalisation utilises a condensation reaction to remove a molecule of water and form a new covalent bond<sup>96</sup>, as shown in figure 31.



**Figure 31.** The condensation reaction of NMA with an alcohol functional group in a macromer backbone<sup>96</sup>



**Figure 32.** Condensation reaction mechanism of NMA with a hydroxy group in a macromer backbone.

The first step in the condensation reaction shown in figure 32 is the attack of the oxygen on the NMA molecule by the positively charged hydrogen. This results in the oxygen becoming positively charged<sup>96</sup>. The oxygen pulls the electrons it needs from the bond it has with the carbon, and water is released from the NMA<sup>96</sup>. In the next step, the oxygen in the alcohol groups present in the macromer backbone acts as a nucleophile and forms a bond with the positive carbon in the NMA molecule<sup>96</sup>. The final step of the condensation reaction is the reformation of the acid catalyst

### **3.2.6 Functionalisation of the macromer: Experimental Procedure**

In a typical functionalisation reaction, 0.4g of the macromer was added to 5.5ml acetonitrile (MeCN) : water (H<sub>2</sub>O) in the ratio 4:6, which was then 3% hydrogen chloride (HCl) acidified. In the case of DH9, 11ml of MeCN : H<sub>2</sub>O in the ratio 4:6 are used again with 3% HCl acidification.

The solution was put onto a shaker bed for 30 minutes until the macromer has dissolved. Then 0.08g NMA and 0.04g chemotropic agent was added to the solution and put on the shaker bed for a further 15 minutes. In the case of DH7 no chemotropic agent is added, as the chemotropic agent was chemically bonded into the macromer during the macromer synthesis. When a hydrogel membrane was to be used for the detection of water in hydrocarbon media such as jet fuel, the addition of a chemotropic agent was not necessary required. The resulting solution was placed into a water bath at 60°C for 2 hours. A needle was put through the sample vial cap to prevent the cap popping off due to an increase in pressure, and the sample vial was shaken by hand every 30 minutes for 2 minutes.

### **3.2.7 Final cross-linking reaction to form a cross-linked hydrogel sensor coating**

The linear polymer is ready to be cross-linked once it has been functionalised with the cross-linking groups. At this stage there is the possibility to add a chemotropic agent such as cobalt (II) chloride to the linear polymer solution, as the final cross-linking reaction will hydrophilically entrap the hydrophilic chemotropic agent in the hydrophobic areas of the polymer network.

For the cross-linking reaction to occur, a free radical reaction is used<sup>59</sup>. Irgacure 184, a photosensitive free radical initiator, is used to provide the radicals needed for the polymerisation. Ebacryl 11 is a polyethylene glycol diacrylate, which makes it an ideal cross-linking agent as there is a unsaturated C=C bond

at either end for the initiator molecules to attack. Also the repeat unit in polyethylene glycol diacrylates can be chosen to give a desired chain length, in order to obtain the required flexibility or rigidity of the final hydrogel. Figures 32 to 35 show the mechanism of the final cross-linking reaction.

In order for the initiation of a free radical reaction to occur, a source of radical centres must be provided. In this instance Irgacure 184 was used as the source of free radicals. Unlike AIBN, Irgacure 184 requires ultra violet (UV) light to provide the energy required to meet the bond dissociation energy. In Irgacure 184 the weak bond is the carbon-carbon bond between the carbon on the ring of the phenol and the carbon of the ketone group on the opposite ring. This bond breaks down homolytically to form two different radical centres for the initiation of the reaction<sup>59</sup>, as shown in figure 33.

Á  
Á



**Figure 33.** The initiation of Irgacure 184

The generated free radical centres will now attack the unsaturated carbon-to-carbon double bonds of the cross-linking agent Ebacryl 11, transferring the propagating radical centres from the initiator to the cross-linking molecule<sup>59</sup>, as shown in figure 34.



**Figure 34.** Propagation of a Irgacure 184 radical centre ( represented as I) with the cross-linking agent Ebacryl 11.

At the same time that the radical centres provided from the initiator attack the unsaturated bonds on the cross-linking agent, they also attack the unsaturated bonds that were added to the linear polymer during the functionalisation step<sup>59</sup>. This transfers the radical centre to the linear polymer backbone, as shown in figure 35.



**Figure 35.** Propagation of the linear macromer cross-linking site (where R represents the linear macromer backbone), with an Irgacure 184 radical (represented as I).

Transfer of the radical centres from the initiator molecules to the linear polymer backbone and to the cross-linking agent during propagation is important for the termination and cross-linking of the resulting polymer<sup>59</sup>. The free radical centres from the linear polymer backbone and the cross-linking agent donate their unpaired electrons to form a new bond between the linear polymer backbone and both ends of the cross-linking agent<sup>59</sup>, as shown in figure 36.



**Figure 36.** Termination of the free radical cross-linking reaction by a propagating cross-linking agent, with a propagating cross-linking site on the macromer.

The reaction shown in figures 33 to 36, is idealised and there is a possibility that the free radical centres may not react as shown. Particularly, two initiator molecules may react together and terminate the free radical centres. Alternatively, two cross-linking molecules may react together and form a longer cross-linking molecule<sup>60</sup>. The insertion of a chemotropic agent into a solution of the macromer, cross-linking agent, and photo initiator before UV curing allows for the entrapping of the chemotropic agent within the hydrogel 3D network<sup>97</sup>. This happens because the chemotropic agent is hydrophilic, and there are

hydrophobic groups in the macromer backbone, which entrap the chemotropic agent within these areas of the hydrogel network once the solution is polymerised<sup>97</sup>. Hydrophobic entrapment is discussed in more detail in section 4.4. Pores within an hydrogel membrane enables the aqueous medium containing the dissolved analyte into the hydrogel network thus allowing the dissolved analyte to interact with the chemotropic agent. The hydrophobic entrapment in the network does not affect its ability to function normally<sup>97</sup>.

### ***3.2.8 Final cross-linking reaction: Experimental Procedure***

For the final cross-linking reaction, a solution of photoinitiator and cross-linking agent was prepared. In a sample vial covered with tin foil 0.3g Irgacure 184 and 1g PEG dicarylate 500 were weighed out. The sample vial is then placed onto a shaker bed for 30 minutes until all the Irgacure 184 was dissolved. Using a Pasteur pipette, 3 drops of this solution were added to the solution of functionalised macromer and chemotropic agent. The resulting solution was shaken by hand for 5 minutes and is ready to be coated onto the surface of a fibre optic cable, as described later in this chapter. Once coated onto the surface, the surface and coating were placed into a box with one side open. A UV lamp was placed onto the open side and turned on for 30 minutes to initiate the reaction. After 30 minutes another coating was applied and the surface and second layer of coating returned to the box for another 30 minutes exposure to the UV lamp.

### **3.3 Nafion®**

Nafion® does not require any preparation work for coating, except for the addition of a chemotropic agent. In a sample vial containing 5.5ml Nafion® 0.04g of the required chemotropic agent was added and left on a shaker bed for 30 minutes. The resulting solution was then coated onto the surface of a fibre optic cable, and the fibre was left in air to evaporate the solvent for 30 minutes. In the case where the fibre optic cable is PMMA, the hair dryer was used intermittently over 5 minutes to prevent deformation of the fibre due to



excessive heating, as the hair dryer does not reach the glass transition temperature of the glass fibre optic cable.

### **3.4 Fibre preparation and coating techniques**

In this project, fibres made from PMMA and glass have been used and, as such, the fibre preparation methods have had to be adapted to suit each material, though the same general principle is followed for each.

#### **3.4.1. "U" bend fibre preparation**

In order to prepare the "U" bend fibre, the first step was to take the fibre from the reel and cut to as short a length as appropriate for handling, to avoid any unnecessary signal loss due to an excessive length of fibre. For glass fibres this is approximately 40cm, and PMMA fibres 30cm. The difference in the preparation of PMMA and glass fibres is that for glass fibres the cladding layer is removed by burning with a flame a length of 4cm in the centre of the fibre, and 3cm at both ends of the fibre. Once the cladding is removed, the glass fibre is heated in the centre where the cladding has been removed until the glass glows bright orange, then quickly removed from the flame and bent to form a "U" shape in the centre of the glass.

For PMMA fibres the reverse is done. The fibre is bent to form a "U" shape in the centre by bending the fibre around a rod of 3mm diameter. Heat from a hair dryer is applied for 30 seconds. While the fibre is still around the rod, the heat is removed and the fibre is allowed to cool for 30 seconds before it is removed from the rod. The cladding layer was then removed only from the centre of the fibre around the "U" bend by using lens tissue that has been soaked in a small amount of acetone (0.5ml approx). Following this the fibre was then rubbed in two circular motions between the thumb and forefinger. This is then repeated with a dry lens tissue, to remove any acetone left on the fibre in order to prevent the core going brittle and snapping upon coating or use. Only the centre of the PMMA fibre cladding is removed, because the connections used for the PMMA fibre do not require the cladding to be removed.

The next step was to polish both glass and PMMA fibre ends to ensure a good optical connection. This is done by inserting the fibre ends into the respective connectors and by removing any excess fibre core protruding from the connector. Then glass fibres were cut using a diamond-cutting pen. Following this the connector and fibre are then screwed into a polishing plate. This plate is next moved in a figure of eight motion eight times on a polishing paper of aluminium oxide particles of 5  $\mu\text{m}$  diameter, placed on top of a glass plate. The whole process of polishing is repeated with a polishing paper of aluminium oxide particles of 0.3  $\mu\text{m}$  diameter. A visual inspection is carried out using a reading magnifying glass, to see if the surface is of a good enough quality and that there is no angle to the surface.

#### ***3.4.2 “End stop” bend fibre preparation***

The term “end stop” has been used to describe a straight fibre optic probe that is 10cm in length (the shortest manageable length of fibre for the probe fabrication), and whereby the light that is passed down the fibre is reflected back up to the detector. For the preparation of an “end stop” fibre, firstly 10cm of fibre is cut, and the cladding is removed using the same method as described in the previous section for PMMA and glass. For glass fibres, 3cm of cladding is removed from both ends, while for the PMMA fibre the cladding is only removed from one end of the fibre. Both ends of the fibre are then polished using the same method as described in the previous section. No bend or shape is put into the fibre; the fibre is allowed to remain straight.

This variation was designed to simplify the production of fibres. With “U” bend fibres, a great precision is required in order to produce fibres with exactly the same path length, to obtain the same signal loss reading each time that they are used. Using a straight fibre overcomes the issue of variation with the “U” bend fibres. However, it poses other production issues. The main issue with the use of “end stop” fibres is that the polished ends must have an angle below 7 degrees, otherwise the light emitted through the fibre will not return back to the

detector from the other end. End stop fibre probes required a special connection to the source and detector, which was provided in the form of a metal cylinder that has two fibre connections out of each end. This tube is called a splitter/coupler. A splitter/coupler is where two fibre optic cables are spliced together. The exact splicing of the fibres allows the light that is launched down the fibre to be split in a ratio of 1:1<sup>98</sup>.

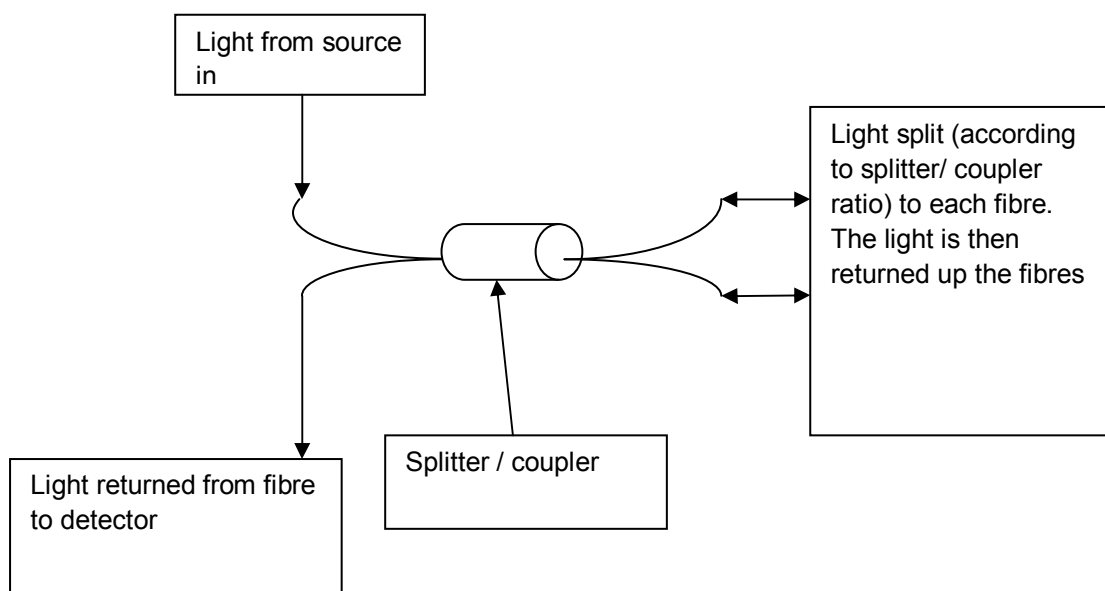


**Figure 37.** Schematic representation of the coupler used with end stop probes.

In the “end stop” setup, a splitter/coupler of 50:50 is used, i.e. the light launched down the fibre is split evenly so 50% of the light is sent down one fibre and 50% down the other fibre. A probe is connected to the end of one of the two fibres. The other end is covered with a rubber cap to keep the signal loss at that end constant, as the light returns through both fibres to the detector and a signal loss is generated. The rubber cap allows for the signal loss that is observed to be due to the interaction of the probe with the sample solution.

### 3.5 Coating of the membrane

Once the fibre optic probe and coating solution have been prepared, the next stage for the fibre optic probe preparation is the coating of the exposed fibre core of the fibre optic cable with the prepared hydrogel. There are several

methods to coat a film/membrane onto a surface, spin coating, painting and dip coating, to name a few.

Spin coating uses centrifugal force to spread an excess amount of a film solution onto a flat substrate<sup>99</sup>. The centrifugal force causes the solution to evenly spread across the substrate<sup>99</sup>. Spinning the substrate causes the solution to spread across the substrate until it reaches the edge of the substrate and is spun off<sup>99</sup>. The solvents used when producing films by this method are volatile, which has an effect on the thickness of the films produced<sup>99</sup>. This method can be used to fabricate reproducible films of the same thickness<sup>99</sup>. The ability to produce films of the same thickness by spin coating would be ideal for the purpose of the project at hand. However, as the fibre optic cable is a tubular shape, spin coating a film onto the surface of a fibre optic cable would be impractical.

Due to the problems associated with spin coating, it was decided that the best route would be to utilise a different method which not only deals with the issue discussed above, but would also reduce complexity and the time needed to coat the fibre. Painting and dip coating were the methods chosen for coating the fibres in the context of the present research. A brush used for art painting was utilised to paint the fibre. The brush was dipped into the coating solution, and the coating was transferred to the exposed fibre core by brushing the exposed area with the loaded brush. This technique proved problematic, as the coating solution would not spread over the exposed fibre core. Instead it would form into droplets on the exposed area, even with repeated brushing. Once painted with the coating (even though the coating was not evenly spread on the core of the fibre), the fibre was placed into an open box on a platform, and a UV face lamp is placed on top of the box and turned on to start the polymerisation. The fibre was exposed to the UV light for 30 minutes, to ensure that the polymerisation is complete.

As an alternative to painting the fibre, the dip coating method<sup>100</sup> was utilised. Hereby, the exposed fibre core was dipped into the coating solution twice to ensure coverage of the exposed core, and then placed onto the platform within

the open box. Which was then exposed to the UV light for 30 minutes to ensure the polymerisation reaction was complete. With the dip coating method it was found that the coating did not form into beads like with the painting method. Moreover, the time taken for the dip coating before exposure to UV light was less, as there was no problem with coverage that was encountered with the painting method.

In the case where Nafion® is used as the coating membrane, there was no need to use UV light to create a film. Once the chemotropic agent was added to the Nafion® and the solution is applied to the fibre optic cable, a hair dryer was used to evaporate the solvent<sup>101</sup> from the surface of the fibre optic cable, leaving a membrane containing a chemotropic agent on the surface of the fibre optic cable.

## **Chapter 4. The design and selection of hydrogel-sensing membranes**

## 4.1 Introduction

Design of the hydrogel membrane is important because the refractive index of the hydrogel is required to respond in a desired way, in order to exploit the conditions for total internal reflection in a specific manner. The membrane needs to be carefully designed with certain parameters, in order to ensure that an effective sensor probe with a sensitivity to a target molecule is obtained and will work with the sensor system requirements. In order for the design to be successful, there are two factors to consider. Firstly, the RI change of the hydrogel coating in the presence of the target species needs to be considered in relation to the refractive index of the core. The second consideration is the way in which the hydrogel and the entrapped chemotropic agent alter the signal loss in the presence of the target species.

The second condition for total internal reflection states that the medium (in this case, the coating) surrounding the core of the fibre must be lower than that of the core of the fibre for total internal reflection to occur<sup>14</sup>. Several approaches can be considered for whether both RI values of the dehydrated and hydrated polymer coating are higher or lower than the RI of the fibre optic cable core, as stated below.

1. Use a coating of higher RI than the core of the fibre.
  - a. Make a coating with an RI that decreases in the presence of the target species.
  - b. Make a coating with an RI that increases in the presence of the target species.
2. Use a coating of lower RI than the core of the fibre.
  - a. Make a coating with an RI that decreases in the presence of the target species.
  - b. Make a coating with an RI that increases in the presence of the target species.

Whilst these approaches are all theoretically valid, in practice they may prove to be problematic.

In the case of a coating with a higher RI than the core of the fibre, which increases RI in the presence of the target species (1b), there is the potential that all the light will be lost from the fibre as the RI of the coating increases to a point where no total internal reflection occurs. In the case of a coating that possesses an RI higher than that of the fibre optic cable core and reduces in the presence of the target species (1a), becoming lower than the RI of the fibre optic core, the signal loss will theoretically become zero as the conditions for total internal reflection are met. However, due to the evanescent field, which is a near standing field, complete total internal reflection is not achievable. In other words, as the RI of the coating lowers past the RI of the fibre optic cables core, some light will still be lost from the cable. Coatings with a RI lower than the fibre core, which decreases further in the presence of the target species (2a) again theoretically already meet the requirements for total internal reflection. As previously mentioned, the effect of the evanescent field means that complete total internal reflection does not occur, but as the RI of the coating lowers further, a point will be reached where the effects of lowering the RI of the coating significantly below that of the core of the fibre will have negligible effects on the light lost. In other words, once the RI of the coating is low enough for all intents and purposes, complete total internal reflection will have been achieved.

The coating material that will be used for the research herein is hydrogels. Due to the properties of hydrogels, the RI change of the hydrogel upon hydration with an aqueous medium containing the target species will be to lower its RI<sup>39</sup>. Therefore careful consideration of the design of a hydrogel with a RI above or below that of the fibre optic cables core is required, i.e., the RI of the dehydrated hydrogel must not be too high as to cause all the light from the system to be lost, or alternatively not be significantly below the RI of the fibre optic cable core so that upon hydration there will be no significant change in the light lost from the fibre.

The reaction of the entrapped chemotropic agent<sup>30,102</sup> in the hydrogel also has an effect on the signal loss that is caused. Chemotropic agents used in the



present research can be divided into two groups. The first includes the chemotropic agents that undergo a displacement reaction<sup>103</sup> forming a precipitate in the presence of the target species. Whereas, the second involves chemotropic agents that undergo a reversible chelation<sup>104</sup> with the target species. Chemotropic agents that undergo a displacement reaction can cause the light lost from the fibres core to scatter. Light from the fibre which is scattered may be scattered back in the direction of the fibre core, or away from the fibre core. The chemotropic agents that undergo a chelation reaction will change colour<sup>104</sup> and the change can be detected by the interrogation system. In an ideal situation, a chemotropic agent that chelates would be ideal for a sensing application, as the probes would be reusable, allowing for an easier calibration and use of the system. In reality, the choice of chemotropic agent is limited by known inorganic chemistry; in some instances there are no alternatives to a chemotropic agent that undergoes a displacement reaction in the presence of the target species.

#### **4.2 Refractive index change as a sensing mechanism – principles and practicalities**

In order to carry out its intended function properly, a membrane needs to be purpose designed for use with a fibre optic sensing platform. Therefore, when designing the membrane, the two main considerations have to be type of aqueous environment that the membrane will be working in, and the target analyte. Target analyte must be able to enter the membrane unhindered, along with the solvent that it is in, whether it be water or a hydrocarbon. The refractive index of the resulting membrane must be lower than that of the optical fibre core used; otherwise the conditions that are required for total internal reflection are not met and the sensor system will not work.

The response of the hydrogel to the targeted analyte will be a change in RI. If the RI of the membrane decreases, the signal loss observed from the fibre will be less. If the RI change of the membrane goes up, the closer it gets to the RI of the fibre core then more loss is observed, until the RI of the membrane is

higher than that of the fibre core when the conditions for total internal reflection are lost and the light escapes from the fibre.

However, coating a fibre optic cable with a membrane is not enough to give sufficient specificity and response required for a fibre optic sensor, where a particular molecule is the desired target. In any aqueous environment there is any possible number of particulates which contribute to the characteristics of that aqueous environment. These particulates can interact with the hydrogel giving a RI change in the hydrogel that is not due to the target molecule. For this reason, the hydrogel needs to be a smart hydrogel, giving a particular response to a particular molecule. This can be achieved with a chemotropic agent, as discussed in 4.3.

#### 4.3 Design and synthesis of membranes to control and exploit refractive index changes

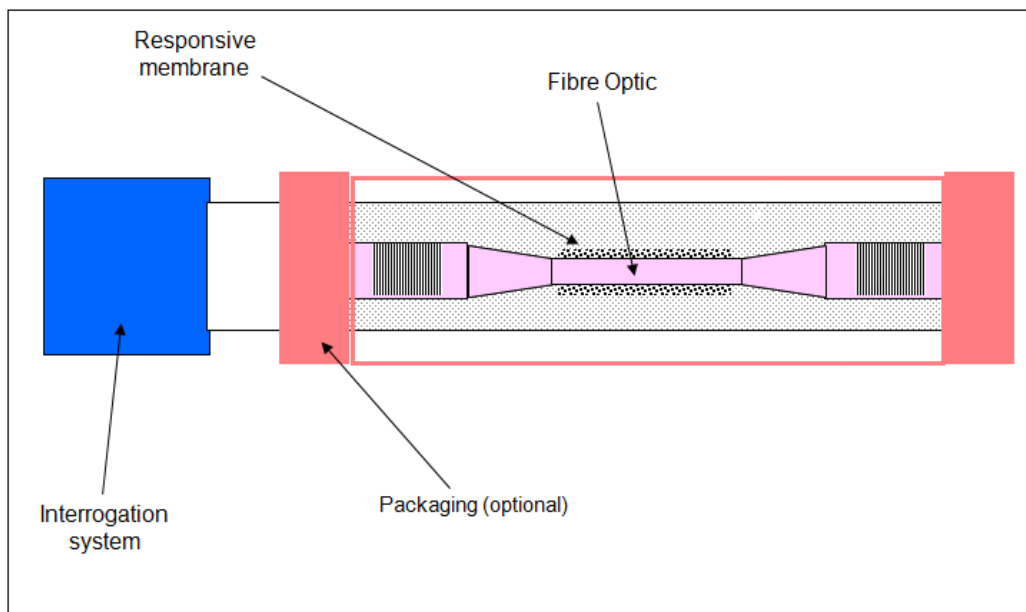


**Figure 38.** A schematic representation of a possible fibre optic cable and interrogation system setup.

The consideration of the choice of a suitable monomer for a membrane dependent on RI has to do with the environment where the sensing will be conducted. Particularly, the membranes can be used in aqueous and in humid environments, and therefore the RI of the hydrogel in both the dehydrated and the hydrated states need to be considered. Therefore, careful consideration to the monomers used in the synthesis of the membrane is required.

The average of the RI of the monomers used is a good indication as to what the final RI of the hydrogel synthesized will be<sup>128</sup>. Thus the choice of monomers used is not only based on the functional groups present in the monomer, which will determine the hydrogel's properties such as hydrophilicity, but also on the RI of the final hydrogel, as this is important as to how the signal loss is generated from the presence of target species.

To design a sensing membrane that has a RI change, the swelling behaviour of hydrogels must be understood. The swelling behaviour of a hydrogel is affected by the following:

- Crosslink density
- Fixed charge density
- Neutral monomers
- Osmolarity of the swelling medium
- pH

Charge density is described as the electrical charge of an atom or molecule over a surface<sup>105</sup>, as shown in equation 2.

$$\text{Charge density} = \text{charge of ion} / \text{surface area of ion}^{105}$$

Equation 2.

Fixed charge density of a molecule affects the swelling properties of a hydrogel<sup>105</sup>. The size and surface area of the charge ion affect the amount of water that can bind to the ion<sup>106</sup>. This is demonstrated by the following example

using the sulfonate functional group, the carboxyl functional and an alcohol group.

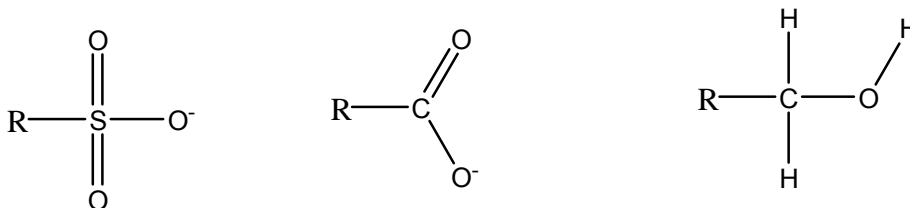


**Figure 39.** A molecular diagram of a sulfonate functional group, a carboxyl functional group and an alcohol group.

Figure 39 shows the common representation of these functional groups in the deprotonated form as having the negative charge on one oxygen molecule. However, in reality when there is no positive ion bound to these functional groups, the negative charge is delocalised over the functional group rather than being associated to one atom<sup>107</sup>.

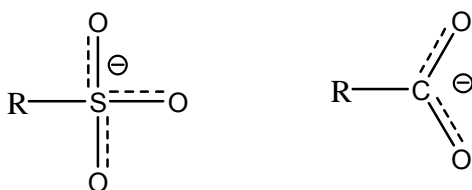


**Figure 40.** A sulfonate functional group and a carboxyl functional group with the negative charge delocalised.

The sulfonate functional group is the largest group, followed by the carboxyl group, and the alcohol functional group is the smallest. The carboxyl group due to its size and charge has a larger charge density than the sulfonate group. Carbon is smaller than sulfur and therefore the charge it possesses is spread over a smaller area. As a result, carboxylic acid groups have a larger fixed charge density and therefore are able to draw more water molecules to solvate itself. As the charge density and the size of the charged group decreases, it becomes hard for the water to be coordinated around the functional group<sup>105</sup>. The charge density of the monomers incorporated into a hydrogel affects the EWC of that hydrogel, a larger charge density results in the hydrogel having a larger EWC. Conversely, if a monomer has a functional group of a smaller

charge density, the hydrogel will have a lower EWC, as the functional groups do not attract as much water into the hydrogel<sup>108</sup>.

Apart from EWC, other considerations have to be taken into account. One such consideration is if the hydrogel had a high percentage of sulfonate functional groups, causing the risk of the hydrogel bursting when hydrated in a medium such as water, compared to if it was to be used in hydrocarbon media.

The effects of neutral monomers, sometimes referred to as inert monomers<sup>109</sup>, on a hydrogel are do not contribute any properties such as hydrophilicity or hydrophobicity to the hydrogels overall properties. Neutral monomers are used to control the structure of the hydrogel, for example to prevent a hydrogel from being overly hydrophilic, without affecting the functionality of the other monomers present in the hydrogel<sup>109</sup>. The prevention of the formation of hydrophobic or hydrophilic areas can be achieved by adding an inert monomer to improve monomer distribution in the polymer backbone.

Osmolarity is a measure of the solute concentration (osmoles, Osm) per litre (L) of the solution (osmol/L or Osm/L)<sup>83</sup>. The osmolarity of the swelling medium is important, as it will affect the movement of water into the hydrogel<sup>83</sup>. For example, in a cell which is separated by a membrane, if one side is pure water and the other a salt solution, water will move across the membrane from the pure water to dilute the salt solution.

A hydrogel is a membrane and as such its swelling behaviour is affected by the monomers used to synthesize it and by the swelling medium. If a hydrogel is made using NaAMPs, and the swelling medium were pure water, the water would enter the membrane to dilute the Na<sup>+</sup> in the hydrogel membrane, causing the membrane to swell. However, if the swelling medium were a sodium chloride (NaCl) solution, an equilibrium between the hydrogel membrane and the solution would occur to equalise the osmotic pressure of the system (dependent on the concentration of the NaCl in the solution).



**Figure 41.** Graph showing the effect of salt concentration in solution on EWC of three hydrogel compositions<sup>110</sup>.

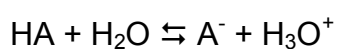
If the hydrogel was made from monomers with functional groups that do not have cations such as  $\text{Na}^+$  in the structure, this type of interaction would still be observed due to the presence of other hydrophilic groups. However, the effects would not be as dramatic, since the hydrogel would not contribute as large an osmotic pressure to cause the water to enter it<sup>91</sup>. The swelling medium could cause the EWC to change if the tonicity of the swelling medium is altered. If the hydrogel contained cations in the structure but the swelling medium had a larger salt concentration, the osmotic pressure would favour the movement of water from the hydrogel to the solution<sup>83</sup>. Conversely, if the concentration of the salt solution were lower than that of the hydrogel, the osmotic pressure would favour the movement of water into the hydrogel.

The effect of pH on a hydrogel, as well as the osmolarity of a swelling solution, can affect the EWC content of a hydrogel, dependent upon the functional groups present in the polymer backbone of a hydrogel<sup>111</sup>.



**Figure 42.** Graph of pH vs swelling ratio of five polymer blends of poly(acrylic acid) (PAA) : poly(vinyl alcohol) (PVA) : <sup>112</sup>.

Increasing the PAA content of a hydrogel increases the swelling ratio of the hydrogel, across certain pH range, as shown in figure 42. This is due to the carboxyl group present in PAA<sup>111</sup>. pH is a measure of the acidity or basicity of a solution<sup>113</sup>. In other words, it is a measure of the concentration of the hydronium ion present in a solution. A Bronsted-Lowry acid is defined as a substance that donates a hydrogen ion, and a Bronsted-Lowry base is a substance that accepts hydrogen ions<sup>113</sup>. The pH scale measures the acidity or basicity, but the strength of an acid or base is described using the equilibrium constant  $K_{eq}$ <sup>113</sup>.



Equation 3.

$$K_{eq} = [H_3O^+][A^-] / [HA][H_2O]$$

Equation 4.

For the measurement of acidity a dilute solution is usually used, and the concentration of water remains almost constant at approximately 55.6M at 25°C<sup>112</sup>. This allows equation 4 to be rewritten to include a new quantity called the acidity constant  $K_a$ , resulting in equation 5.

$$K_a = K_{eq}[H_2O] = [H_3O^+][A^-] / [HA]$$

Equation 5.

The equilibrium constant multiplied by the molar concentration of pure water gives the acidity constant for any generalised acid  $HA$ <sup>113</sup>. A strong acid has an equilibrium that lies to the right of equation 3, as a strong acid dissociates easier than a weak acid. This means that a strong acid will have a larger  $K_a$  than a weak acid<sup>113</sup>.  $K_a$  values for a weak acid range from  $10^{-60}$  to  $10^{115}$ . The strength of acids is normally expressed as the negative logarithm of  $K_a$ <sup>113</sup> as shown in equation 6.

$$pK_a = -\log K_a$$

Equation 6.

As  $K_a$  is expressed as the negative logarithm, there is an inverse relationship between  $K_a$  and  $pK_a$ . Therefore, if an acid has a high  $K_a$ , it will have a low  $pK_a$ <sup>113</sup>. The dissociation constant of an acid or a base in a solution is important if the hydrogel contains acidic or basic groups within the polymer backbone.  $pK_a$  is the measure of the dissociation constant of the hydrogen ion from an acidic group in solution<sup>113</sup>. As applied to a hydrogel, this means that if it has an acidic functional group (such as acrylic acid) that donates its  $H^+$  when in solution, if the pH of the solution increases and becomes basic, the hydrogel will swell because the basic molecules (such as NaOH) are increasing in concentration and interact with the carboxyl group of acrylic acid.



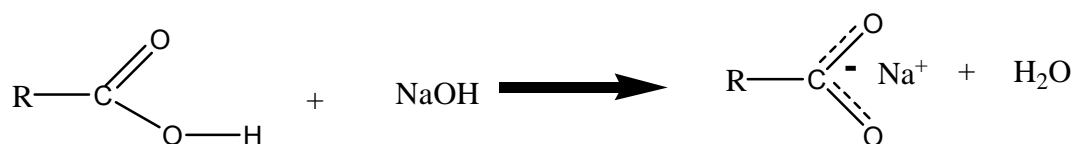


**Figure 43.** A carboxylic acid group reacting with a sodium hydroxide molecule.

The degree of swelling of the hydrogel is also controlled by the amount of the acidic functional group present. Increased levels of acidic groups means that more of the alkali solution will interact with the acidic groups in the hydrogel, causing a greater degree of swelling<sup>111</sup>, as seen in figure 42. In other words, as the ratio of acrylic acid increases from 3:7 to 7:3, so does the degree of swelling. Figure 42 shows a curve of increased swelling ratio from pH 10 to 13 with the maximum swell ratio observed at approximately pH 12. This is due to the equilibrium of the solution being maintained between the protonated and deprotonated forms of the acid<sup>111</sup>. The position of the curve is related to the fact that some acids are stronger than others, thus the dissociation of the proton from the acid will happen at different pH<sup>111</sup>. A strong acid will donate its proton to a stronger base. If the acid group were a stronger acid, the curve seen in figure 42 would lie further to the right<sup>111</sup>. Conversely, if the acid were a weak acid, the curve would lie further to the left, but not past pH. If the curve lied to the left of pH 7, the acid group would be replaced with a base functional group.

#### 4.4 Chemotropic membranes – the use of entrapped colourimetric agents

The use of a chemotropic agent in a hydrogel is another way to make the hydrogel smart, i.e. the hydrogel will respond to a specific stimulus<sup>56</sup>. A chemotropic agent is a compound that responds to stimuli by changing colour, the colour change can be due to the chemotropic agent either complexing with a target species or undergoing a displacement reaction to form a precipitate<sup>103,104</sup>. This response can be utilised within a hydrogel membrane. The response is twofold because the membrane will have an associated RI change with the presence of the stimulus. In addition, a colour change can be

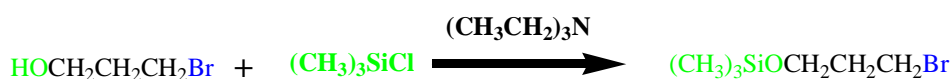
observed and detected by the fibre optic sensor system. The membrane utilised must be able to entrap the chemotropic agents used without loss of functionality and without them leaching out of the membrane and into the surrounding environment. Most commonly the chemotropic agent is held in the membrane by a simple hydrophobic interaction<sup>46,47</sup>. Alternatively, the chemotropic agent can be chemically bound into the polymer backbone; however this is a more time consuming and resource intensive process making the simple hydrophobic bond the preferred route. An ideal chemotropic agent has a reversible colour change when the stimulus has been removed, as this can allow for a real-time sensor system to be developed and used in a quality control process. An example is the on-site detection of water level in jet fuel. Chemotropic agents that have a displacement reaction to form a precipitate can be used for one-off measurements where a constant monitoring is not needed. For example, the level of potassium in the eye could be detected for the medical diagnosis of eye conditions by obtaining a tear sample or taking a direct eye measurement.

#### **4.5 Design and synthesis of membranes to control and exploit colourimetric changes**

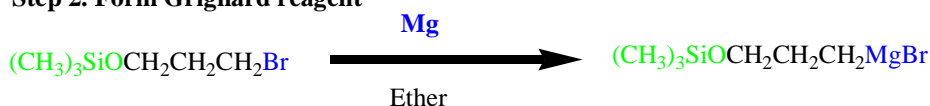
The design parameters for a membrane that exploits RI change discussed in sections 4.0, to 4.2 need to be taken into account for the design of a membrane that entraps chemotropic agents causing a colourimetric change. Colourimetric membranes must be optically clear, as the chemotropic agent used in these membranes will change colour. Therefore, there should be no interference from the membrane, obstructing the coloured light from getting to the fibre core. The entrapment of the chemotropic agent is another important factor; the membrane must allow the solvent and the molecules for detection to enter it, and not interfere with the interaction of the chemotropic agent and the target molecule. A chemotropic agent could be bound through covalent bonds or through hydrophobic entrapment (the entrapping of a hydrophilic molecule by surrounding hydrophobic groups). Bonding a chemotropic agent in a membrane using covalent bonds would reduce the functionality of the chemotropic agent. To covalently bond a chemotropic agent into the polymer backbone, the

chemotropic agent requires a functional group that can be reacted to form a new bond. This removes one of the groups that give the chemotropic agent its functionality. The bonding of the chemotropic agent into the polymer backbone is not specific to a particular functional group present on the chemotropic agent. This means that the chemotropic agent could bond into the polymer backbone using one of the functional groups that may have more affinity to the target molecule. The only method to ensure that the specific functional group is used for the bond to hold the chemotropic agent into the backbone is to protect the other functional groups that are present, and de-protect them after the chemotropic agent has been bonded into the backbone. One example of protecting a functional group is in the preparation of a Grignard reagent from a halo alcohol<sup>114</sup>. The carbon-magnesium bond is not compatible with an acidic alcohol group in the same molecule<sup>114</sup>. In this instance, the alcohol needs to be protected to prevent it from interfering with the formation of the Grignard reagent. The second step is to form the Grignard reagent, followed by the carrying out of the Grignard reaction, and finally the removal of the protecting group<sup>114</sup>.

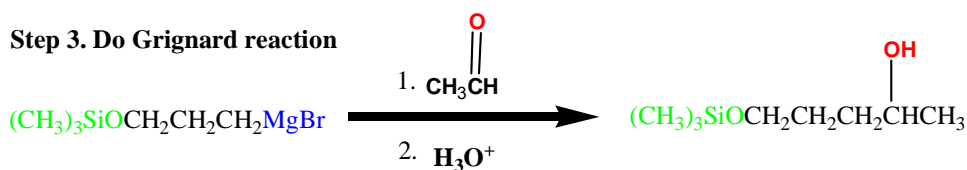
**Step 1. Protect alcohol**



**Step 2. Form Grignard reagent**



**Step 3. Do Grignard reaction**



**Step 4. Remove protecting group**

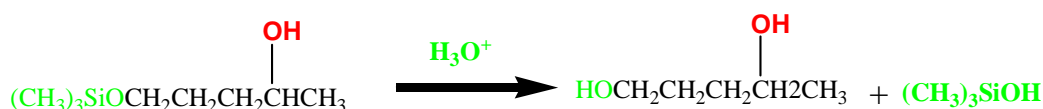


**Figure 44.** The four steps of creating a Grignard reagent by protecting the alcohol group, forming the Grignard reagent, Grignard reaction, and the removal of the protecting group from the alcohol<sup>114</sup>.

The process outline in figure 44 requires more time and effort than hydrophobic entrapment, with the inclusion of three extra steps to the process, namely the protection of the functional group, the reaction to bond the chemotropic agent, and finally the deprotection for enabling the full functionality of the chemotropic agent. The covalent bonding of a chemotropic agent is another factor that reduces the degree of rotation that the chemotropic agent can go through. This may result in a target molecule not being able to approach the chemotropic agent due to the functional groups being inaccessible to the target molecule.

Hydrophobic is the preferred method utilised in this project for the entrapment of a chemotropic agent. The chemotropic agent is held within the membrane by the incorporation of hydrophobic groups in the linear polymer backbone. To achieve hydrophobic entrapment, the chemotropic agent is added to a solution of the linear polymer, a cross-linking agent, and a photo initiator before the photo polymerisation. The chemotropic agent is then held in by hydrophobic interaction between the chemotropic agent and the hydrophobic parts of the hydrogel network, as shown in figure 45.

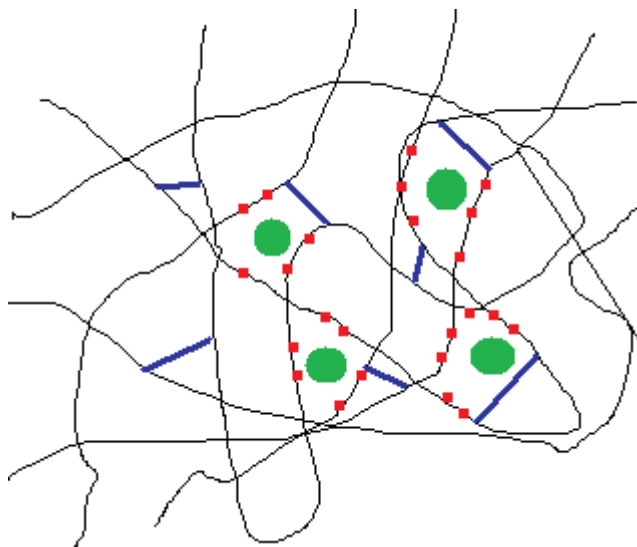


**Figure 45.** A representation of the entrapment of chemotropic agents within a hydrogel network. The red dots represent hydrophobic groups. The large green circles represent the chemotropic agent trapped by the hydrophobic groups within the hydrogel network.

This method of entrapment allows the solvent and the dissolved analytes to enter the hydrogel network and into the regions of the hydrogel where the chemotropic agent is entrapped. Dissolved analytes can then interact with the entrapped chemotropic agent. The hydrogel network does not hinder the chemotropic agent's functionality with the target molecule. While the hydrophobic entrapment of the chemotropic agent does not allow it to escape the network, it is not enough to prevent the solvent and the target molecule in it from entering the hydrogel network, reaching the chemotropic agent and interacting in its intended way. This method of entrapment, however, has a maximum loading dependent on the amount of hydrophobic groups present and the number of hydrophobic groups it takes to hold one molecule of chemotropic agent.

## **Chapter 5. The design and development of a sensing platform.**

## 5.1 introduction

The design and development of a fibre optic sensor system has to be carefully considered in terms of choosing the most appropriate system available. There are different hardware types in terms of the light source emitting light through a fibre optic cable.

One of the simplest forms of a fibre optic sensor system is that of a light source connected to a light detector via a fibre optic cable<sup>115</sup>. Light launched through the fibre makes a single pass from the light source to the detector<sup>115</sup>. The light source for this type of system does not need to be a laser, which produces coherent light. An LED could be used as the length of the pathway that the light takes is not large enough for attenuation to pose a significant problem. The change in light is then turned into a signal loss by calculating the difference in the intensity of the light emitted from the source and the light that reaches the detector. This type of a system generates one data point for the light emitted from the light source. It is suitable where great levels of accuracy are not needed to achieve the required results. The main advantage of this type of system in comparison to other systems, such as cavity ring down, is the cost. For a single pass fibre optic system a light source such as an LED is suitable. The cost of an LED is considerably less than that of a laser light source. An LED can be used in a single pass system because in a single pass system the light only goes through the system once. As a result, the issue of attenuation is not as important as in a system where light has to travel through the system many times. If a light source such as an LED were used for a cavity ring down system, the light would lose intensity too quickly to be adequate enough for analysis. The hardware required for a single pass system in terms of the light source and the analysis equipment is fairly compact. When using an LED light source, a photodiode is adequate to detect the intensity of the light that reaches the end of the cable. In addition, the analysis of the signal received by the photodiode can be easily done on a laptop or desktop computer with the appropriate software.

Cavity ring down sensor systems are highly sensitive optical systems<sup>116</sup>. These types of systems use lasers as the light source. Light from a laser is launched into a cavity, which in its simplest form comprises of two highly reflective mirrors<sup>116</sup>. The laser is turned on until the amplitude of the light caught in the cavity is at maximum. At this point the laser is turned off and the decay of the light measured as it passes back and forth between the two mirrors<sup>116</sup>. A path length of a few kilometres is created before all of the light has dissipated<sup>116</sup>. The time it takes for the light to dissipate is called the ring down time<sup>116</sup>. This system can be turned into a sensor system by the addition of a sample in the cavity that absorbs the light, as this causes the light intensity to decrease faster<sup>116</sup>. One example of this setup is cavity ring down spectroscopy, which is used to measure the concentration of gases that absorb light of different wavelengths<sup>117</sup>. The cavity is filled with the gas and the light is passed back and forth between the two mirrors. A time measurement is taken for the light to decay to  $1/e$  of its intensity<sup>117</sup>.

Cavity ring down spectroscopy systems have two main advantages over other spectroscopic systems that use light<sup>106</sup>. Firstly, in order to calculate the concentration, the ring down time is measured as the time it takes the light decay to  $1/e$  of the original intensity<sup>106</sup>. The results are not affected by any variation in the light source's initial intensity<sup>106</sup>. This technique is more accurate, as other techniques assume that the light source intensity is constant for both the calibration and sample measurement<sup>106</sup>. In reality the light source intensity diminishes over its lifetime. The second advantage is that because the light will travel many times between the mirrors, it has a very long path length and therefore a greater sensitivity can be achieved<sup>106</sup>. One disadvantage of using this type of setup is the limited range of analytes that can be tested for<sup>106</sup>. This is due to the availability of tuneable laser light and the corresponding high reflectance mirrors at the correct wavelength<sup>106</sup>. The main disadvantage of this type of system is the cost associated with all the equipment required. Size is also another matter, as it is not a compact and easily transportable spectroscopic system.



## 5.2 The fibre optic probe: materials and configurations

The fibre optic probe used in this system is the location of the interaction between the sensor coating, the interrogation system and the environment that the potential target analyte is in. There are several implications in the choice of the fibre optic probe material. In this project, the fibre optic cables that were investigated were PMMA 1mm core diameter fibre optic cables and 400µm core diameter low -OH glass fibre optic cables. Therefore, considerations based on these two fibres will be discussed. The EvanesCo EV5000 red LED light source, sensor system has been used. This sensor system uses an LED to provide the light launched down the fibre optic cable. This type of light source is not coherent<sup>119</sup>, i.e. the waves of light emitted from the LED are not all in phase with each other, as shown in figure 46.

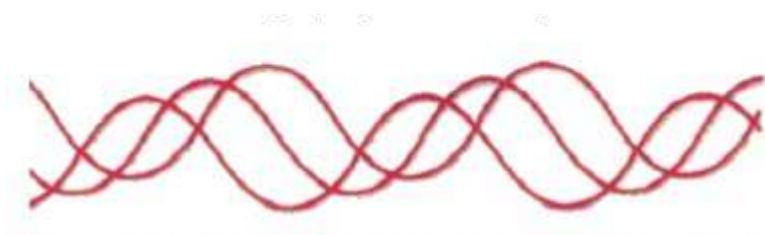


**Figure 46.** Light emitted from an LED represented as waves that are not in phase with each other.

On the contrary, the light from a laser is coherent because all the waves are in phase with one another<sup>119</sup>, as shown in figure 47.



**Figure 47.** The light from a laser represented as waves, all in phase with each other.

The advantage of light emitted from a laser is that the light can be launched down fibre optic cables that have a core diameter of only ten times the wavelength of light<sup>119</sup>. This allows for very precise transmissions to be made down the fibre. Contrarily, the light emitted from an LED requires a fibre optic core of a larger diameter to allow the light to enter the core<sup>119</sup>. In addition, because the light is incoherent, waves emitted from the LED simultaneously may not reach the end of the fibre at the same time<sup>119</sup>. The EvanesCo fibre optic sensor systems measure the light emitted from the LED and the light received at the end of the fibre to calculate a signal loss. For the purpose of the signal loss calculation, an LED light source is suitable enough, as whilst it does not produce as coherent light as a laser, it is less expensive and the light produced from the LED is more than sufficient for a sensor system where the difference in light within the system is measured.

Initially, the PMMA fibre optic cables were the only cables used for the sensor system developed. Throughout the course of the research, different coatings for different sensing purposes were developed. The coatings required different solvent systems, including toluene and methanol. These solvents caused problems with the PMMA fibre because they would dissolve the fibre optic core, and this created the need for a different material for the fibre optic cable to be used. Glass seemed the ideal solution, as it is very resistant to solvents. The use of glass fibre optic cables increases the cost of the system. A glass fibre optical cable with a core of 1mm would be an ideal choice. With a glass fibre of 1mm core, more of the parameters of the work carried out would remain constant, but the chosen 400µm core fibre was more cost-effective. The choice of a suitable fibre optic probe material is dependent on the environment where the sensing is taking place and the time that the probe is exposed to the environment. For example, if a deuterated PMMA<sup>2</sup> fibre were to be used to take sample readings of an analyte in water, there would be a potential for ingress of water into the fibre due to deuterated hydrogen atoms present in the fibre<sup>2</sup>. Thus the long-term use of a deuterated PMMA fibre in water environments would be problematic and a glass fibre would be the preferred type. Some scenarios would require the use of a PMMA fibre optic cable, as the glass fibre has flexibility when there is a cladding layer, but when that cladding

layer is removed, as our system requires, that section of fibre becomes very brittle and breaks easily. Thus, in cases such as sensing in a body site or where flexing of the probe is required, the use of a glass fibre optic cable would not be ideal.

The fabrication process of a fibre optic probe with either material is very simple, and both use “butt to butt” connections<sup>120</sup>. However the difference between these two fibres is the precision needed for the connection. A PMMA fibre with a core diameter of 1mm needs less precision to get more of the light from the LED, compared to the 400µm diameter glass fibre<sup>120</sup>. This means that more attention is needed for the cleaving of the glass fibre. The ideal cleave would be 0° and the higher this angle is, the more difficult for the light to enter the fibre<sup>120</sup>.

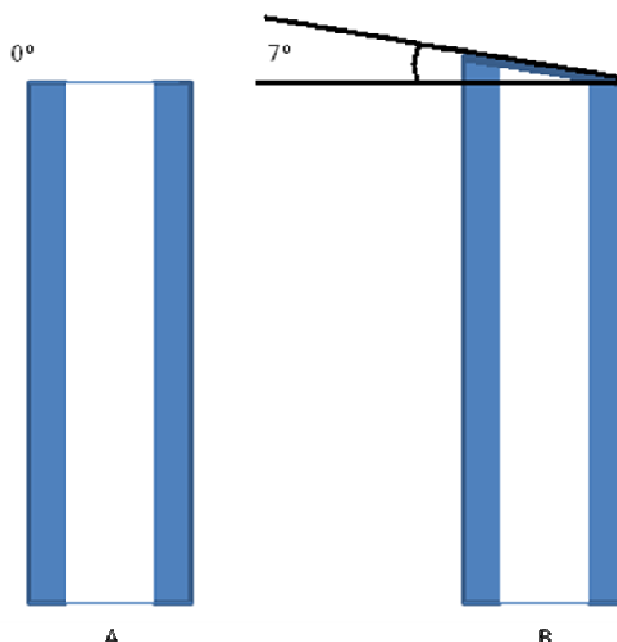


**Figure 48.** A Schematic representation of two cleaved fibres. A, shows a fibre that has been cleaved with an angle of 0°. B, shows a fibre that has been cleaved with a 7°, angle at the end of the fibre.

This has knock-on effects for the system as a whole. The PMMA fibre will transport more light as it has a larger core diameter. Hence, the signal loss changes observed when taking a sample reading using a glass fibre would be smaller compared to the PMMA fibre. Therefore, if there is only a small signal loss in the presence of the target analyte, this could be overshadowed by

interference factors (such as vibration in the probe) causing signal loss or changes in natural light intensity, when the glass fibre is used.

### 5.3 Hardware of the sensor system

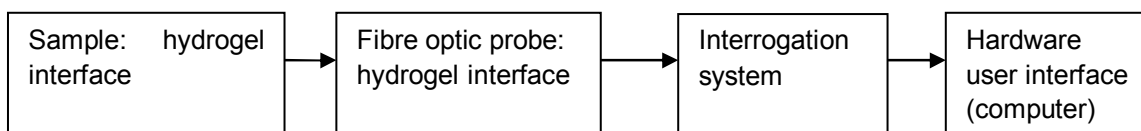


**Figure 49.** Schematic overview of the four sensor system components.

The sensor system developed for the work conducted in this project comprises of four distinct components, shown in figure 49. First is the sample containing the target species and the hydrogel coating that is applied to the fibre optic cable probes. The target species interacts with the hydrogel coating exhibiting a desired response. Second is the interaction of the hydrogel and the fibre optic probe. When the hydrogel has been saturated with the sample, and exhibiting the desired response, the hydrogel coating: fibre optic probe interface causes light to either be lost or reflected back into the fibre optic cable. The increase or decrease in light escaping the fibre is detected by the third component of the system, the interrogation system. Finally, the fourth component of the system is the hardware user interface. This is a software program which calculates and interprets the amount of light lost from the fibre optic cable.

#### 5.3.1 The hydrogel membrane

The first stage of detection begins at the interface between the target species, and the hydrogel. As the aqueous sample containing any dissolved species enters and swells the hydrogel membrane, allowing the dissolved target species to interact with the entrapped chemotropic agent. This is followed by the interaction between the hydrogel and the core of the fibre.

The second stage occurs once the sample has entered into the hydrogel, and the interaction between the target species and the chemotropic agent has occurred. At this point, the hydrogel will change RI and there may also be an associated colour change. The change in RI of the hydrogel, as previously discussed, alters the amount of light that is lost from the fibre. As the hydrogel is only a thin layer, the time it takes for the EWC of the hydrogel to be achieved is relatively short<sup>156</sup>. Any change of the hydrogel's RI is registered almost instantaneously, as the time it takes for this change to be detected by the interrogation system is based on the time it takes for light to travel through the fibre from the source to the detector.

In this way, the hydrogel acts as the sensing mechanism for the system, exploiting the dependence of the fibre optic system on total internal reflection.

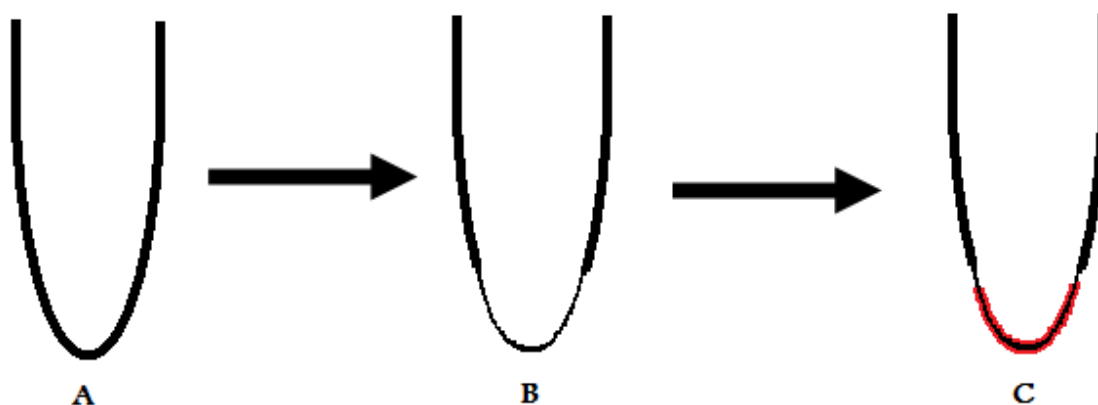


**Figure 50.** A. “U” bend fibre optic cable with cladding layer. B. Cladding layer removed to expose the fibre core. C. The core of the fibre coated with a hydrogel coating (red area).

Figure 50 shows a probe setup in a “U” bend configuration. The first stage is to remove the cladding layer from the fibre optic cable to expose the core. Following this the second stage is to replace this removed cladding with the sensing hydrogel. The interface between the core of the fibre and the hydrogel controls the light lost from the system due to the changes that occur in the hydrogel from the presence of the target species.

### 5.3.2 The fibre optic probe

Probe is the term used to describe the fibre optic cable that is used to connect the light launched from the LED light source to the photo diode where the light is returned to. The fibre optic cable could be made from various materials, including PMMA and glass. For each application the configuration of the probe can be altered to suit the application requirements before it is coated with a smart hydrogel. The hydrogel is used as the mechanism to control the light lost from the fibre due to the presence of a particular stimulus. One example of a configuration that can be used for measuring metal ions in tear in an *ex-vivo* contact lens is that of a fibre optic cable with a “U” bend put into the fibre to encourage signal loss from the fibre, as shown in figure 51. This “U” bend is then coated with the smart hydrogel to give the probe sensitivity to a particular stimulus.



**Figure 51.** A PMMA fibre optic cable that has a “U” bend in it to encourage signal loss, coated with a smart hydrogel, to attain sensitivity to a particular stimulus.

An alternative probe configuration is that where a straight piece of fibre is used and both ends are polished with an angle of less than  $7^{\circ}$ <sup>19</sup>. The end of this fibre is coated with a smart hydrogel. Light is then launched down the fibre and reflected back up the length of this fibre to the photo diode. This type of probe could be used for the measurement of metal ions in water systems, or for taking lower tear meniscus readings of tear analytes, as shown in figure 52.



**Figure 52.** A straight fibre optic probe coated with a smart hydrogel being used to perform a direct assay of the lower tear meniscus.

### ***5.2.3 The interrogation system***

The data collected is generated by the interrogation system, in this case the EvanesCo EV5000 sensor box. This interrogation system comprises of a LED light source and two photo diodes. One photo diode is set to measure the intensity of the light source, and the other the amount of light that is returned to the EV5000. This difference in light is then interpreted into a signal loss. For the measurement of a sample, the light is continuously emitted through the fibre and data points are generated at set time intervals between 0.1 seconds and 99 hours. Due to the above particular features of the system, it can be used for detection of the target molecule in static samples, or for measuring the target molecule in a flowing sample, such as a stream. In a flowing sample the aim of the device is to measure increases or decreases in the target molecules concentration. In such cases the accuracy that could be achieved with systems such as cavity ring down spectroscopy is not required<sup>106</sup>. The size of the interrogation unit gives it the versatility to be used almost anywhere, whether it be water sampling at remote locations, or measurement in a laboratory setting. Spectroscopy techniques that use light, such as IR spectroscopy, rely on the intensity of the light source remaining constant through its use to measure the presence and concentration of samples<sup>106</sup>. In reality, however, light sources will change intensity with use<sup>106</sup>. This does not apply to the

EV5000 system, as there are two detectors in the unit. One detector measures the intensity of the light that is returned to the box after traveling through the probe, and the other measures the intensity of the light transmitted from the light source. The signal loss is generated as the difference in the intensity of the light returned to the unit from the intensity of the light emitted from the unit.

### 5.3.3 The user interface

The hardware user interface is in the format of a software program that can be supported on a laptop or a desktop computer. This software interface shows the signal loss in decibels in numerical and a digitised “analogue” needle format, as shown in figure 53.

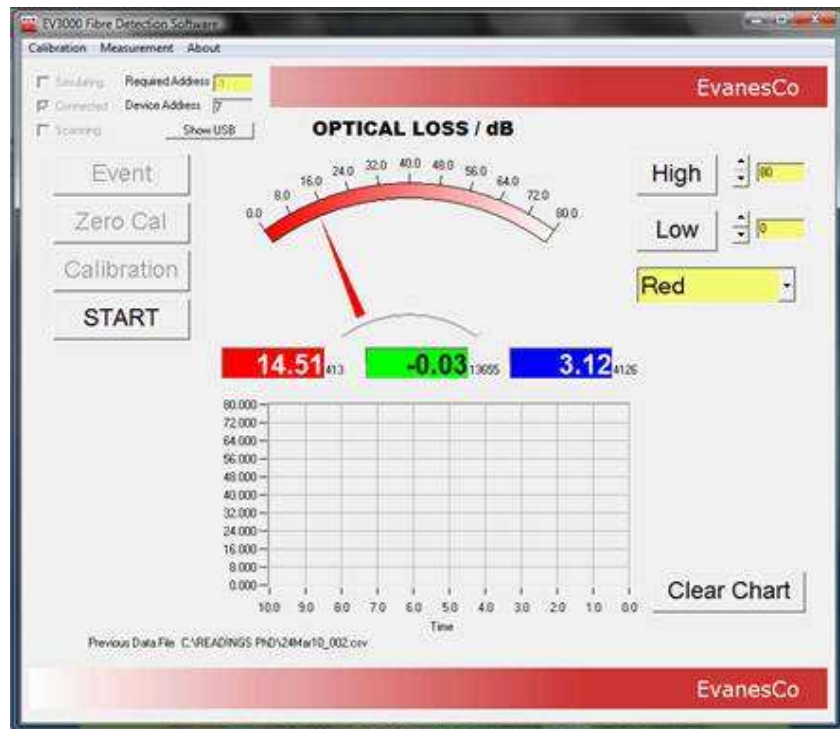
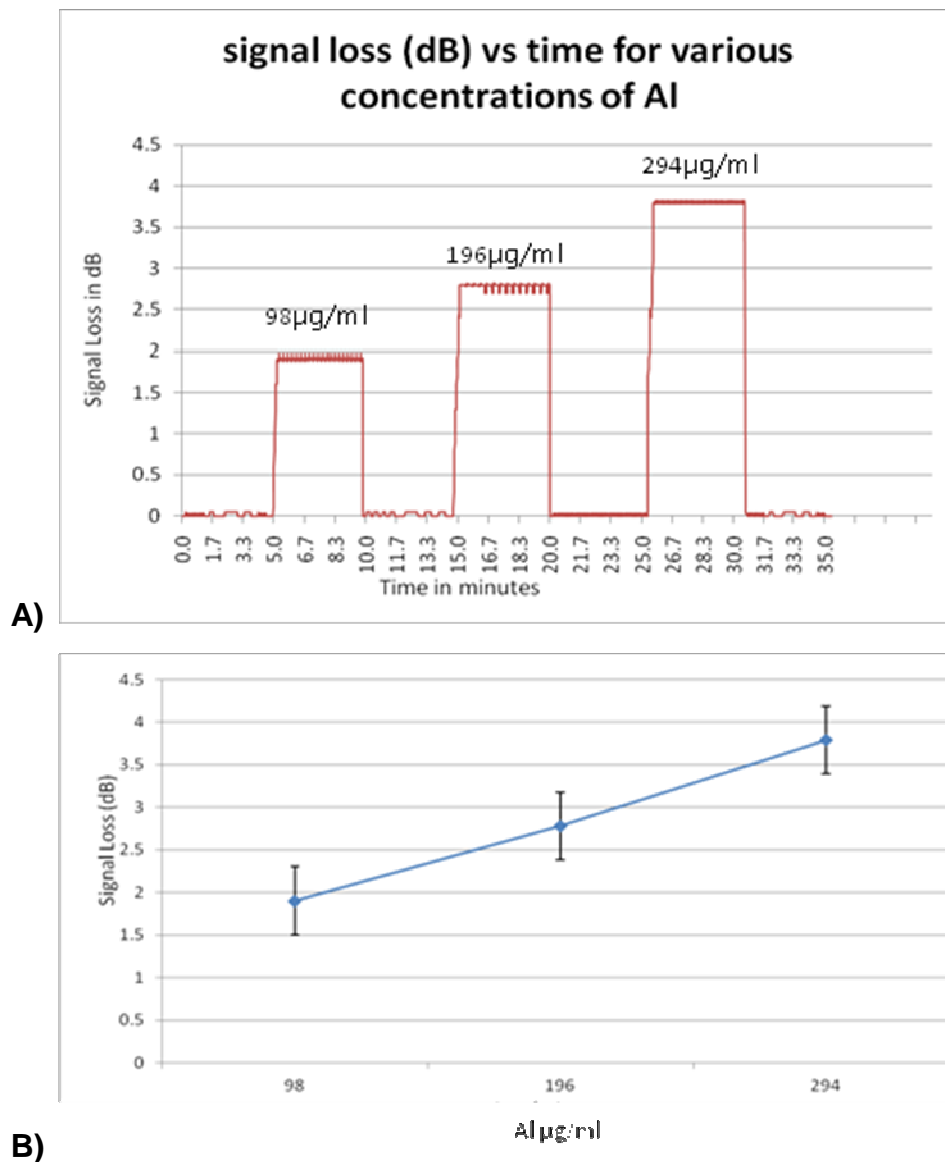


Figure 53. Hardware user interface.

This interface gives real time signal loss and produces a graph of the real time information for the last 10 seconds of data collection, so that a visual comparison of increase or decrease of signal loss can be viewed. The data collected is saved in a Excel spreadsheet, which can be manipulated to



produce a graphical representation of all the signal loss data collected over a given time frame, as shown in figure 54.



**Figure 54.** A) Signal loss vs time of three concentrations of aluminium (Al) in water. B) The average signal loss vs concentration of three samples of aluminium solution.

The time between readings can be altered to suit the application, ranging from 0.1 seconds between data point samples and up to 10 hours between readings, with a maximum of 40000 data points being collected. Figure 54A shows only time and signal loss. A record has to be made of the time that the probe was subjected to a sample and the time it was removed, in order to ensure the cause of the signal loss is assigned to the correct samples. This data can be

further manipulated to obtain the average signal loss due to a sample. Figure 54B shows the average signal loss obtained for each sample plotted against the known concentration of the aluminium solution. The graph in figure 54B shows an almost linear relationship as would be expected, which is ideal to make a calibration graph to use when determining the concentration of unknown samples. In the next section the calibration of the sensor system is discussed in more detail. Section 7.5 discusses in more detail the detection of aluminium.

#### **5.4 Calibration and use of the system – coating and configuration issues**

As with all spectroscopic techniques including sensors, a calibration has to be made using samples of known concentration so that the corresponding readings can be linked to the value of the target species<sup>120,121</sup>. In this case, signal loss has to be linked to corresponding concentrations of the target molecule. This is achieved by taking readings of samples of known concentrations with the sensor equipment and creating a calibration graph. The calibration graph allows the user to determine the concentration of the target species in an unknown sample by comparing the signal loss of the unknown sample to that of the calibration graph.

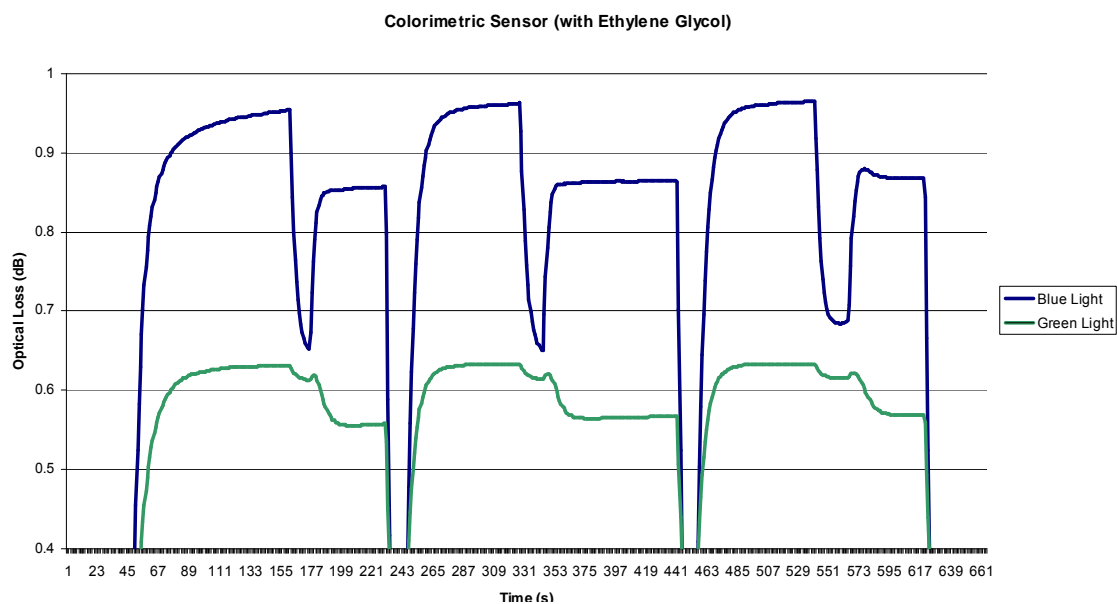


**Figure 55.** A Colourimetric probe of methyl orange, in a coating of NBNMA, NVNMA and MMA (crosslink density 0.8%). The probe was dipped into a solution of HCl, and sodium hydroxide (NaOH) alternatively three times.

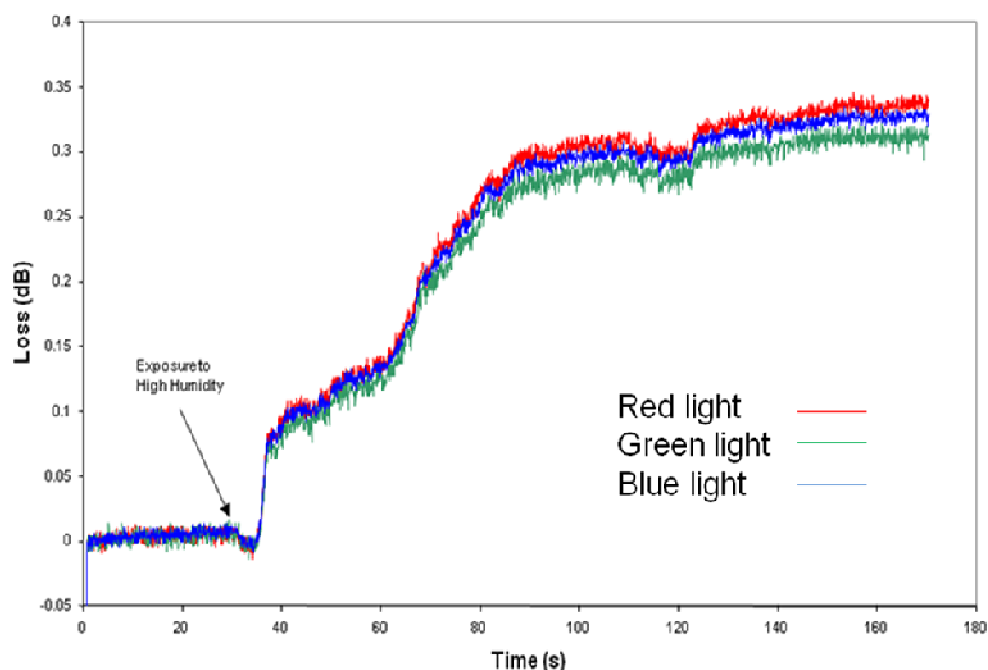


**Figure 56.** A probe coated in a PVA/sulfonated macromer (crosslink density 1%) in ambient air then placed over a beaker of water at room temperature. The light source used was a white LED, the red, green and blue lines represent the data collected from each channel, i.e. red, green and blue wavelengths.

As can be seen in figures 55 and 56, the probes are exposed to a range of target species that they are designed to sense. The sensor system is able to detect and differentiate between acidity and basicity using the pH probe, and differences in humidity using the moisture probe. Because the sensor system is able to sense not only the presence, but also the concentration of the target species, a calibration graph can be made from this data.

In figures 55 and 56 the response times that are seen differ from a couple of seconds to tens of seconds. The variation that is seen is due to the cross-link density. A higher level of cross-link density in a hydrogel network, makes it harder for the solvent to enter the network<sup>55</sup>. This is because a higher cross-link density results in a more tightly bound network. Conversely, a hydrogel network with a lower cross-link density allows solvents to enter the network easier. The choice in cross-link density is based on the required response time, as well as on other properties such as the structural integrity of the hydrogel. Another factor affecting the choice of cross-link density is the loading of chemotropic agents into the hydrogel network. If the network is more loosely bound, the likelihood of the hydrophobic monomers in the polymer backbone being in close enough proximity to each other to hold the chemotropic agent is reduced.

### **5.5 The rationale for the sensor system selection.**

One of the objectives of designing this system was to create a cost effective alternative to the available laboratory methods of quantitative measurement of stimuli such as metal ions, without sacrificing accuracy of measurement.

To do this we took a novel approach of combining existing technologies, namely the fibre optic sensor and smart hydrogel technology. Both technologies have been used to create sensor systems in their own rights, whether it be smart hydrogels used to measure glucose levels<sup>41</sup>, or fibre optic sensor systems to measure parameters, such as distance or stress levels in buildings<sup>20</sup>. There are many variations in fibre optic sensor systems used,

ranging from the light source, the way light is transmitted through the fibre before it is analysed, and the type of fibre used. Keeping in mind that the goal was to provide a cost effective alternative, we developed the simplest possible system, as simplicity is often related to cost-effectiveness and therefore to the successful development of a single sensor platform.

One of the simplest forms of a fibre optic sensor measures the difference in the strength of the light emitted from the source and detects the light returned from a single pass system. The system itself has a user-friendly interface that gives an immediate and simple signal loss measurement, and allows for further manipulation of the data in an Excel spreadsheet. Probes that are manufactured for this system are easy to use, as they only require contact with the sample.

Hydrogels are a well-established material, with well-known synthetic routes that make them ideal for a simplistic manufacturing process<sup>36,37,122,39,41,42</sup>. The RI changes observed, as well as the colour changes which can occur in smart hydrogels, make them suitable for fibre optic sensing systems. Removal of the cladding layer of the fibre and the coating of the exposed fibre core with the smart hydrogel makes the signal sent through the fibre susceptible to the changes that occur in the smart hydrogel<sup>32,79</sup>.

Another appealing factor for the development of this sensor system is the low cost, the ease of fabrication and variation of the probes which can be fabricated in the laboratory. The basic material for the fabrication of the fibre probes is a reel of fibre optic cable of the desired material. In order to manipulate the probe, all that is needed are the appropriate cutting tools and a heat source (like a hair dryer) to manipulate the shape of polymer fibre optical cable, or a flame to manipulate a glass fibre optical cable. For the polishing of the ends of the fibre optic cable, a polishing paper and a fibre holding disc are needed. The exact details of the probe fabrication are covered in the experimental methods chapter.

These factors show that the combination of smart hydrogels and fibre optic sensor technology is ideal, and an attractive field of research with promising potential.

## **Chapter 6. Hydrogels for the detection of water: Results and Discussion**

## 6.1 Introduction

The choice of method of detection of a target species will depend upon the target species, the environment in which the hydrogel will operate in, and the choice of the available chemotropic agents.

For the detection of water, whether it is moisture in the air or water in hydrocarbon media, the hydrogel coating itself can be the sensing agent. Hydrogels by nature are a hydrophilic material; their response to the presence of water will be an associated RI change proportional to their level of hydration<sup>123</sup>. The interaction between the hydrogel and water is a reversible interaction thus such allows for the probe to be used many times<sup>41</sup>.

In the case of sensing a soluble analyte, the ideal sensing molecule would not chemically bind to the target species. The preferred interaction would be a reversible non-chemical binding. One such example is the reversible complexation of water with cobalt, resulting in a colour change of the cobalt<sup>124</sup>. The incorporation of a sensing molecule that has an associated colour change to accompany the RI change of a polymer membrane would be ideal, as sensing the target molecule would be two-fold. Both changes can be detected by the sensing unit.

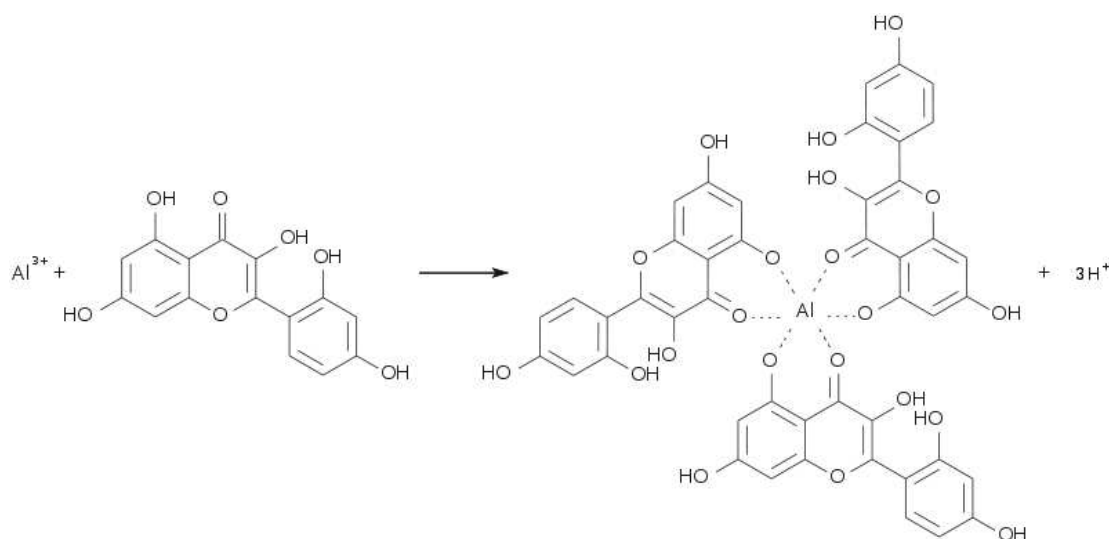


**Figure 57.** Morin chelating with aluminium.



However, this is not always achievable. A more common alternative to a chelating agent for the target analytes is a compound that will have a metal ion that is displaced by the target molecule, resulting in the formation of a precipitate<sup>103,104</sup>. The use of this type of chemotropic agent means that the probe can only be used once.

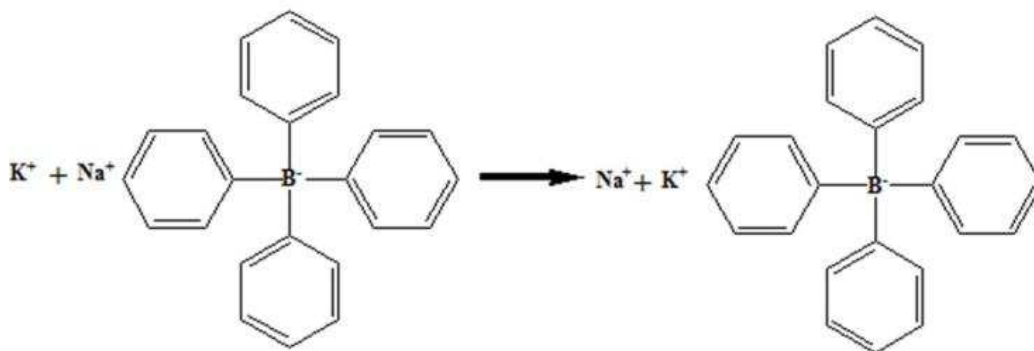


**Figure 58.** Sodium tetraphenylborate undergoing a displacement reaction with potassium to form potassium tetra phenyl borate.

In both systems there is a maximum threshold that the fibre can detect. This threshold will be the maximum amount of the sensing molecule that the polymer membrane can be loaded with. The threshold exists because once all the chemotropic agent has been interacted with, the addition of more target species would not result in any further interactions.

Other factors that have to be considered when choosing the sensor molecule are any known interference from the presence of other molecules and whether the sensor molecule will interact more strongly with one molecule over another. If, for example, a crown ether (like 4'-aminobenzo-15-crown-5) was used, the crown ether will have an affinity to bind positively charged ions. Ions such as magnesium and calcium chelate with crown ethers<sup>125</sup>. However, calcium ions have a higher affinity to chelate with the crown ether, as calcium possesses a larger charge<sup>125</sup>. Therefore if the crown ether was used to sense magnesium then it would be possible for calcium to interfere with sensing. The use of this chemotropic agent as a sensor could only be justified if the solution that the

probe was to be used in could guarantee that no species that could interfere were present.

## **6.2 Hydrogels used for the detection of water**

The desired level of sensitivity of the hydrogel membrane to moisture will determine the ratio of hydrophilic to hydrophobic monomers used in the design of the membrane. For example, the level of hydrophilicity required is higher if the end application is the detection of water in jet fuel at levels of less than 100 ppm. However, the detection of moisture in air requires a hydrogel that is less sensitive, as the levels of moisture in air are a lot higher. A hydrogel that is to be used for the detection of moisture in jet fuel required a higher hydrophilicity, due to the need to aggressively draw moisture into the membrane. Another consideration is that the hydrogel that is to be used in a hostile environment, such as a hydrocarbon media, must have structural integrity that does not allow the hydrogel to break down in the presence of the hydrocarbon.

In both cases, a hydrogel with the appropriate hydrophilicity would be sufficient for the detection of moisture in air or a hydrocarbon media, provided that there are no other molecules or compounds in the hydrocarbon sample that would cause a RI change, resulting in a false reading to be obtained. In cases where this cannot be guaranteed, a chemotropic agent is required.

Another factor that must be considered is the temperature that the probe would be expected to operate in. The glass transition temperature of PMMA is 93.8°C to 149.8°C<sup>126</sup> depending on the composition of the PMMA. At temperatures higher than this, the probe would soften and begin to bend (due to gravity), changing the path length of the light. This would also change the angle of incidence at which the light hits the boundary of the fibre core, resulting in a change in the signal loss and therefore giving a false reading. The use of glass fibre optic probes would overcome this problem. If the operating temperature range were below the glass transition temperature of PMMA, the cost of using a glass fibre probe would be deemed unnecessary.

In the case of fibre optic probes coated with a hydrogel that is extremely sensitive to moisture, an airtight packaging is required for its transportation, in order to prevent the hydration of the hydrogel by moisture from the air. Alternatively it could be possible to calibrate the probe on site. For the purpose of the present project conducted in a laboratory environment, the hydrogel membrane is robust enough that the fibre can be placed into a microwave to dry the coating.

### ***6.2.1 Hydrogels using refractive index change for the detection of water***

Figure 59 shows the relationship between the RI of a hydrogel and the EWC of an hydrogel. As the EWC of a hydrogel increases the RI of the hydrogel decreases. This relationship occurs because water has a lower RI than the hydrogel, thus as more water is incorporated into the hydrogel membrane the RI of the membrane lowers.



**Figure 59.** Variation of refractive index (RI) with EWC for various methacrylate hydrogels at 20°C (filled dots) and at 34°C (empty squares)<sup>127</sup>.

The RI of a hydrogel is dependent on the monomers used in the synthesis of the hydrogel, and the ratio in which these monomers are used. For example, polystyrene has an RI of 1.589 in both dehydrated and “hydrated” forms, because the polymer takes up no water. In contrast, a typical hydrogel such as poly HEMA has an RI of 1.512 in the dehydrated form and 1.435 in the hydrated form. These facts form the basis for an understanding of the design of moisture-sensitive hydrogel-based sensing membranes.



**Figure 60.** Variation in refractive index (RI) with composition for polymers of styrene:HEMA, in both hydrated (triangles) and dehydrated (diamond) state<sup>128</sup>.

Figure 60 shows that an increase in the levels of HEMA present in styrene:HEMA copolymers lowers the RI of the copolymer. For the dehydrated copolymers the relationship is linear; however for the hydrated copolymer the relationship also involves another element - the EWC of the hydrogel. The effect seen here is an additive relationship, described in equation 7. Consequently, as the water becomes part of the network it affects the resultant RI<sup>128</sup>. The amount of water taken up by the copolymer is dependent on the comonomer composition. For example, styrene is a hydrophobic monomer, whereas HEMA is a hydrophilic monomer, thus the refractive index decrease on hydration becomes greater as the proportion of HEMA in the copolymer increases<sup>128</sup>. The RI of a hydrogel decreases as the water content increases because water has a RI of 1.33, which is lower than that of organic monomers<sup>128</sup>. In the absence of water, the RI of the hydrogel is controlled by the RI of the constituent monomers. With the addition of water to a hydrogel it becomes part of the network and therefore also contributes to the RI of the hydrated hydrogel, lowering the hydrogels RI with the addition of water to the

hydrogel membrane<sup>128</sup>. These principles are applied in the contact lens field. For example, the contact lens material Sauflon 70, is a cross-linked copolymer of N-vinyl-2-pyrrolidone and methyl methacrylate. The resulting hydrogel has an EWC of 60%, with a RI of 1.54 when dry, and 1.39 when hydrated<sup>128</sup>. This makes hydrogels ideal for the exploitation of the second condition required for the phenomenon of total internal refraction to occur.

The RI of a hydrogel is an additive property, the value of which is based on the weighted average of the hydrogel components. A hydrogel that has a 20% EWC when hydrated will have a RI that can be calculated using equation 7<sup>128</sup>.

$$\text{RI of hydrated polymer} = (0.2 \times \text{RI water}) + (0.8 \times \text{RI of dehydrated hydrogel})$$

Equation 7.

The hydrogel coated onto the fibre optic cable core will lower the RI of the medium surrounding the fibre optic cable core, when exposed to water. As the RI of the PMMA fibre optic cable core is 1.49, if the hydrogel coating to be used was for example the Sauflon 70 material with a dry RI of 1.54<sup>128</sup>, this would cause light to be lost from the fibre as the RI of the medium surrounding the fibre core is higher than that of the fibre core. If this hydrogel became progressively hydrated until its EWC was reached, the RI of the medium surrounding the fibre core would reach 1.39. The RI of the hydrated Sauflon 70 would result in the occurrence of the second condition for total internal reflection and the light (signal) lost from the fibre would reduce to zero.

It is possible to exploit the first condition for total internal reflection by bending the fibre optic cable to encourage signal loss. This results in a change in the angle of incidence, causing light to be lost from the fibre optic cable. In the work carried out in this project, the fibre optic cables have a "U" bend to form a probe to encourage a signal loss. This is done so that the RI change of the hydrogel in the presence of water reduces the signal loss as the concentration of water increases.

The probes used for testing were prepared using the method stated in the experimental methods chapter for “U” bend PMMA probes. For the blank control fibre, the cladding layer was removed and no coating was applied to the exposed section of the fibre core. The connection to the interrogation system was made with butt-to-butt connections of the polished probe ends to the PMMA patch cables (connection cables) attached to the interrogation box, which again were butt-to-butt joints. As the core of the fibre used for both the patch cables and the probe cable was 1000 $\mu\text{m}$ , the light lost from these connections was negligible compared to the light that it transmitted across the connections. The interrogation system was clamped using a retort stand and clamps, so that the system and the connected probe were in a vertical position to allow for samples to come into contact with the probe, without bending the probe between samples and thus avoid any signal loss due to cable bending.

The first test run was the control blank carried out with the PMMA probe. In this test, the probe was prepared as any other “U” bend probe, except that no coating is applied to the core of the probe. In the testing procedure the uncoated fibre optic probe is subjected to three samples of jet fuel, containing 0%, 3% and 5% water by volume. The signal loss is initially recorded with the probe in air as a reference medium. These levels were chosen because at approximately 5% water becomes immiscible with hydrocarbon liquids. In this test it would be expected that as the concentration of water in jet fuel increases, the signal loss would decrease, because the RI of the jet fuel, which is mainly octane, typically is 1.395 at 25°C<sup>129</sup>. Addition of water (which has a RI of 1.33) to jet fuel lowers the RI of the resulting solution. The RI of the PMMA fibre core is 1.49<sup>13</sup>, thus the addition of the water to the jet fuel, whose RI is already below that of the RI of the fibre core, should reduce the observed signal loss.

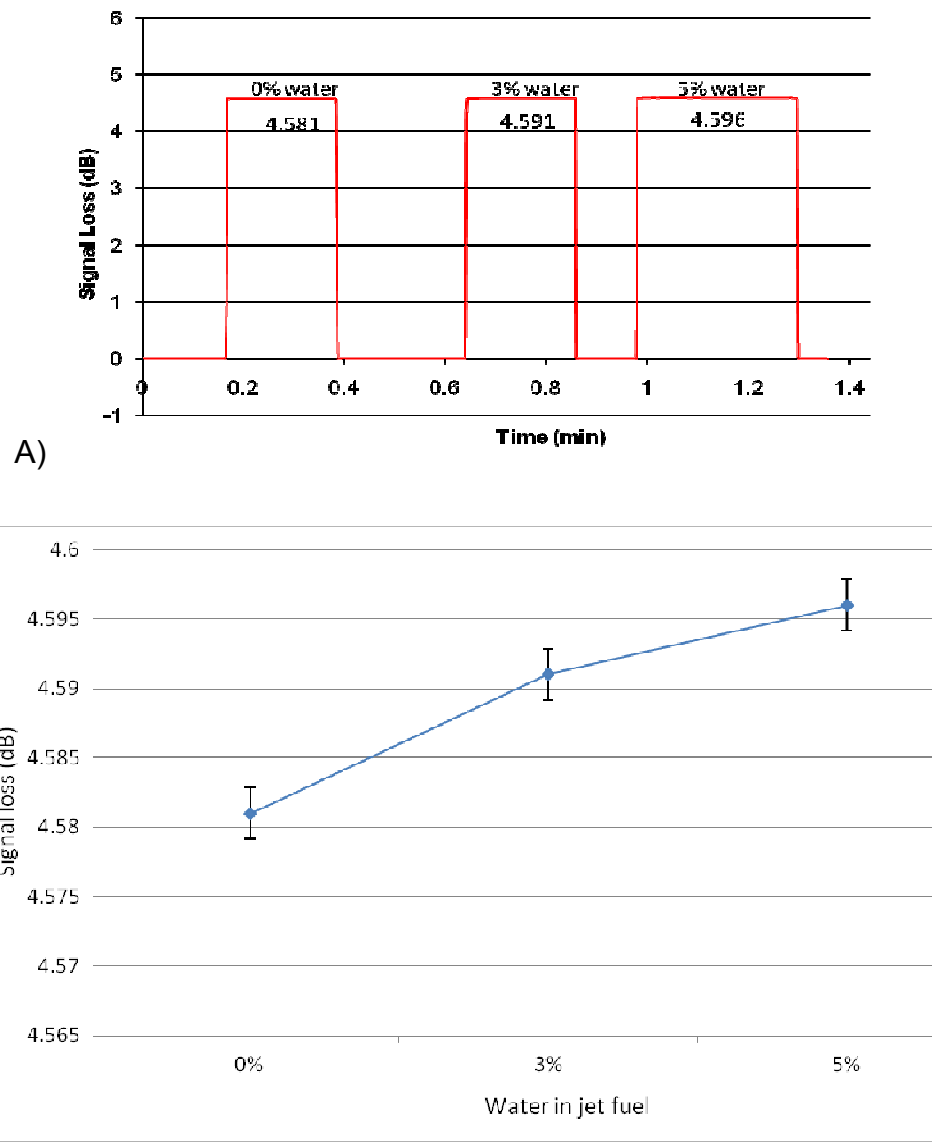


**Figure 61** A) An uncoated PMMA “U” bend fibre subjected to jet fuel samples containing 0, 3 and 5% water. B) Average signal loss values for 0, 3 and 5% water in jet fuel obtained from an uncoated “U” bend PMMA fibre.

The results from the experiment show a pattern of increasing signal loss with increasing levels of water. From the obtained results, the signal loss does not follow the predicted pattern. Increasing the level of water should reduce the RI of the jet fuel/water solution, therefore reflecting the light that hits the core-resolution boundary at the necessary angle of incidence. If the two criteria for total internal reflection are met, the light should be totally reflected back into the fibre optic cable core. However, when this phenomenon is observed most of the light is reflected back into the fibre core. However, some light escapes from the



core of the fibre. This light is called the evanescent wave. The escaping evanescent wave is a near standing wave, and its strength exponentially decays from the boundary where the wave originated<sup>138</sup>. Since the evanescent wave model is only a theoretical one, the developed system may not conform to it. The contact fluid of the sample may not have a uniform RI. This may partly explain why the developed system does not follow the pattern for signal loss vs water content that would be expected.

For the detection of water in jet fuel, three coatings, namely DH5, DH8 and DH9 were investigated (compositions listed below).

**Table 4.** The compositions of hydrogels used for sensing water in jet fuel.

<i>Macromer</i>		<i>DH5</i>	<i>DH6</i>	<i>DH7</i>	<i>DH8</i>	<i>DH9</i>
<b>Monomer</b>	RI of monomer					
2,2,2, trifluoro- ethylacrylate	1.35				6.25g (25%)	
HEA 45% sol	1.505	4.5g (6%)	2.25g (10%)	2.25g (10%)	1.5g (6%)	4.5g (20%)
SPA	-		4.5g (20%)		6.25g (25%)	1.13g (5%)
NVNMA	1.484	4g (5.5%)	5.6g (25%)	5.6g (25%)	10.94g (44%)	7.88g (35%)
ACMO	1.472	4g (5.5%)	5.6g (25%)	5.6g (25%)		7.88g (35%)
AGA	-		4.5g (20%)			1.13g (5%)
CoSPA				4.5g (20%)		
NaAMPs 50% sol	1.4220	60g (83%)		4.5g (20%)		

The coating DH5 was designed as a water scavenging hydrogel to attract water from the jet fuel. NaAMPs is a hydrophilic monomer due to the sulfonate group

at the end of the molecule, which is negatively charged and attracts and binds water. HEA contains a hydroxyl group which is used to attach NMA to the macromer backbone via a condensation reaction. The use of NMA allows for the addition of an unsaturated C=C bond to enable the macromer to be cross-linked. ACOMO and NVNMA are used as inert monomers, because of their lack of functionality (except for the C=C bond), in order to control the properties of the resulting hydrogel, i.e., their hydrophilicity, pH-sensitivity and so on.

The DH5 hydrogel is designed to give specificity to the fibre optic probe for water detection. Signal loss from an uncoated (uncladded) fibre optic cable probe is caused by the change in the RI of the solution, controlled by the component parts of the solution. Any adjustment in the component parts would cause a RI change in the solution, and therefore a signal loss change. Hence the use of a hydrogel that is designed to bind water has an associated RI change. This means that the signal lost from the system will be due to changed water levels and not some other component of the solution.

Coating DH5 was prepared by mixing the monomers listed in table 4 in 95% of the solvent system (listed in the same table) in the polymerisation rig described in the experimental methods chapter. The solution was mixed for 30 minutes in the reaction vessel at 60°C, under nitrogen. In parallel, the initiator was mixed with the other 5% of the solvent system and left on a shaker bed for 30 minutes. The resulting initiator solution was then added to the monomer mixture in the reaction vessel via a syringe through one of the side arms. Next the reaction mixture was left stirring at 60°C for two hours under nitrogen. Once the reaction was complete, the reaction vessel was shut down and the solution is left to cool to room temperature for one hour. At this point, a visual observation of a change in the viscosity of the reaction mixture is an indication that polymerisation has occurred. Once cooled to room temperature, the reaction mixture was transferred to a beaker containing one litre of acetone to precipitate the linear macromer. The precipitate is then transferred to a watch glass, put in a vacuum oven at 40°C and left over night to remove any solvent. Next the linear macromer is functionalised to allow for the macromer to be cross-linked to form a hydrogel. In a sample vial covered in tin foil, 0.4g of the

linear macromer was dissolved in 5.5ml of a 0.3% HCl MeCN:H<sub>2</sub>O (1:1) solution, and left on a shaker bed for 30 minutes to ensure that the macromer was completely dissolved. To this solution 0.08g NMA was added and vigorously shook by hand for 5 minutes. The sample vial was then placed into a water bath at 60°C for 2 hours, and was shaken by hand every 30 minutes for 2 minutes. Using a Pasteur pipette, 3 drops of a solution of 1g ebacryl and 0.3g Igracure 184 were added to the resulting solution and it was placed on a shaker bed for 15 minutes. The U bend PMMA fibre prepared using the method described in the experimental methods chapter is dipped into the solution and placed under a UV lamp for 30 minutes to cure the coating on the fibre. This step was repeated one more time.

When conducting the test, the sensor system was set up in the same manner as for the blank fibre test, using a retort stand and clamps to put the system and the probe in a vertical position. The sensor system was set to record signal loss at a rate of one reading per second, in air. Next the sample vials containing the samples are then introduced to the fibre.

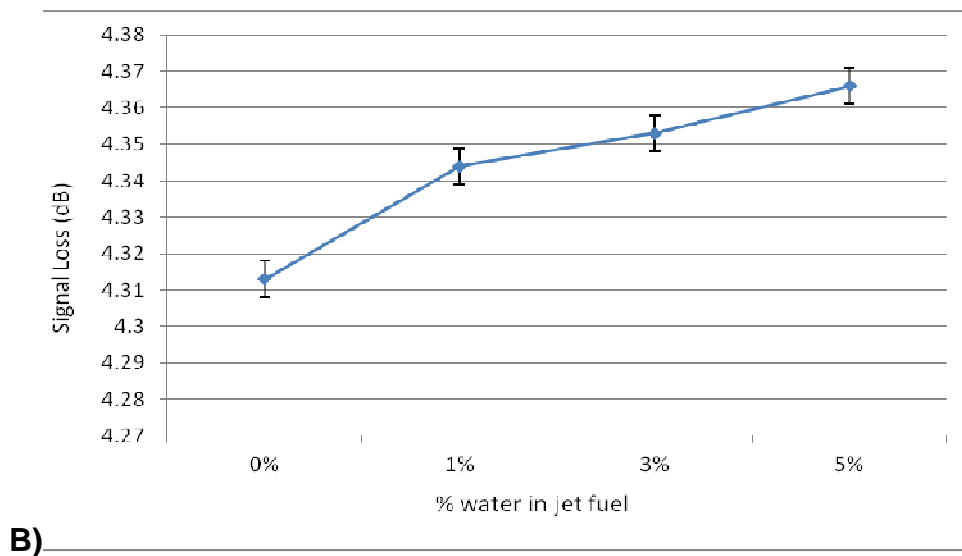
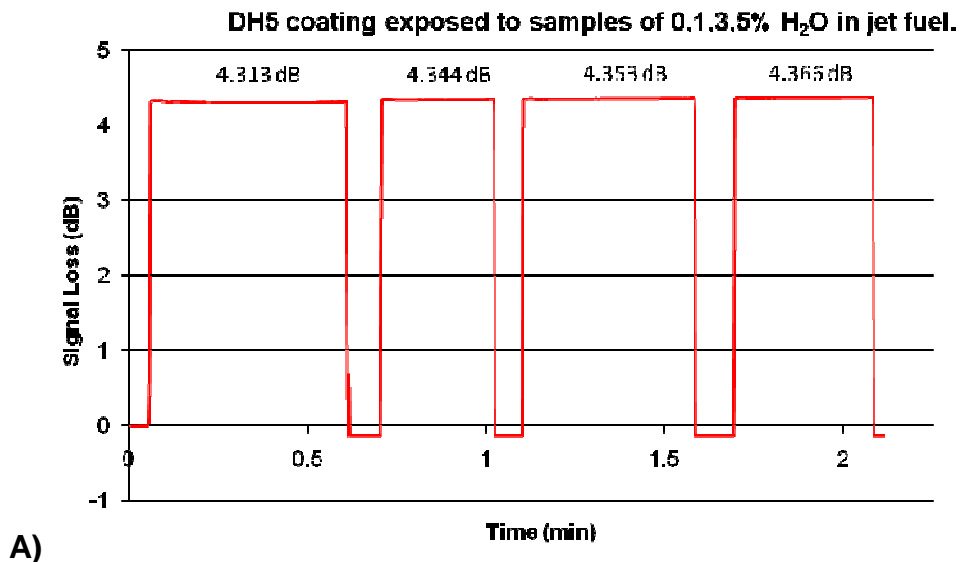


**Figure 62.** A) A plot of signal loss vs time for a PMMA “U” bend probe coated with the hydrogel DH5 exposed to samples of jet fuel containing from left to right, 0, 1, 3 and 5% water. B) A plot of the average signal loss vs the % water in jet fuel.

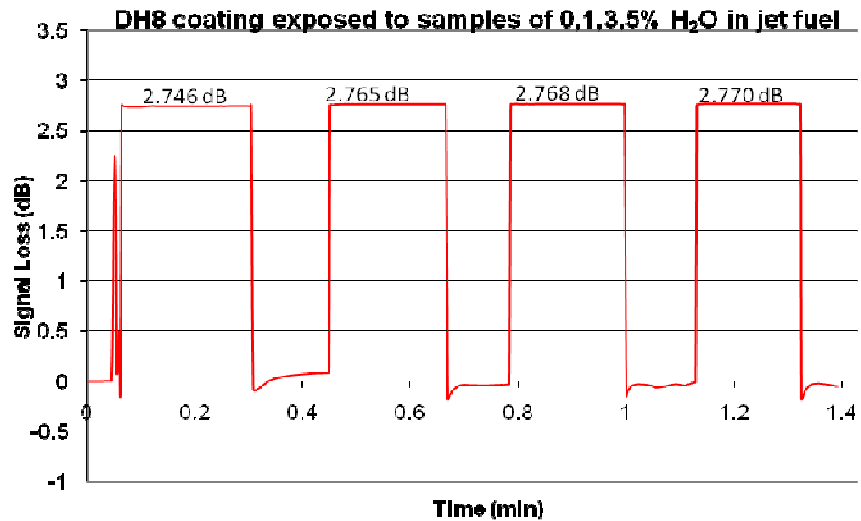
Figure 62 shows increasing signal loss with increased levels of water in jet fuel. These results do not conform to the ideal model of signal loss decrease with the increased levels of water, i.e. with the reduction in RI of the medium surrounding the fibre core. This pattern is repeated every time the test has been carried out. It is therefore accepted for the purpose of the research in hand that

the desirable pattern is an increase in signal loss with increase in the levels of water.

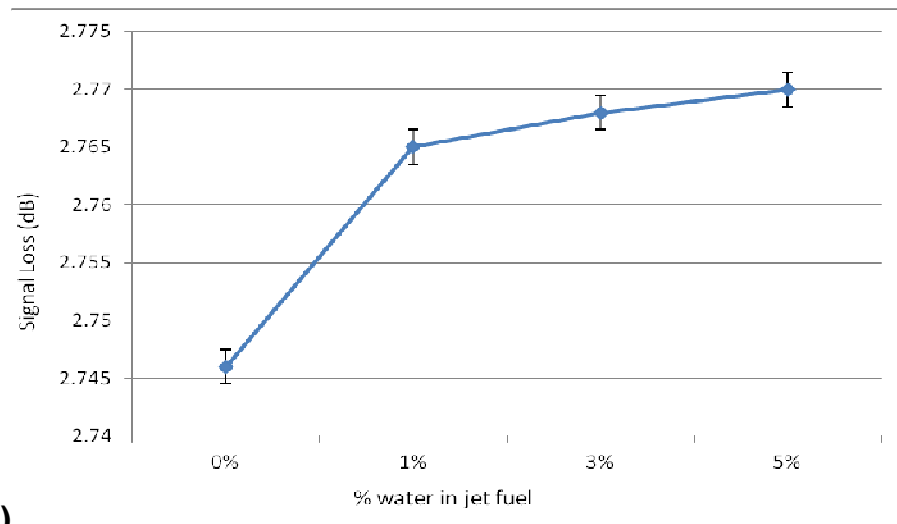
When the sample solution enters the hydrogel membrane, it causes the RI of the hydrogel to change causing the pattern observed in figure 62. The difference between samples is the introduction of higher levels of water, which has a RI of 1.33. This increased level of water results in a change of the base RI of the jet fuel, which is mainly octane with a RI of 1.395. As the solution enters the hydrogel and becomes a part of the hydrogel matrix it lowers the RI of the hydrogel, causing more signal to be lost from the fibre optic cable probe.

The coating DH8 was designed to have a low RI in order to observe how this affected the signal loss in comparison to a hydrogel coating with a higher RI. A lower RI coating is achieved by incorporating monomers such as fluorinated with a low RI into the linear polymer backbone. DH8 is a low RI hydrogel used for sensing low levels of water in hydrocarbon media. The monomer 2,2,2-trifluoro ethylacrylate is used to lower the RI of the DH8 hydrogel coating. In addition, SPA is used to increase the hydrophilicity of the hydrogel, as it contains sulfonate groups. SPA enables the hydrogel to absorb the low levels of water present in the sample.

The method for the preparation of the DH8 hydrogel membrane and its coating onto a U bend PMMA fibre is the same as for DH5 described earlier. The monomers used and quantities are listed in table 4.



A)



B)

**Figure 63.** A) A plot of signal loss vs time for a “U” bend probe coated with the hydrogel DH8 exposed to samples of jet fuel containing from left to right, 0, 1, 3 and 5% water. B) The average signal loss vs % water in jet fuel for a U” bend probe coated with the hydrogel DH8

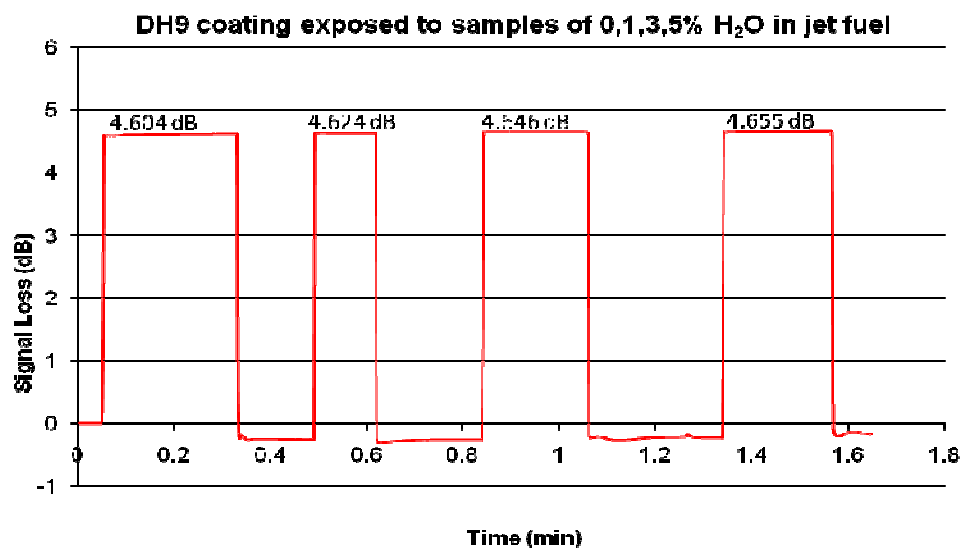
Figure 63 shows that the increase in water in jet fuel causes an increase in signal loss. The pattern that emerged when using a low RI monomer is in accordance with the patterns observed for an uncoated and a DH5 coated U bend PMMA fibre optic probe. However, the signal loss observed with a DH5 and an uncoated PMMA fibre in the water:jet fuel samples were of an intensity

of over 4dB. The use of the fluorinated monomer in DH8 resulted in the signal loss observed to be lowered to below 3dB.

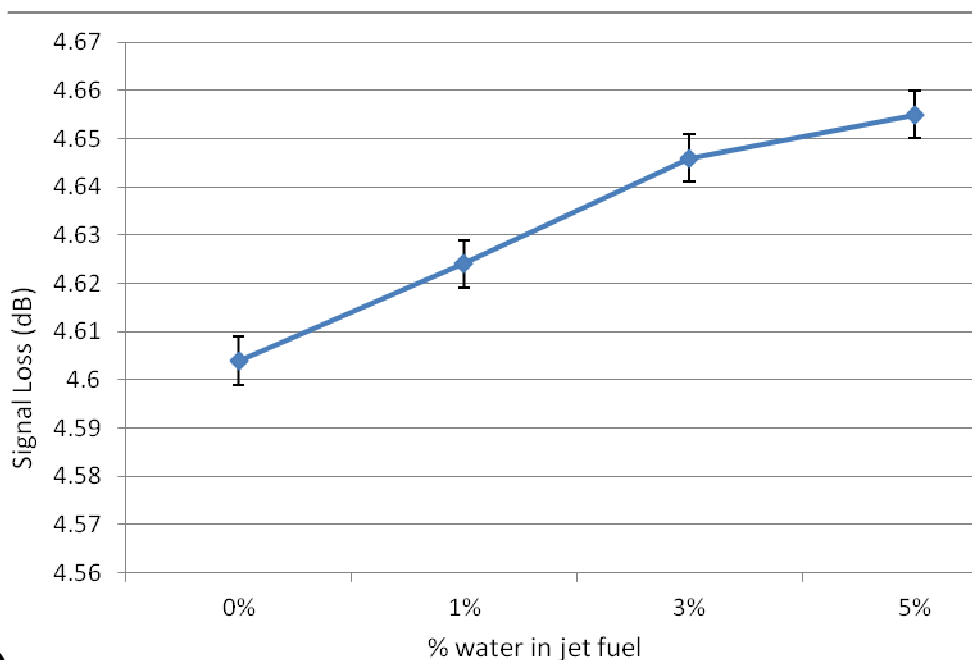
In order to increase the hydrogel's maximum sensitivity to water and ensure the absorption of the water present in the sample into the hydrogel matrix, the hydrogel needs to have maximum hydrophilicity. Carboxylic acids have a larger fixed charge density than sulfonate groups. This is due to the size difference of sulfur and carbon. Carbon is smaller than sulfur and therefore the charge it possesses is spread over a smaller area. As a result, carboxylic acid groups have a larger fixed charge density, making them more hydrophilic than sulfonate groups.

DH6 was prepared by following the same method as for DH5 preparation, and using the monomers listed in table 4. However, the needed to dissolve 0.4g of linear macromer was 22ml of 0.3% HCl MeCN:H<sub>2</sub>O (1:1) solution. When the DH6 coating was exposed to samples of jet fuel containing water, the visible swelling was over double of its initial unhydrated thickness. On the contrary, the DH5 and DH8 coatings did not show any visible size changes when hydrated. When removed from the water:jet fuel sample, the DH6 coating had swollen and in parts detached from the fibre optic probe. The low level of cross-linking and the high hydrophilicity of the coating caused the hydrogel matrix to become saturated to the point where the cross-linking within the hydrogel network broke. This meant that the coating was no longer structurally sound and had no binding to the fibre optic cable surface, resulting in its detachment from the fibre.

DH6 did not produce a useable coating due to its hydrophilicity. A new composition was prepared, DH9 (listed in table 4), with lower levels of SPA and AGA, and higher levels of HEA, in order to allow for a higher cross-link density.



**A)**



**B)**

**Figure 64.** A) A plot of signal loss vs time for a “U” bend PMMA probe coated with the hydrogel DH9 exposed to samples of jet fuel containing from left to right, 0, 1, 3 and 5% water. B) a plot of average signal loss vs % water in jet fuel for a “U” bend PMMA probe coated with the hydrogel DH9



Figure 64 shows that the increase in water in jet fuel causes an increase in signal loss. The effect of increasing levels of water in jet fuel is a lowering of the RI of the hydrogel, causing a signal loss increase.

The effect of the hydrogel composition on signal loss can be seen in figure 65.

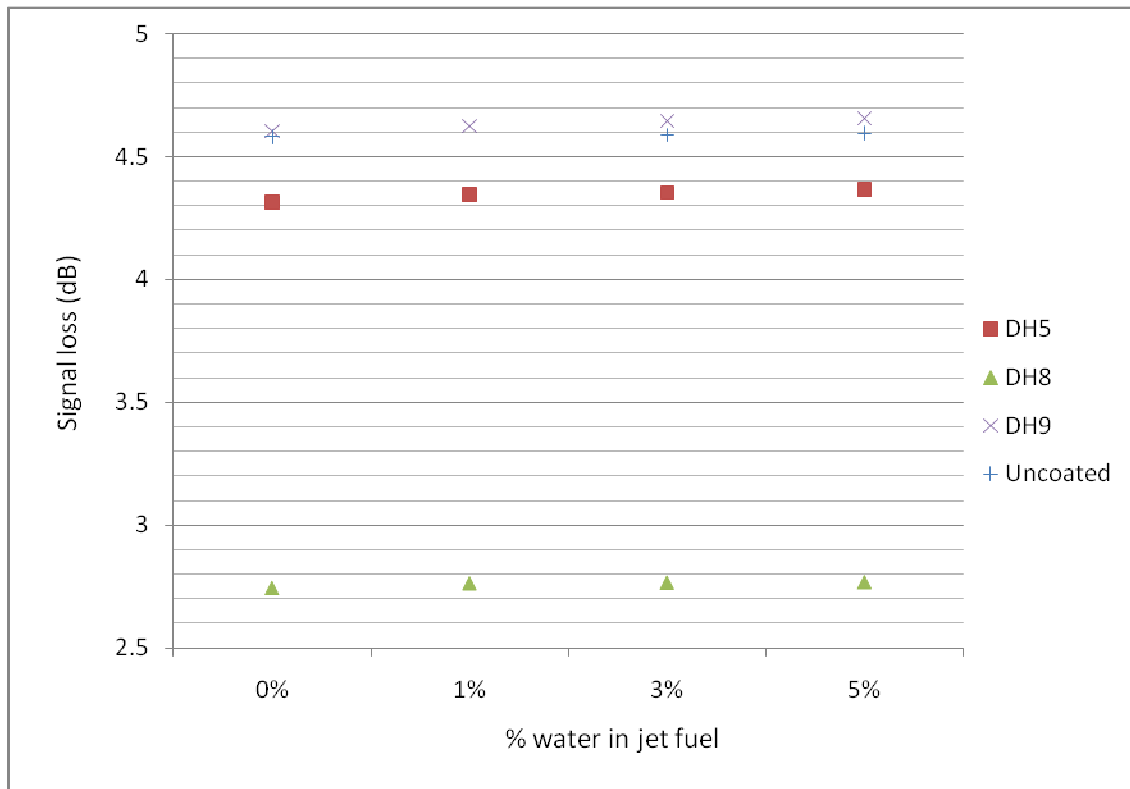


**Figure 65.** A comparison of the average signal loss values generated by an uncoated, and DH5, DH8 and DH9 coated “U” bend PMMA fibres optic probe for a range of jet fuel containing water.

With and without a hydrogel coating the signal loss is increased with the increase of water (however the addition of any liquid with a RI lower than jet fuel would cause the same signal loss change, hence the need for a hydrogel membrane which is sensitive to water). This is observed because the addition of water to jet fuel lowers the RI of the solution. In turn this causes the RI of the medium surrounding the core of the fibre optic cable probe to lower. In theory, the lower RI of the medium surrounding the fibre core should decrease the signal loss observed. The reason is that the conditions of total internal reflection require that the RI of the medium surrounding the core of the fibre be lower

than that of the RI of the core of the fibre. However, the observed signal loss follows the opposite pattern; an increase in signal loss when the RI of the medium surrounding the core of the fibre is lowered. This is because the evanescent wave model is a theoretical model, and the developed sensor system may not conform to this ideal model. Furthermore, the RI of the sample solution may not be uniform and the hydrogel may have areas that are more hydrophilic than others. Nevertheless, the experimentation so far has shown the pattern without exception.

Hydrogel composition plays an important role in terms of the signal loss observed. The signal loss difference from 0% to 5% water in jet fuel in the 3 hydrogels tested and the blank fibre test does not exceed 0.1 dB. This range over which the observed signal loss occurs is dependent on the hydrogel. For a U bend PMMA probe with no coating around the exposed section of the fibre core the signal loss ranges from 4.581 dB to 4.595 dB. The DH5 hydrogel coating showed a signal loss range from 4.314 dB to 4.366 dB, which is lower than the range of a blank fibre. This is observed due to the fact that the hydrogel has a lower RI than jet fuel. In this sensing experiment, the RI change of the hydrogel in response to the lowering of the RI due to the presence of water in jet fuel has caused signal loss to rise. However, when the DH8 coating is compared to the DH5, the DH9 and the blank fibre, the expected pattern should be a decrease in the signal loss as the RI of the medium surrounding the core of the fibre lowers, as seen in figure 65. The DH8 coating shows a signal loss range of 2.746 dB to 2.770 dB, which is approximately 1.6 dB lower than the DH5 coating, with a signal loss range of 4.314 dB to 4.366 dB. This difference in the signal loss range is due to the fluorinated monomer used in the synthesis of the linear macromer for the DH8 hydrogel. The RI of the DH8 is significantly lower than that of the coatings DH5 and DH9, resulting in the difference in the intensity of the signal lost from the fibre.

### **6.2.2 Hydrogels containing cobalt salts for the detection of water**

Although the signal loss in these experiments shows an opposite relationship, to what would be expected this has remained constant throughout testing.

Another way to enhance the control mechanism for signal loss due to external stimulus is to use a chemotropic agent. A chemotropic agent can be one of two types; a chelating molecule which gives rise to a colour change when the molecule that it chelates with is present, or a chemotropic agent which undergoes a displacement reaction with a particular molecule to form a precipitate.

In the case of a chemotropic agent entrapped in a hydrogel membrane, a colour change is observed in the presence of the target species. This causes light to be emitted from the hydrogel and back into the fibre optic cable. The colour change of the hydrogel due to the chemotropic agent will be proportional to the amount of stimulus present, and therefore the intensity of the colour will be dependent on the amount of the stimulus. In the particular setup the stimulus is water and the amount of water will determine the intensity of the colour, and a decrease in signal loss should be observed. In addition to the signal loss decrease from the lowering RI of the hydrogel due to the addition of water, the chemotropic agent will increase the amount of light reflected back into the fibre core, causing a further decrease in signal loss. From the experiments conducted with the sensor system for the detection of water using RI-changing hydrogels, the expected result is an increase in signal loss with increasing level of water in jet fuel.

Within the structure of a chemotropic agent there is a central atom or molecule which acts as a Lewis acid, coordinated by one or more atoms or molecules which act as Lewis bases<sup>104</sup>. One example is cobalt (II), which can be coordinated by six ligands<sup>104</sup>, as seen in Figure 66.

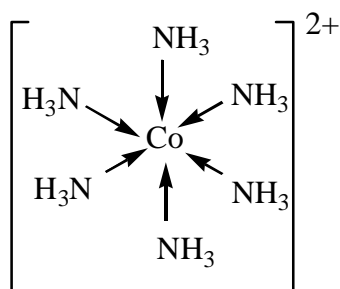


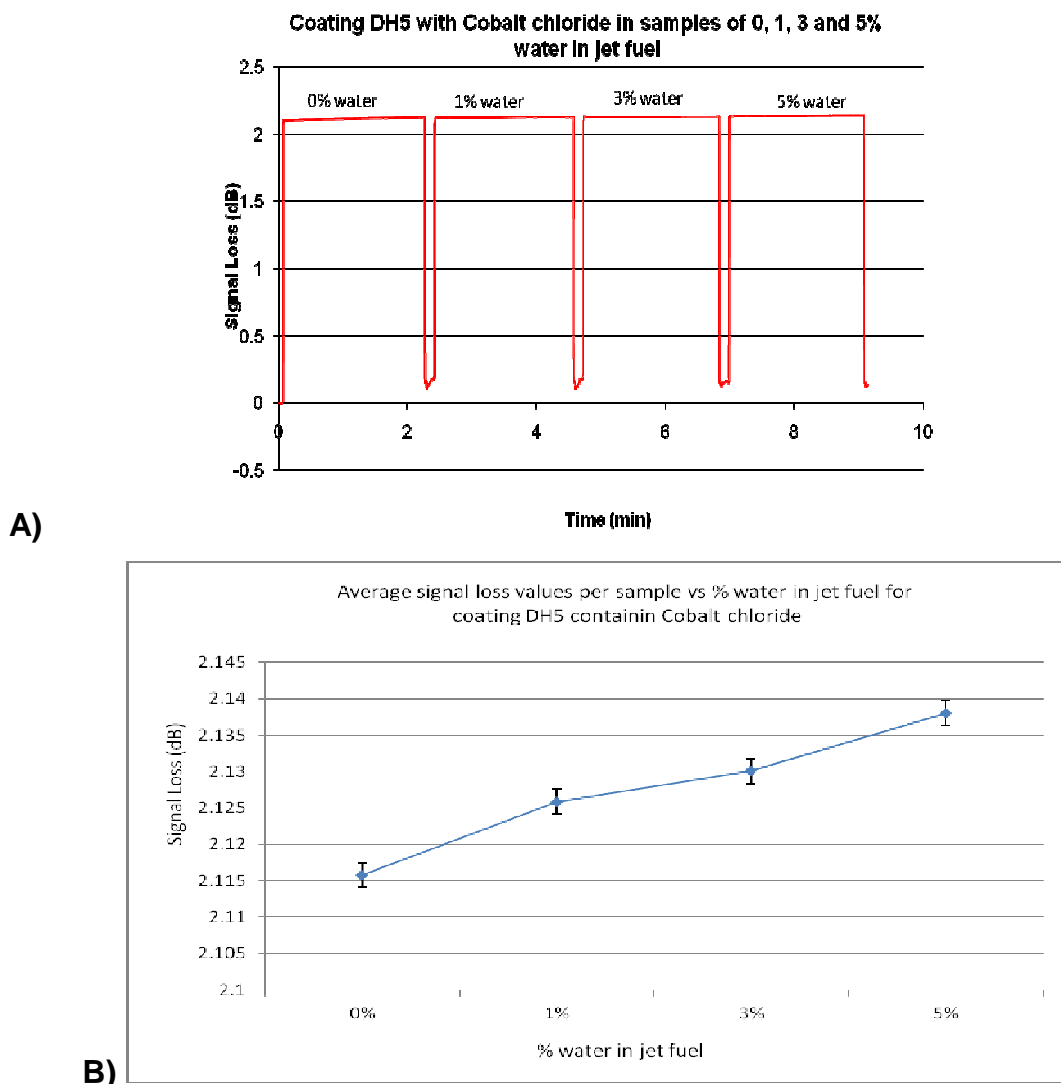
**Figure 66.** Example of a coordinated complex. Cobalt (II) being coordinated by 6 ammonia ligands.

For the detection of water in jet fuel the chemotropic agent cobalt (II) chloride was used. When water is introduced to cobalt (II) chloride it turns colour from blue to red.

Cobalt (II) Chloride was entrapped into the hydrogel membrane by hydrophobic entrapment<sup>97</sup>. Hydrophobic entrapment uses the hydrophobic parts of a hydrogel membrane to surround the hydrophilic cobalt (II) chloride. This prevents the cobalt (II) chloride from moving from its position within the membrane<sup>97</sup>. Whilst this method entraps the chemotropic agent, it does not affect the ability of the solvent to enter the hydrogel and hydrate the chemotropic agent within the hydrogel network<sup>97</sup>. In the ideal case, the presence of the stimulus in the solvent would cause a decrease in the signal lost from the sensor system. The presence of the stimulus causes a colour change within the hydrogel as it chelates with the chemotropic agent to form a coordinated complex<sup>104</sup>. Any colour change will also have an intensity change associated with it, because the more stimulus present the more coordinated complexes form, resulting in a more intense colour change. The colour change of the hydrogel will cause some of the light to be reflected back into the fibre core, causing a signal loss change. In the case of the sensor system under investigation, a red LED is the light source and cobalt chloride is the chemotropic agent, which goes from blue when dehydrated to red when hydrated. The signal loss that should be observed from increased levels of water in jet fuel is a decrease in signal loss as the colour change of the cobalt chloride occurs. However, given the fact that the observed pattern is reversed

to the ideal situation in the sensor system previously discussed, the expected signal loss observed will be an increase in signal loss with an increase in water.

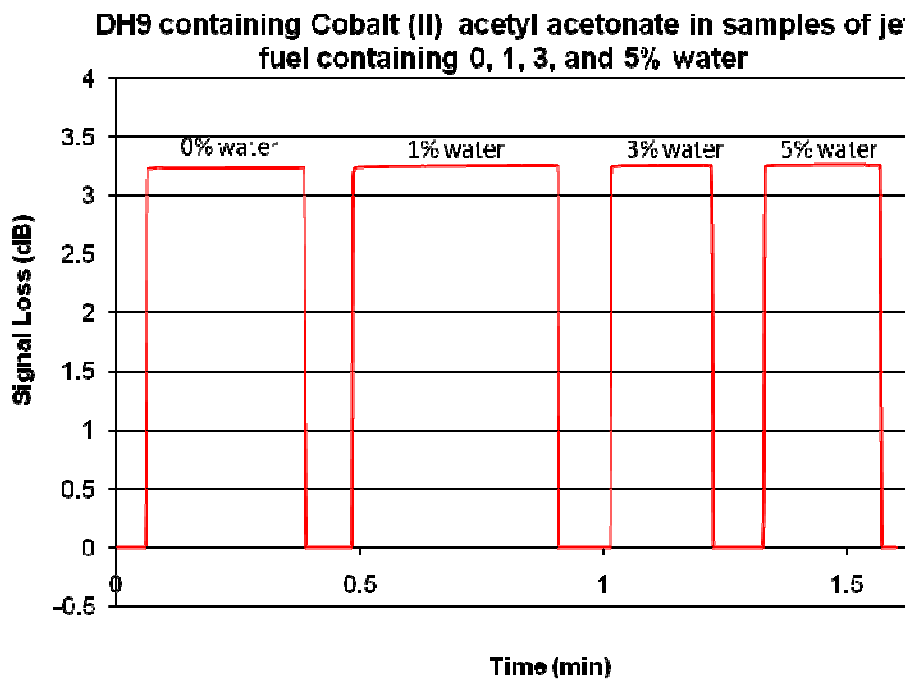
The DH5 coating was prepared as described in section 6.2.1, except from 3 drops of a solution of 1g ebacryl and 0.3g Igracure 184, 0.04g of cobalt (II) chloride was also added. Following this the resulting solution was placed on a shaker bed for 30 minutes to ensure that the cobalt (II) chloride has dissolved. The coating was then applied to a “U” bend PMMA fibre optic probe using the same method described in 6.2.1.



**Figure 67.** A) Signal loss data collected for a “U” bend PMMA fibre probe coated in hydrogel DH5 containing cobalt (II) chloride, for a range of water in jet fuel. B) The average signal loss values obtained for each sample of jet fuel containing water.

As shown in figure 67, the relationship observed is that with increasing levels of water in jet fuel, the signal loss recorded also increases. The observed signal loss is in line with the established pattern. Figure 67 B graph shows an almost linear relationship between signal loss and the level of water in the sample, as expected. An increase of water in the sample causes more complexes to be formed between the water and the cobalt chloride entrapped within the network. With increasing number of coordinated complexes, the intensity of the colour change is visually observed. In addition, the RI of the hydrogel changes, as discussed in section 6.2.1, and this is registered as an increasing signal loss by the sensor system.

Coating DH9 was prepared using the method described in section 6.2.1, except that 0.04g of cobalt (II) acetyl acetonate was added in addition to the 3 drops of a solution of 1g ebacryl and 0.3g Igracure 184. The resulting solution was placed on a shaker bed for 30 minutes to ensure that the cobalt (II) acetyl acetonate has dissolved. Finally the coating was then applied to a “U” bend PMMA fibre optic probe, using the same method described in 6.2.1. Cobalt (II) acetyl acetonate, like cobalt chloride, is coordinated by 6 water molecules.



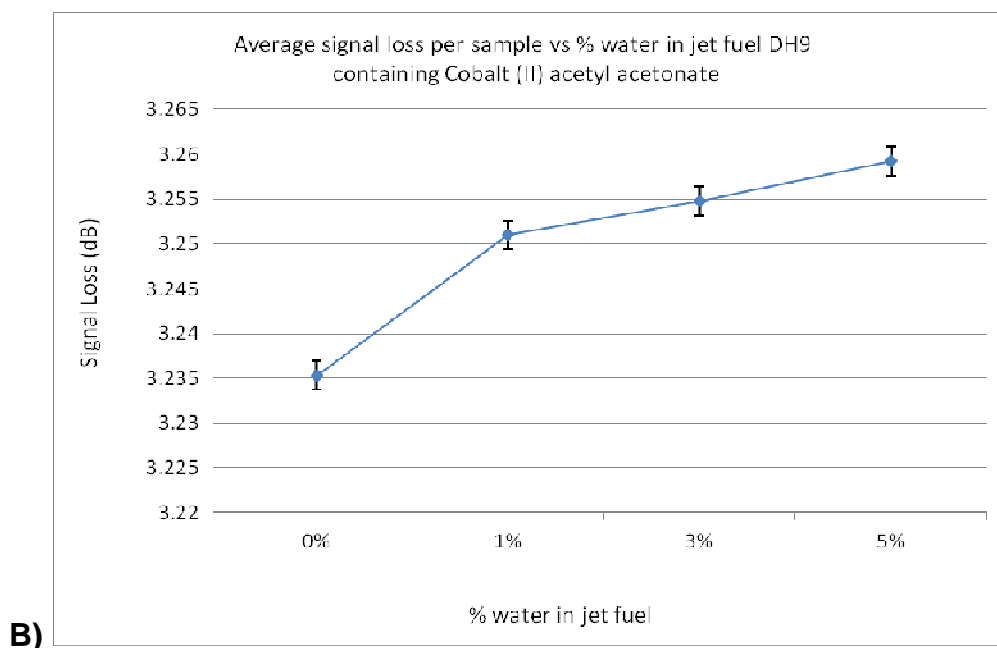
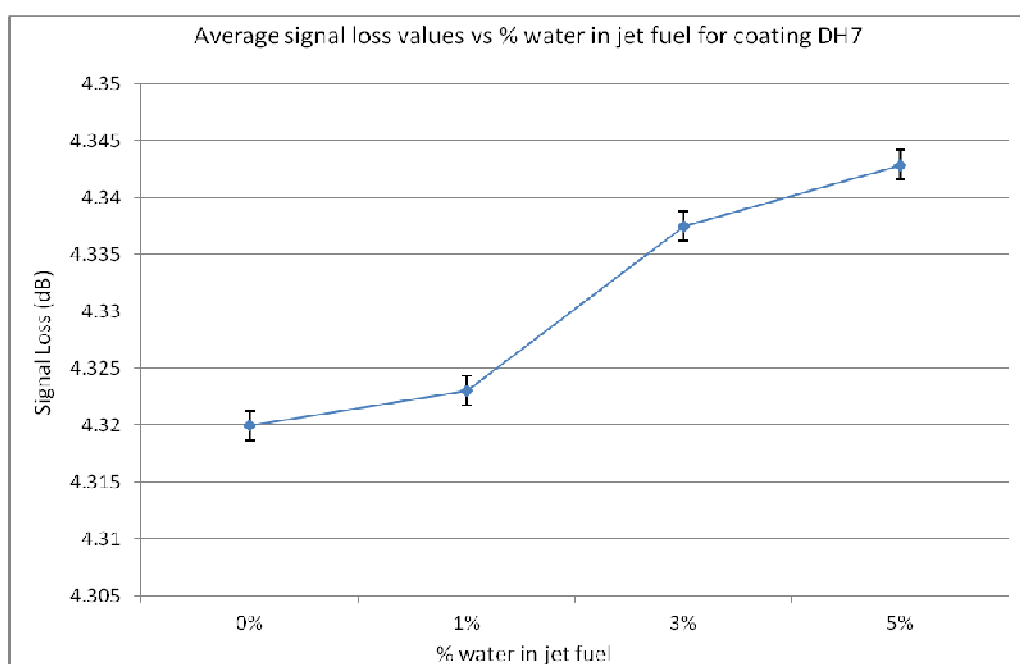


**Figure 68.** A) Signal loss data collected for a “U” bend PMMA fibre probe coated in hydrogel DH5 containing cobalt (II) acetyl acetonate, for a range of water in jet fuel. B) The average signal loss values obtained for each sample of jet fuel containing water.

From figure 68 it is observed that with increasing levels of water in jet fuel, the signal loss increases. Again, the pattern observed with the DH9 cobalt (II) acetyl acetonate coating is the same as with DH5 cobalt (II) chloride, due to the increasing levels of water presenting more ligands to complex with the cobalt (II). This in turn causes a more intense colour change, which, together with the RI change, causes more light to be lost from the system.

Another method of entrapment of a chemotropic agent within the hydrogel network is to chemically bind the agent to the polymer backbone. This can be achieved utilising a displacement reaction to replace one metal ion in a monomer with a different one. SPA was the monomer used to undergo a displacement reaction in the presence of excess ammonia. Cobalt (II) chloride was used to displace potassium. Cobalt (II) is the chemotropic agent to be used to chelate with water molecules. The resulting CoSPA was then used as one of the monomers for the free radical polymerisation to synthesize the linear macromers used to produce the DH7 coating. Advantages of utilising this

method of entrapment is that because the chemotropic agent is chemically bound into the backbone of the hydrogel, it cannot leach out. Another advantage lies in the fact that the chemotropic agent is one of the monomers used to form the hydrogel, making it possible to increase the levels of chemotropic agent and therefore the maximum amount of water it can detect. However, consideration must be given to the other properties of the hydrogel. The properties that an hydrogel exhibits is due to the functional groups present in the monomers used in the synthesis of the hydrogel. Just like with the chemotropic agent, the degree to which each individual property is exhibited is related to the proportion of the monomer to which the property is attributed.



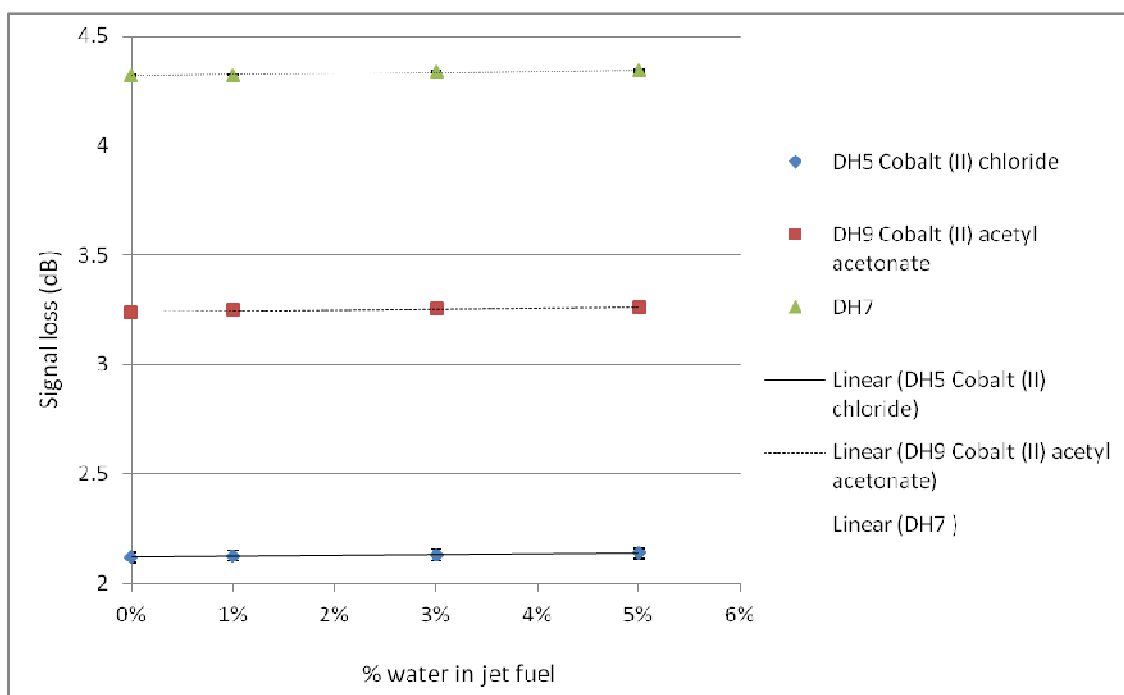
**Figure 69.** The average signal loss values obtained for a “U” bend fibre optic probe coated in DH7 exposed to 0, 1, 3 and 5% water in jet fuel.

Figure 69 shows that with increasing levels of water the signal loss increases. As in the cases where the coatings DH5, containing cobalt (II) chloride, and DH9, containing cobalt (II) acetyl acetonate, were used, the increased signal loss occurs due to the higher level of water causing the formation of more coordinated complexes. This in turn causes a more intense colour change which, (in combination with the RI change), is detected by the sensor system.



The method of chemically binding the chemotropic agent into a monomer showed a positive relationship between signal loss and level of water in jet fuel. Nevertheless, for the purpose of detecting low levels of water the need for such a high level of loading which could be achieved by chemically binding the chemotropic agent into the polymer backbone, is not required. Therefore, the additional steps of chemically binding the chemotropic agent into a monomer are unnecessary for the purpose of this application. Leaching of hydrophobically entrapped chemotropic agents is not an issue if the amount of the chemotropic agents within the hydrogel is sufficiently low, but still enough for the level of detection required.

The above holds true wherever low levels of target molecules are to be detected. If the sensing of higher levels of water was desired, where hydrophobic entrapment of higher levels of chemotropic agent could not be achieved through hydrogel composition manipulation, this route of chemically binding the chemotropic agent would be a viable solution.



**Figure 70.** A comparison of the average signal loss values generated by the coatings DH5 containing cobalt (II) chloride, DH9 cobalt (II) acetyl acetonate,

and DH7 coated onto a “U” bend PMMA fibre optic probe for a range of jet fuel containing water.

All three coatings when tested show an increase in signal loss with increasing levels of water in jet fuel, as shown in figure 70. The increase in water levels causes the chemotropic agents to undergo a colour change, which is more intense with increased levels of water, because water causes more coordinated complexes to form. The DH7 coating uses the monomer CoSPA as the chemotropic agent. Incorporating the chemotropic agent into the macromer backbone prevents any of the chemotropic agent from leaching out of the hydrogel coating, as the cobalt is ionically bonded to the covalently bonded SPA. This technique of incorporating the chemotropic agent into the hydrogel allows for a higher loading of the chemotropic agent to be achieved. The higher loading would allow for a higher level of water to be detected. Dependent on the level of water to be sensed, the method can be used where suitable loading via hydrophobic entrapment could not be achieved. In the detection of low levels of water this method of entrapment is unnecessary, as the low levels of water require less chemotropic agent. Therefore the additional synthetic steps for the production of CoSPA are unnecessary, in terms of costs and time. The levels of loading achieved with coatings DH5, and DH9 proved adequate for the detection of water in the levels tested.

### ***6.2.3 Sulfonated hydrogels containing organic dyes for the detection of water- methyl orange***

Another method for the detection of water is to use a chemotropic agent such as methyl orange, typically used as pH indicator in order to measure the acidity of the solution.

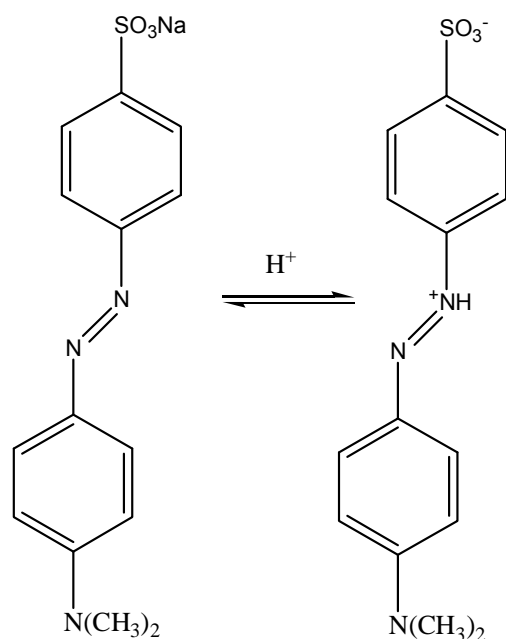


**Figure 71.** Methyl orange being protonated by  $H^+$ , undergoing a colour change from orange to yellow.

In the presence of acids, methyl orange becomes protonated and has a colour change from orange to yellow. The amount of  $H^+$  available in solution will determine the intensity of the colour change, as the colour observed is due to the number of protonated methyl orange molecules. As discussed in section 4.3 and 4.4, pH indicators can be hydrophobically entrapped within a hydrogel network and this principal of entrapment can be used for a wide variety of colourimetric agents, as seen in section 6.1.2, and as demonstrated in the following chapter. This method of entrapment is used to entrap methyl orange into the DH9 hydrogel coating.

Coating DH9 was prepared using the same method as in section 6.2.1, except that additionally to the 3 drops of a solution of 1g ebacryl and 0.3g Igracure 184, 0.04g methyl orange was added. The resulting solution was placed on a shaker bed for 30 minutes to ensure that the methyl orange had dissolved. Finally the coating is then applied to a “U” bend PMMA fibre optic probe using the same method described in 6.2.1.

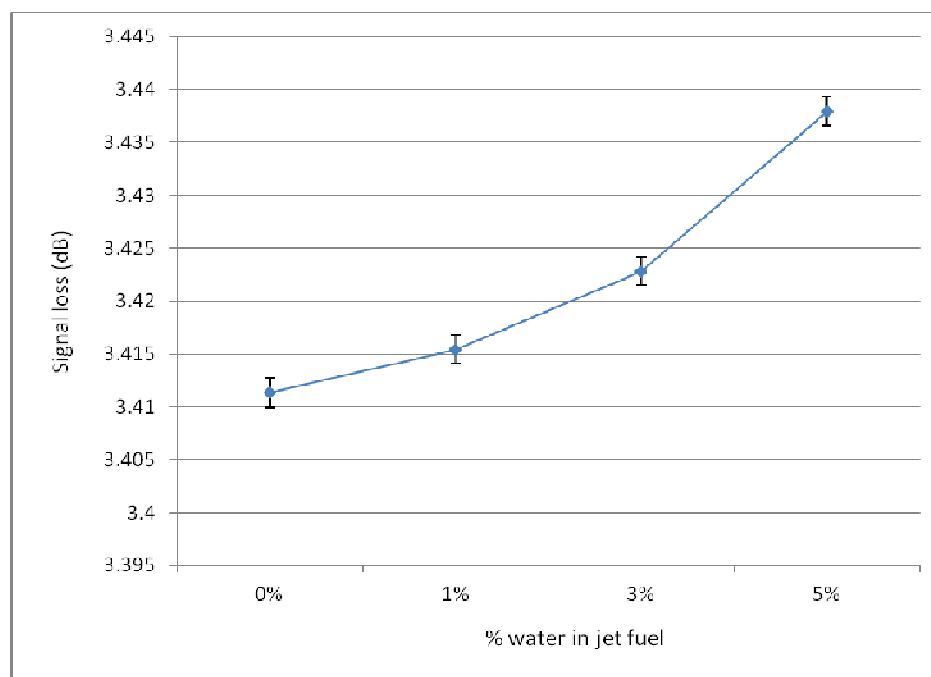
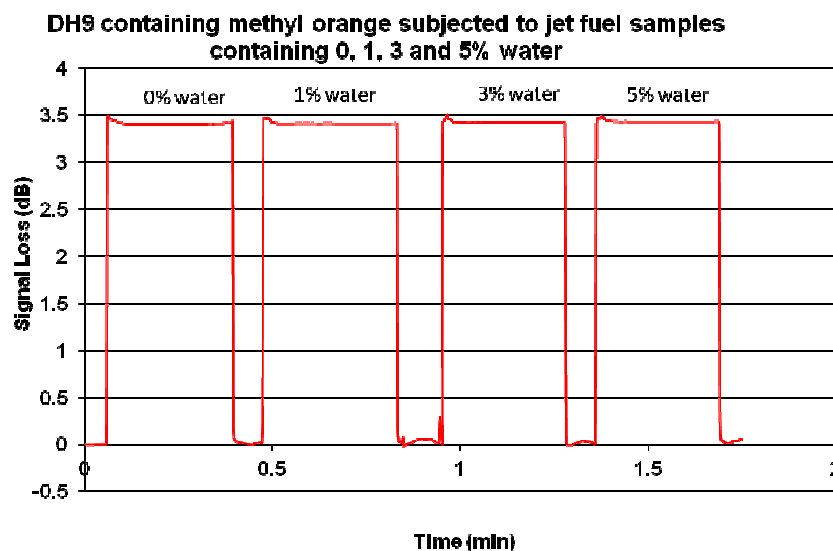


**Figure 72.** A) Signal loss data collected for a “U” bend PMMA fibre probe coated in hydrogel DH9 containing methyl orange, for a range of water in jet fuel. B) The average signal loss values obtained for each sample of jet fuel containing water.

Figure 72 shows the signal loss observed when the coating DH9 containing methyl orange is placed into samples of fuel containing increasing levels of water. The signal loss observed is increasing with increasing levels of water. As more water and  $H^+$  ions are present, the number of protonated methyl orange

molecules increases. This increase is visually observed as a colour change, which is measured by the sensor system as an increase in the signal lost from the fibre optic cable probe. In figure 72 A, it can be seen that for each sample there is a small peak in the observed signal loss before the signal loss settles as the sample is introduced to the hydrogel coated fibre optic probe. This peak is observed because the hydrogel is becoming saturated with the sample solution before an equilibrium is established within in the hydrogel. Whilst the hydrogel is becoming saturated with sample solution, this change in the hydrogel affects the RI of the hydrogel which is seen as a peak for each sample.

#### **6.2.4 Sulfonated hydrogels containing organic dyes for the detection of water- crystal violet**

Crystal violet is a dye from the triarylmethane family<sup>128</sup>. In solutions of pH 0.0-1.8, crystal violet undergoes a colour change from yellow to blue. The colour change of crystal violet is observed due to H<sup>+</sup> ions attacking the nitrogen and changing the electron configuration, therefore changing the light absorbed by the crystal violet.

In a dehydrated sulfonated membrane such as Nafion®, a DuPont trademark, in its acid form, the sulfonic acid groups are not dissociated. The addition of water to a sulfonated membrane causes the sulfonic acid group to dissociate, giving up a H<sup>+</sup> ion to the water.

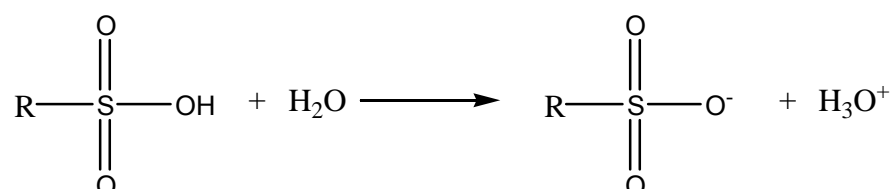


**Figure 73.** The dissociation of a sulfonate group in the presence of water.

The concentration of the  $\text{H}_3\text{O}^+$  ion is directly equivalent to the water that is taken into the hydrogel. This property of the sulfonic acid groups means that if a pH indicator such as crystal violet is entrapped in the hydrogel membrane, a water sensor coating can be fabricated. In the case of water detection in jet fuel, the sulfonate groups in the Nafion® membrane would draw the water molecules into the membrane. The sulfonic acid group would dissociate a  $\text{H}^+$  to the water molecule, forming  $\text{H}_3\text{O}^+$ .  $\text{H}_3\text{O}^+$  would then be able to protonate the crystal violet in the membrane, as shown in figure 74.

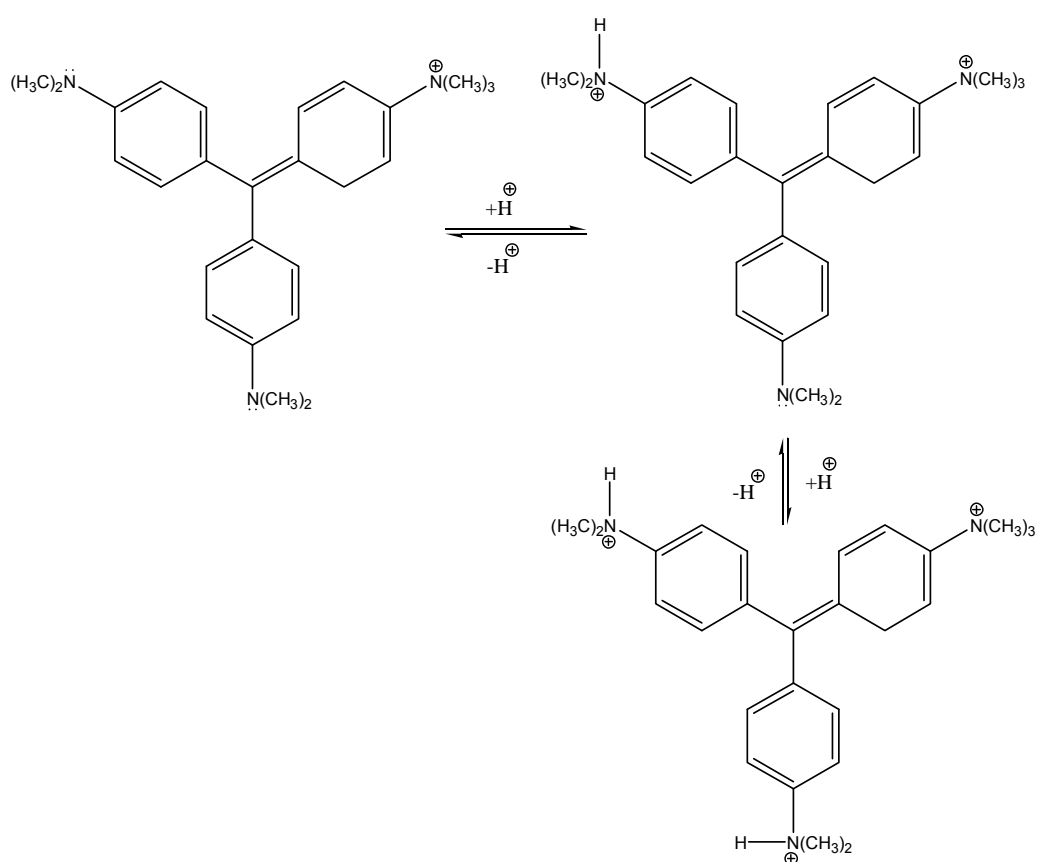


**Figure 74.** The protonation of crystal violet.

As with previously discussed chemotropic agents which undergo a colour change, the light emitted from the membrane coating would be transmitted back into the fibre optic cable core. This results in a change in the signal lost from the sensor system.

Nafion® is a perfluorinated copolymer, which is prepared by copolymerising tetrafluoroethylene, with a sulfonyl acid fluoride derivative of a perfluoro vinyl alkyl, or perfluoro vinyl alkyl ether<sup>157</sup>. Nafion® is supplied as a linear polymer solution in aqueous aliphatic alcohols. Due to the hydrophobic nature of the fluorinated backbone of the polymer, Nafion® does not need to be cross-linked to form a membrane. Instead, Nafion® uses hydrophobic interlocking to maintain the integrity of the film or membrane. Hydrophobic interlocking is also used to entrap the crystal violet within the Nafion® network. The Nafion® polymer backbone is stored in a solution of lower aliphatic alcohols, which are evaporated leaving a hard Nafion® film on the surface.

A coating solution was prepared by dissolving 0.04g crystal violet in 5.5ml of a 20%wt Nafion® solution of lower aliphatic alcohols. The resulting solution was placed onto a shaker bed for 30 minutes. A “U” bend PMMA fibre optic probe was prepared using the method described in the experimental methods chapter. The fibre was dipped into the crystal violet Nafion® solution and the aliphatic alcohol solvent was left to evaporate in air for 30 minutes. This step was repeated once more.

The sensor system was clamped in a vertical position using a retort stand and clamps. A fibre optic probe was connected via butt joints to the interrogation unit. Finally, the interrogation unit was connected to a computer with the suitable software to run the sensor system.

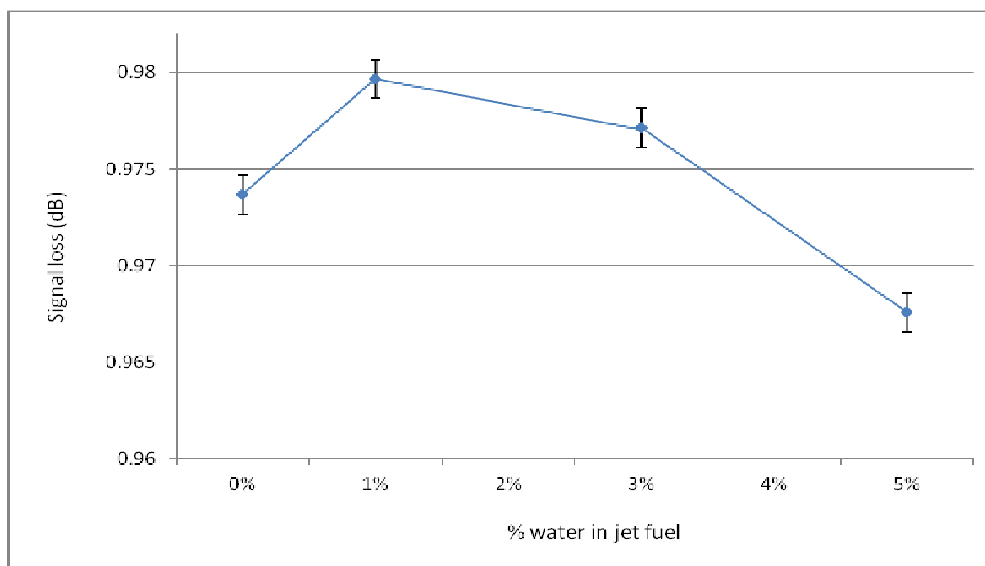


**Figure 75.** The average signal loss obtained from a PMMA “U” bend probe coated with Nafion® containing crystal violet when exposed to jet fuel containing water.

Figure 75 shows the relationship between the % water in jet fuel, and the signal loss obtained by a “U” bend PMMA probe coated in Nafion® containing crystal violet. The signal loss for jet fuel containing 0-1% water increases, and from 1-5% the signal loss decreases. This is observed due to the pH range being very low when the sulfonic group picks up the moisture from the jet fuel. For this reason, crystal violet was chosen as the chemotropic agent in this coating, as it has a low pH detection range. As such, the Nafion® / crystal violet coating only detects the presence of water at very low levels. At higher levels, any signal loss detected is past the detection threshold of the crystal violet, and is attributed to other factors. Above 1% water in jet fuel, the signal loss observed is caused by the water swelling the membrane. The sensitivity range of the crystal violet to moisture is useful where only very low concentrations of water are to be detected, for instance relative humidity.

### 6.3 Applications in the fuel industry

The detection of water is important for the fuel industry, particularly in the case of aviation fuel. Water in jet fuel can have potentially catastrophic



consequences<sup>97</sup>. In recent years, there have been several incidents where water in jet fuel has been speculated as the reason for aircraft crashes<sup>131</sup>. Water and hydrocarbon media (like jet fuel) become immiscible at approximately 5% water content. At high altitudes, water in the fuel freezes into pellets and may be drawn into the fuel lines<sup>133</sup>. This has the potential to cause damage to the engine, or even cause the engine to stall. Water in the fuel also causes the growth of certain bacteria in fuel tanks, causing more problems for the aircraft<sup>133</sup>. Finally, water can cause corrosion, which cannot be easily seen on a routine inspection of the fuel tank. The corrosion can also happen in other larger vehicles, such as ships, which have large fuel tanks that are costly to repair or replace.

In the aircraft industry, the current methods for the detection of water in fuel comprise of two tests. The first is conducted when an aircraft lands. A fuel sample is drawn from underneath the wing into a large jar. An inspector will visually check for any immiscible water<sup>133</sup>. If the test is negative, they will shake the sample to see if any water separates out. A positive result, results in the fuel tanks being drained<sup>133</sup>. The second test is a test kit provided by Shell. This kit comprises of a plastic tablet with a disc of green paper in its centre. A sample of fuel is drawn up into a syringe, and then passed through the tablet and paper. If the paper changes colour, the level of water in the fuel is more than 30 ppm and the test has been failed<sup>134</sup>. The cut-off point of 30 ppm is chosen as the industry standard not because it is the safest limit for water in fuels, but because the available laboratory test is not sensitive enough to detect lower levels of water.

The sensor system that has been developed herein could potentially be used to detect the level of water in fuels with quantitative, rather than qualitative, readings. An in-line sensor attached to the fuel browser could potentially be developed from the developed sensor system. This way, the sensor can detect water while the aircraft is re-fuelled, and the fuelling can be stopped if the level of water is unacceptably high. Alternatively, a sensor within the fuel tank could detect the level of water in the fuel and if it is high, the tank could be drained.

#### **6.4 Applications in humidity detection**

The sensor system is not just limited to the detection of water in fuels, but could also be used in a humidity-sensing paradigm. Humid environments, such as the habitats of exotic animals or plants, require a close and accurate monitoring of humidity in the air. The sensor system developed here could be used for such a purpose, as part of an integrated system to control the humidity.

## **Chapter 7. Hydrogel coatings for the detection of inorganic analytes: Results and Discussion**

## 7.1 Introduction

In the previous chapter, the use of RI change and chemotropic agents for the detection of the target species has been discussed. The focus was on chemotropic agents that chelate with the target species. This chapter on the other hand, will discuss the use of chemotropic agents that undergo a displacement reaction in the presence of the target species, forming a precipitate.

The design of a hydrogel coating for the detection of water soluble analytes using chemotropic agents which form a precipitate in the presence of the target species rather than a colour change, has a different set of criteria. Of which, the most important criterion is the choice of the chemotropic agent. Firstly, the chemotropic agent used must be soluble in the coating solution to enable it to be hydrophilically entrapped in the hydrogel membrane. Secondly, the resulting precipitate must not be soluble in the sample solution. This is important because the change in signal loss is reliant on the target species causing a precipitate, which will scatter the light in the hydrogel coating layer. If no precipitate is formed, it is unlikely that a significant signal loss will be observed.

The hydrogel coating must be able to transport the sample solvent and the dissolved target species within the hydrogel network to the entrapped chemotropic agent to allow for interaction between the two.

As discussed in chapter 1, one of the first considerations of the design of a hydrogel for a sensor application is the response time of the hydrogel. The response time of a hydrogel can be defined as the time it takes to reach its EWC. For applications such as microswitches, the response time of the hydrogel needs to be in the order of a few seconds<sup>41</sup>. The response time of a hydrogel for a sensor application needs to be relatively short for two reasons. Firstly, sensor systems are expected to give a reading within a couple of minutes. Secondly, the time it takes for the hydrogel to return to its original state is important. For a sensor system to give real time readings, the hydrogel must not only respond quickly to the presence of the stimuli, but also return to its original state ideally in the same time frame. If the time it takes for the hydrogel

to respond is too long, in a real time sensing scenario where the sample is flowing the obtained reading would be somewhere between the actual value and the value of the sample that passed over the sensor probe some time before.

The thickness of the hydrogel used also plays a role in determining its response time<sup>41</sup>. As the thickness of the hydrogel increases, the more time it takes for it to reach EWC.

The response time of a hydrogel can be manipulated by controlling the ratio of the monomers used to synthesize it, and therefore the percentage of the functional groups present<sup>77</sup>. Designing a hydrogel is not straightforward; it is a trade off between properties. For example if a gel was required to have a stronger structural integrity, this could be achieved by increasing the level of cross-linking in the hydrogel. Whilst this would make the hydrogel structurally stronger, it would affect other properties such as the EWC<sup>135</sup>, the response time, the pore size<sup>135</sup>, and the transparency of the hydrogel. As discussed earlier in section 6.2.1, the hydrogel's properties are not only affected by its composition and its structure, but also by external environmental factors including temperature and concentration gradients. Therefore, the environment needs to be taken into consideration, as well as the desired properties of the hydrogel and how changes in the selection of the monomers and their ratios to synthesize the hydrogel affect the final properties and performance of the hydrogel.

The main driving factor in designing the appropriate hydrogels that entrap chemotropic agents that form precipitates for the detection of dissolved analytes has been the detection in clinical applications. This chapter builds on the principles developed for the detection of water in hydrocarbon media. The developed sensor test bed is combined with hydrogel coatings, whose optical properties change proportionally in the presence of the target species. Dissolved analytes other than the target analyte do not affect the chemotropic agent. The basic principles guiding the design of a sensor system using

chemotropic agents that form precipitates allow for applications in various settings, including the point of care diagnostics.

## **7.2 Point of care assays: Tear Electrolytes**

Point of care assays are increasingly important and rely on self-contained, user-friendly desktop systems that can be used in the clinical environment. They desirably combine rapid diagnosis with minimum handling of the patient's sample, thereby reducing the time, the cost, and the potential for errors. The need for rapid analysis is clearest in the case of critically ill patients and potential means of improving sensitivity, speed and versatility of biochemical assays is a key aspect of technique development<sup>137</sup>.

In such cases, point of care bioassay technology competes directly with established laboratory methods. In others, the availability of point of care assays will create new opportunities for biochemical screening as an adjunct to certain types of routine assessment – such as visits to an optometry clinic, for example. In such situations, the technology must be robust, compact and suitable for use in a clinical rather than analytical setting. In environments other than the hospital clinic, non-invasive alternatives to blood samples – such as saliva or urine – are already under active investigation. The use of tears as an assay medium has been less actively pursued, largely because of small available sample volumes and difficulties in reproducible sample collection. This section discusses the use of tears with emergent fibre-optic technology sensor systems as a potential route to a new area of point of care diagnostics in optometric practice.

The potential advantages of the use of tears as a means of obtaining representative analytical data relating to blood constituents was recognised in earlier studies. Khuri<sup>129</sup> made the point that the constituents found in tears are representative of those found in the blood supply to the brain, because the palpebral conjunctiva is supplied by the ophthalmic artery, a branch of the internal carotid artery, which is a major supplier of the brain.

However, the problem lies in obtaining large enough tear samples to allow measurement or detection of constituents by conventional techniques. Attempts to overcome this problem by use of artificial stimulation of tear production are confounded by the fact that the concentration of some tear components is flow-dependent. The method of tear collection has, in consequence, a significant influence on the analytical data obtained. Khuri proposed the use of Schirmer strips as a means of overcoming this problem and demonstrated that this method of collection does allow determination of organic components such as glucose and urea together with inorganic such as potassium and calcium<sup>129</sup>. Although the principle of this collection method is sound and readily adaptable to point of care analysis, it has not been matched by a simple and sensitive assay technique that would enable one or more important tear constituents to be measured conveniently and quantitatively in the clinic.

The last fifteen years have seen little advance in point of care tear assays. Perhaps the most important recent development of this type has been the nano-osmometer<sup>138</sup>, the potential importance of which derives directly from the work of Gilbard<sup>139</sup>. Gilbard pointed out that tear film osmolarity can potentially be increased by any condition that increases tear evaporation or decreases tear secretion. His studies translated the theoretical link between keratoconjunctivitis sicca (KCS) and tear film osmolarity to observation with practical clinical utility. Many specialised studies have emphasised the importance of the link between tear electrolyte balance and concentration on one hand, and the health of the ocular surface on the other<sup>139</sup>. Notwithstanding its acknowledged importance, there has been until recently no point of care method for even determining total undifferentiated electrolyte concentration in tears.

It is clear that total tear electrolyte concentration (i.e. osmolarity) has important clinical significance, and that it has only been the lack of an appropriate affordable point of care assay that has prevented its widespread use in optometric practice. A similar situation exists with individual tear electrolytes: an ability to identify abnormal levels of potassium or calcium at point of care, for example, would have considerable potential clinical diagnostic value. The fact that such methods are not available means that the diagnostic

significance of abnormal levels of these electrolytes is not widely appreciated amongst practitioners.

Perhaps surprisingly, potassium disorders, which range from hyperkalemia (in which the serum potassium ion concentration is greater than 5.5 mM/l) to hypokalemia (in which the serum potassium ion concentration is less than 3.5 mM/l)<sup>140</sup> are second only to hydrogen ion disorders as causes of mortality and morbidity. Hyperkalemia is the more dangerous and can lead to fatal cardiac arrhythmias<sup>141</sup>. The underlying condition is reversible, provided that it is recognised in time and appropriate measures are taken. Hypokalemia can be caused either by inadequate potassium salt intake or by excessive potassium ion renal excretion or gastrointestinal loss<sup>142</sup>. The clinical manifestations of the condition may be cardiac (irregular heartbeats), hemodynamic (decrease in blood pressure), renal and endocrine or neuromuscular<sup>142</sup>. Though the measurement of serum potassium via conventional blood tests has saved many lives, many crises are missed because of the lack of a non-invasive monitoring system. Tears contain about 15-30 mEq/litre of potassium ions, much higher than serum levels, which are about 4.5 mEq/litre, indicating that there is active potassium secretion in tears<sup>143</sup>.

The value of analytical screening procedures, particularly at point of care, has been made both by many of the authors previously cited and others who emphasise the point that sample collection and assay of tears presents particular problems<sup>144</sup>. It is clear that in comparison with general observations of tear osmolarity, elevated levels of specific electrolytes are associated with specific conditions and thus offer diagnostic potential. Elevated potassium levels are an early marker of dry eye<sup>145</sup>. The availability of a suitable point of care assay would enable the general applicability of a system for analytes such as potassium to be readily determined<sup>146</sup>.

### **7.3 Potassium as a target analyte**

The hydrogel coating DH2 was chosen for this research over existing and well-researched hydrogels such as poly HEMA due to the different properties of these. As mentioned in section 6.2.1, poly HEMA is a hydrophilic hydrogel, due



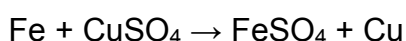
to the hydroxyl group present. The method used in this work utilises the hydrophobic groups within a hydrogel network to entrap the chemotropic agent. Hydrogels such as poly HEMA do not have hydrophobic functional groups (although the polymer backbone is hydrophobic), which means that they would not be able to effectively entrap the chemotropic agent within the hydrogel network. Coating DH2 was designed to have hydrophobic areas provided by the monomer NBNMA. When homopolymerised, poly NBNMA forms a high RI polymer of 1.585, that possesses an EWC of 5%<sup>158</sup> due to its hydrophobic nature. NVNMA and MMA are used for their hydrophilic and hydrophobic properties respectively, to ensure that water enters the hydrogel matrix and any chemotropic agent entrapped within the hydrogel. Unlike the other hydrogels synthesized that use a cross-linking agent and photo initiator to form a cross-linked network, the hydrogel DH2 coating uses hydrophobic interlocking to form a hydrogel network. A cross-linking agent and a photoinitiator are used to form cross-links via free radical hydrogen abstraction from the benzyl groups in the NBNMA, though this is not necessary to form a hydrogel matrix.

The principles used to design the DH2 coating are transferable to use in the detection of other analytes of clinical importance, as well as non-clinical analytes that will be discussed later in this chapter.

As mentioned earlier, the collection of tear samples in large quantities for an assay is problematic. One possible route to solve this problem is to use an assay technique that does not require larger amounts of tear samples, and that could actually be carried out with tears present in the eye environment. For this purpose, and to overcome the issues of reproducibility that are discussed later, the end stop probe was developed. The end stop probe uses glass fibre optic cable in short lengths with the cladding layer removed at one end of the fibre, which is then coated with the hydrogel coating containing the appropriate chemotropic agent. Light transmitted from the light source travels along the fibre to the end of the fibre that is coated in the hydrogel membrane, and it is reflected back through the fibre to the detector. The amount of light reflected is dependent on the hydrogel coating on the tip of the fibre optic cable probe, and its interaction with the sample. This type of sensor probe would allow

optometric clinicians to carry out routine tests when patients visit the clinic, without the need to extract a tear sample to be sent off for testing.

As mentioned in section 6.1.2, there are two types of chemotropic agent. The first, discussed in 6.1.2, are chemotropic agents which chelate with the target molecule to give rise to a colour change. A chemotropic agent that undergoes a displacement reaction to form a new compound, which is no longer soluble in the solvent that it is in is the second type of chemotropic agent. One example of a displacement reaction is that between iron and copper sulfate.



Iron has an electro negativity of 1.83<sup>147</sup>, and copper of 1.9<sup>147</sup>. Iron is a stronger oxidising agent and therefore displaces the copper. The detection of potassium as a target analyte in a solution utilises the chemotropic agent sodium tetra phenyl borate. This chemotropic agent undergoes a simple displacement reaction in the presence of potassium, forming potassium tetra phenyl borate, which is a white precipitate in a solution. The sodium tetra phenyl borate entrapped in the hydrogel coating precipitates in the presence of potassium. As the precipitate is a white solid, any light that escapes the core of the fibre will hit the precipitated potassium tetra phenyl borate and be scattered. Some of the light will be scattered back into the fibre core, and the rest will be scattered out of the hydrogel. As the levels of potassium present in the sample increase, more potassium tetra phenyl borate will be precipitated in the hydrogel membrane. This will cause more of the light that escapes the fibre to be scattered, either back into the core of the fibre, or out of the hydrogel. Building on the observed relationship during experimentation with water in jet fuel, the signal loss is expected to increase with increasing levels of potassium.

**Table 5.** The composition of DH2.

<b>Macromer Monomer</b>	<i>DH2</i>
NBNMA	38.1ml
NVNMA	20.7ml
MMA 48%sol	38.1ml
<b>Initiator</b>	
AIBN (AZBN)	0.88g
<b>Solvent system</b>	
Toluene :	
MeOH (1:1)	103.5ml

Coating DH2 was prepared by mixing the monomers listed in table 6 in 95% of the solvent system (listed in the same table) in the polymerisation rig, as described in the experimental methods chapter. The solution was mixed for 30 minutes in the reaction vessel at 60°C, and under nitrogen. In parallel, the initiator was mixed with the other 5% of the solvent system and left on a shaker bed for 30 minutes. Next the resulting initiator solution was then added to the monomer mixture in the reaction via a syringe through one of the side arms. The reaction mixture was left stirring at 60°C for two hours under nitrogen. Once the reaction is completed, the reaction vessel was shut down and the solution was left to cool to room temperature for one hour. At this point a visual observation of a change in the viscosity of the reaction mixture is an indication that polymerisation had occurred. Once cooled to room temperature, the reaction mixture was transferred to a beaker containing one litre of acetone to precipitate the linear macromer. The precipitate was then transferred to a watch glass, put in a vacuum oven at 40°C and left overnight to remove any solvent. The next stage was to functionalise the linear macromer to allow for it to be cross-linked to form a hydrogel. In a sample vial covered in tin foil, 0.4g of the linear macromer was dissolved in 5.5ml of a 0.3% HCl MeCN:H<sub>2</sub>O (1:1) solution and left on a shaker bed for 30 minutes to ensure that the macromer is completely dissolved. To this solution 0.08g NMA was added and shook by hand vigorously for 5 minutes. The sample vial was then placed into a water

bath at 60°C for 2 hours, and was shaken every 30 minutes by hand for 2 minutes. Using a Pasteur pipette, 3 drops of a solution of 1g ebacryl and 0.3g Igracure 184, and 0.04g sodium tetra phenyl borate was added to the resulting solution. Following this the solution was placed on a shaker bed for 30 minutes, to ensure all the sodium tetra phenyl borate was dissolved. The glass “end stop” fibres were prepared using the method described in the experimental methods chapter. A fibre was dipped into the solution and placed under a UV lamp for 30 minutes to crosslink the coating on the fibre. This step is repeated once more.

Using a retort stand and clamps, the sensor system is clamped in a vertical position and the coating fibre optic cable probe attached by butt-to-butt connections to PMMA patch cables. The sensor system was set to record measurements every 1 second initially in air for 5 minutes. A sample vial containing the sample was then introduced to the probe, and left to record the signal loss of the sample for 5 minutes. The sensor is then stopped, and the probes changed as the displacement reaction is non-reversible and the probes are not re-usable. This method is repeated for each of the samples. The mean average signal loss for each sample is calculated and plotted in figure 76.

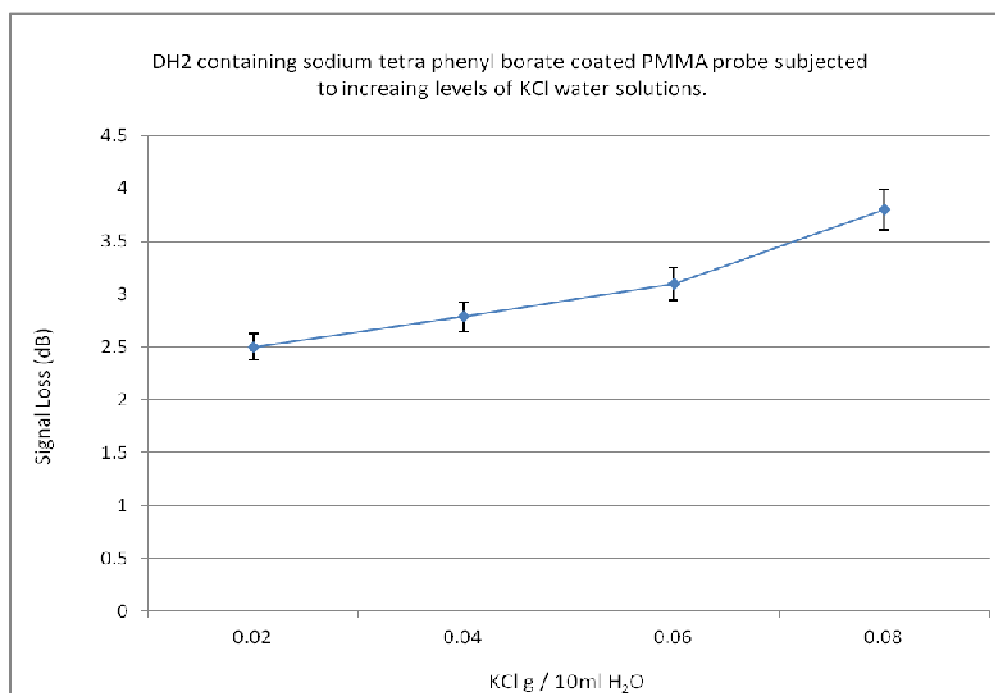


**Figure 76.** DH2 coated “end stop” glass probe with sodium tetra phenyl borate entrapped in the hydrogel, subjected to samples of potassium in water.

From figure 76, the mean average signal loss increases with increasing levels of potassium concentration in the test solution. The signal loss observed in this instance is not due to a large RI change of the hydrogel, as observed in the detection of water in jet fuel and discussed in sections 6.2.1, and 6.2.2. Whilst the addition of potassium chloride to the samples of distilled water will alter the RI of the solution, the change in RI is negligible. This signal loss pattern observed is due to the amount of potassium tetra phenyl borate that is precipitated in the hydrogel membrane. The precipitate causes the light lost from the fibre optic probe to be increasingly scattered with increasing levels of potassium, which causes more precipitate to form. As mentioned earlier in this section, the reaction that occurs between sodium tetra phenyl borate and potassium is non-reversible and the chemotropic agent is used up in each reading. Therefore the fibre optic probe can only be used for one sample. As a result, if the sensor was to be used in another sample of potassium chloride solution, the signal loss reading would not be accurate, as the signal loss observed would be an accumulated effect of the precipitate formed from the current and previous sample.

## 7.4 Calcium as a target analyte

Calcium is another clinically important tear analyte. Typical concentrations of ionic calcium in tears are around 0.4-0.8 mM<sup>148,149</sup>. Elevated calcium levels in tears have been shown to be a key characteristic of primary acquired nasolacrimal duct obstruction<sup>145</sup>. It has also been suggested that elevated tear calcium levels predisposed patients to form white spots during the wear of contact lenses. The availability of a suitable point of care assay would enable the general applicability of such propositions to be readily determined<sup>147</sup>, and could aid in the fitting of contact lenses without the need for a trial and error approach based on the fitter's experience with previous patients.

A crown ether is a chemical compound that contains a ring of ether groups. The lone pair of electrons on the oxygens in the ether groups creates a "ring of charge". This "charged ring" allows the crown ether to form coordinated complexes with interesting properties. As mentioned in section 6.1.2, a central atom or molecule is coordinated by one or more ligands resulting in an associated colour change. In the case of crown ethers, the oxygen atoms within the ring of the crown ether act as donor atoms to hold in place any cation within the ring. The stability of any complex the crown ether forms is dependent on the relative size and diameter of the cavity of the crown ether, and the diameter of the cation<sup>135</sup>. This is not in line with the relationship between size and charge, which states that the smaller the size and the larger the charge of a cation, the more stable a complex is formed (further discussed in section 6.1.2). The relationship between stability and the charge and size of a cation in a coordinated complex becomes more complicated when formed with a crown ether<sup>125</sup>.

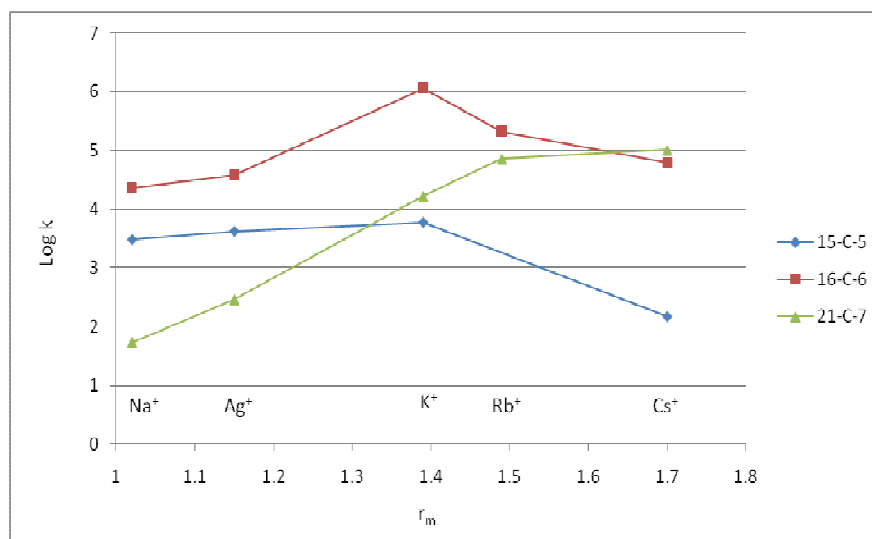


**Figure 77.** The log of the stability constant for complexes of three crown ethers plotted against the size of several cations<sup>125</sup>.

**Table 6.** The radii of several cations and three crown ether cavities<sup>125</sup>.

Cation	Ion radius (Å)	Crown Ether	Cavity radius (Å)
Na <sup>+</sup>	1.02	15-C-5	0.85
Ag <sup>+</sup>	1.15	18-C-6	1.38
K <sup>+</sup>	1.38	21-C-7	1.70
Rb <sup>+</sup>	1.49		
Cs <sup>+</sup>	1.70		
Ca <sup>2+</sup>	1.00		
Ba <sup>2+</sup>	1.36		

The stability of the formed complex depends on the relationship between the size of the cavity and the size of the cation<sup>125</sup>. Particularly, the larger the cation, the more stable it is, until the size of the cation exceeds the size of the cavity<sup>125</sup>. When this happens, other factors become more important in determining the stability<sup>123</sup>. Similarly, when the cavity is much larger than cations, the contribution of size becomes meaningless<sup>125</sup>. In these instances the charge on the cation plays a more crucial role in the stability of the formed complex<sup>125</sup>. For

example, although a  $K^+$  cation and a  $Ba^{2+}$  cation are similar in size, in a complex with 18-C-6 they are both similarly sized to the cavity, but the  $Ba^{2+}$  cation has a higher stability than the  $K^+$  cation<sup>125</sup>. In cations smaller than the cavity radius, such as  $Na^+$  and  $Ca^{2+}$ , the stability is reversed with  $Na^+$  showing a larger stability than  $Ca^{2+}$ . Therefore, where there is competition between similar sized cations that are close to the size of the cavity radius, a divalent cation will form a more stable complex<sup>125</sup>. When two similarly sized cations are much smaller than the cavity, the monovalent cation will form a more stable complex<sup>125</sup>.

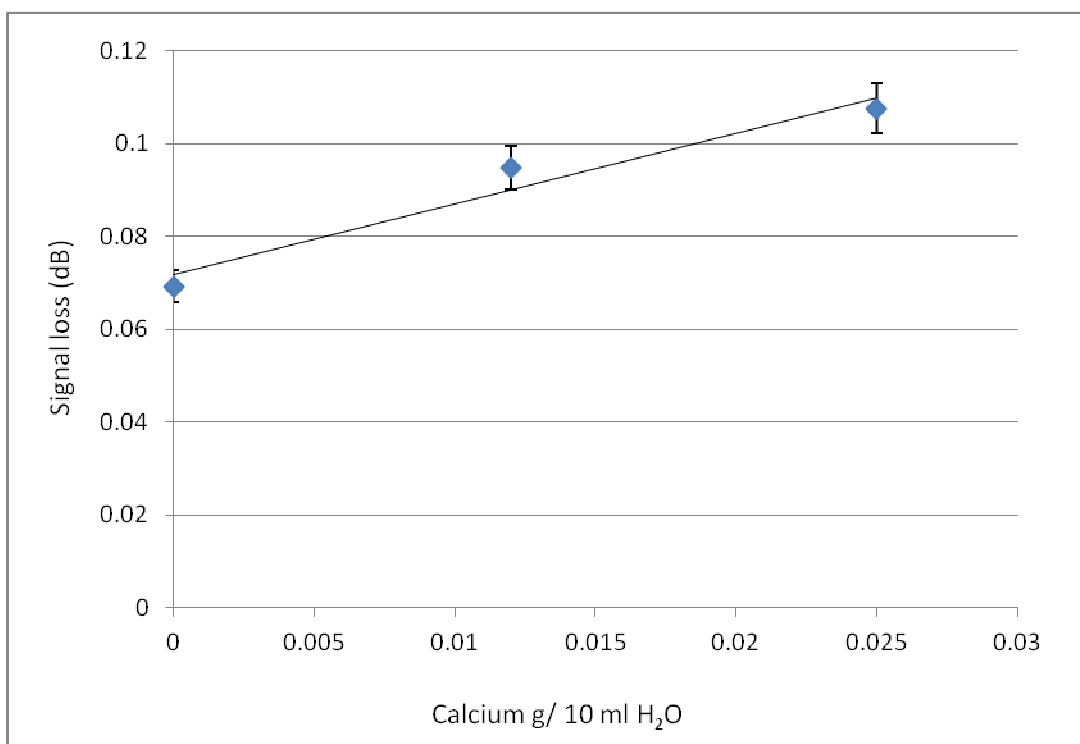
For the detection of calcium, benzo-18-crown-6 is used as the chemotropic agent. The calcium ion in a water solution will enter the hydrogel and coordinate with the entrapped benzo-18-crown-6 to form a complex. This new coordinated complex will have an associated colour change due to the new electron configuration. This in turn will create a signal loss, which should follow the pattern established in previous experimentation with chemotropic agents. The expected pattern seen previously is a more intense colour change causing an increased signal loss with increasing levels of the target species.

Coating DH2 was prepared by mixing the monomers listed in table 6 in 95% of the solvent system (listed in the same table) in the polymerisation rig, as described in the experimental methods chapter. Next the solution was mixed for 30 minutes in the reaction vessel at 60°C, and under nitrogen. Simultaneously, the initiator was mixed with the other 5% of the solvent system and left on a shaker bed for 30 minutes. The resulting initiator solution was added to the monomer mixture in the reaction via a syringe through one of the side arms. The reaction mixture was left stirring at 60°C for two hours under nitrogen. After the completion of the reaction, the reaction vessel was shut down and the solution left to cool to room temperature for one hour. At this point a visual observation of a change in the viscosity of the reaction mixture was an indication that polymerisation had occurred. Once cooled to room temperature, the reaction mixture was transferred to a beaker containing one litre of acetone to precipitate the linear macromer. The precipitate was then transferred to a watch glass and put in a vacuum oven at 40°C and left overnight to remove any



solvent. The next stage was to functionalise the linear macromer to allow for the macromer to be cross-linked to form a hydrogel. In a sample vial covered in tin foil, 0.4g of the linear macromer was dissolved in 5.5ml of a 0.3% HCl MeCN:H<sub>2</sub>O (1:1) solution, and left on a shaker bed for 30 minutes to ensure that the macromer had completely dissolved. To this solution 0.08g NMA was added and shook by hand vigorously for 5 minutes. The sample vial was then placed into a water bath at 60°C for 2 hours, and shaken by hand every 30 minutes for 2 minutes. Using a Pasteur pipette, 3 drops of a solution of 1g ebacryl and 0.3g Igracure 184, and 0.04g sodium tetra phenyl borate was added to the resulting solution. The solution was placed on a shaker bed for 30 minutes, to ensure all the benzo-18-crown-6 had dissolved. The glass “end stop” fibre was prepared using the method described in the experimental methods chapter and was dipped into the solution and placed under a UV lamp for 30 minutes to cure the coating on the fibre. This step was repeated once more.

For the experimental setup in hand, the interrogation unit was clamped in vertical position using a retort stand and clamps. A coupler/splitter was used instead of patch cables to connect the “end stop” probe to the interrogation system. The coupler/splitter used was in the ratio of 50:50. Two cables from one end of the coupler/splitter were connected to the interrogation system. The metal cylinder of the coupler/splitter was clamped in a vertical position. The uncoated end of the glass “end stop” probe was carefully pushed into a bare fibre termination unit, with a 400 µm SMA connector attached, which was then screwed into one of the two unconnected ends of the coupler/splitter. The probe was then clamped in a vertical position around the bare fibre termination unit. Finally the last cable had a Pasteur pipette teat placed over the end to prevent any light entering or escaping the system.



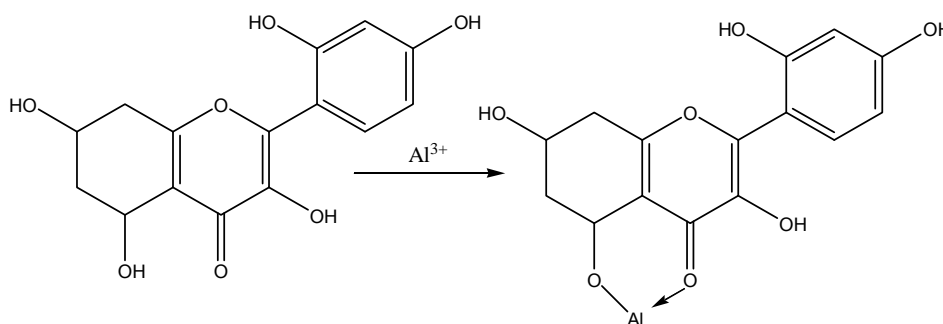
**Figure 78.** The average signal loss of a PMMA “U” bend coated with DH2 containing benzo 18 crown 6, exposed to three samples of water containing varying levels of calcium ions.

Figure 78 shows a signal loss pattern that when increasing the level of calcium in water, the signal loss increases. The signal loss observed shows the same pattern as the other coatings that utilise a chemotropic agent which undergoes a colour change, with an intensity proportional to the presence of varying levels of the target species. However, in this instance the intensity of signal loss that is observed is much less than in previous experiments. The reduction in intensity of signal loss is not due to the efficiency of the sensor system at retaining light. Light generated by the interrogation system first enters the coupler/splitter, which uses PMMA fibre of 1000  $\mu\text{m}$  core. It is then transmitted into the glass fibre optic cable probe with a 400  $\mu\text{m}$  core. The signal that is actually transmitted though the system is small. Therefore the signal loss caused by the “end stop” probe and the hydrogel coating is proportionally smaller.

## 7.5 Aluminium as a target analyte

In moving away from clinical applications to other areas of commercial interest for fibre optic sensors, water purity is an important target area. Metal ions such as iron, aluminium, nickel and cobalt to name a few are the analytical target. In this section the detection of aluminium is discussed.

Morin is a compound that has been used for the detection of aluminium in the form of flash powder in explosives and explosive residues<sup>150</sup>. Aluminium forms a coordinated complex with Morin, and fluoresces. This simple test can be carried out in neutral or acidic conditions<sup>150</sup>.



**Figure 79.** Morin complexing with aluminium to form the aluminium salt of Morin.

Morin is a yellow/brown powder, which, when dissolved in water, forms a yellow/brown solution. Upon the addition of aluminium to the solution, the aluminium salt of Morin is formed; a complex that fluoresces green. Just like other chemotropic agents, Morin can be hydrophilically entrapped in a hydrogel membrane, where a solvent like water can enter, carrying dissolved aluminium into the hydrogel network. Morin can complex with the aluminium and the new complex fluoresces green<sup>150</sup>. The coating of the hydrogel containing Morin onto a fibre optic cable probe can be used with the interrogation system to measure the levels of aluminium in water in the same manner as cobalt chloride is used with a hydrogel coating to measure water levels in hydrocarbon media, as described in section 6.1.2.

Coating DH2 was prepared by mixing the monomers listed in table DH2 in 95% of the solvent system (listed in the same table) in the polymerisation rig, as described in the methods chapter. The solution was mixed for 30 minutes in the reaction vessel at 60°C, and under nitrogen. In parallel, the initiator was mixed with the other 5% of the solvent system and left on a shaker bed for 30 minutes. The resulting initiator solution was added to the monomer mixture in the reaction via a syringe through one of the side arms. Following this, the reaction mixture was left stirring at 60°C for two hours under nitrogen. Upon the completion of the reaction, the reaction vessel was shut down and the solution left to cool to room temperature for one hour. At this point a visual observation of a change in the viscosity of the reaction mixture was an indication that polymerisation has occurred. Once cooled to room temperature, the reaction mixture was transferred to a beaker containing one litre of acetone to precipitate the linear macromer. The precipitate was then transferred to a watch glass and put in a vacuum oven at 40°C where it was left overnight to remove any solvent. The next stage was to functionalise the linear macromer to allow for the macromer to be cross-linked to form a hydrogel. In a sample vial covered in tin foil, 0.4g of the linear macromer was dissolved in 5.5ml of a 0.3% HCl MeCN:H<sub>2</sub>O (1:1) solution, and left on a shaker bed for 30 minutes to ensure that the macromer had completely dissolved. To this solution 0.08g NMA was added and shook vigorously by hand for 5 minutes. The sample vial was then placed into a water bath at 60°C for 2 hours, and shaken by hand every 30 minutes for 2 minutes. Using a Pasteur pipette, 3 drops of a solution of 1g ebacryl and 0.3g Igracure 184, and 0.04g Morin was added to the resulting solution and placed on a shaker bed for 30 minutes, to ensure all the Morin was dissolved. A U bend PMMA fibre was prepared using the method described in the experimental methods chapter. It was dipped into the solution and placed under a UV lamp for 30 minutes to cure the coating on the fibre. This step was repeated once more.

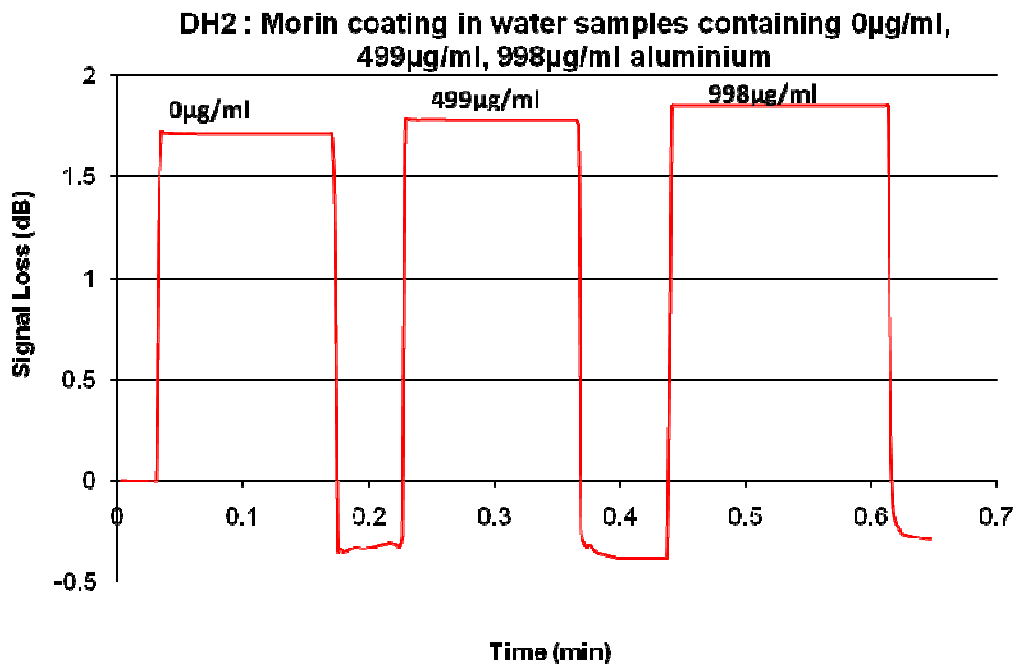


**Figure 80.** Time vs Signal loss for a probe coated with smart hydrogel DH2 containing the chemotropic agent Morin. The probe is subjected to three samples of water containing increasing levels of aluminium.

From figure 80, it can be seen that when a sample has been removed from the probe the signal loss in air becomes negative. This is due to the Morin coordinated aluminium fluorescing causing the negative signal loss.

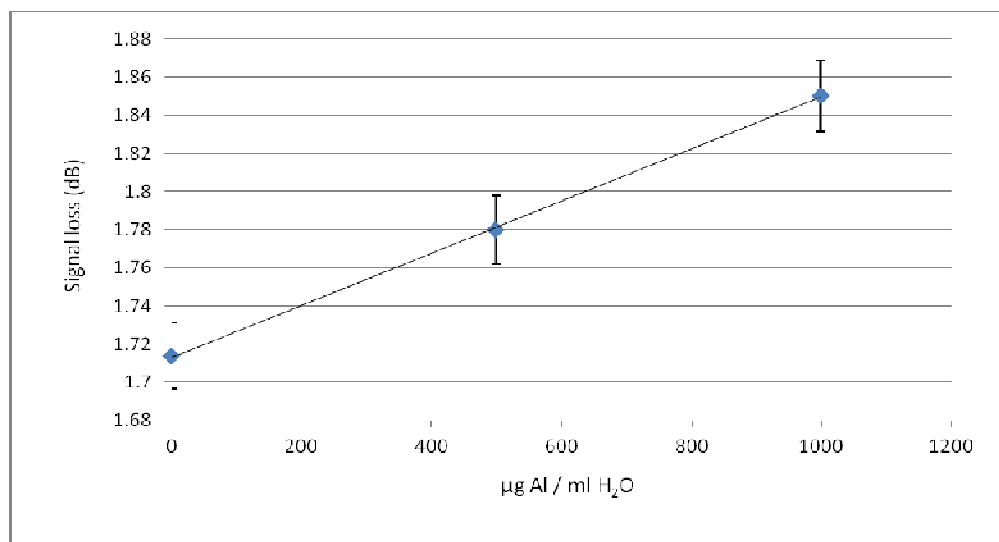


**Figure 81.** The average signal loss for a probe subjected to three samples of water containing 0, 499 and 998 µg/ml Al.

The signal loss observed for coating DH2 containing morin, shows a pattern of increasing signal loss with increasing levels of aluminium in water in a linear relationship. This is due to the increasing levels of aluminium forming more coordinated complexes of the morin aluminium salt. This in turn causes a greater intensity of the fluorescence proportional to the level of aluminium present, causing an increased signal loss.

## **7.6 Possible applications of the sensor system**

Due to the type of medium that this sensor system is designed to detect in, i.e., liquid environments, the knowledge used for its development is widely transferable. Any liquid that contains a dissolved analyte, or a liquid that is not water and water is the target species, can be used as a medium for sensing in. In addition, the fact that hydrogels can be designed to suit a particular set of criteria makes this system highly versatile and applicable in a variety of sensing settings.

### ***7.6.1 Applications in ophthalmic diagnosis***

Diagnosis techniques need to be improved in clinical point of care assistance. Optometric practitioners rely upon diagnosis from visible symptoms that patients display. These symptoms are normally the result of tear abnormalities; one such example is the increased levels of potassium, one of the causes of dry eye<sup>145</sup>. A method of diagnosis based on visible symptoms is not always reliable, as it relies upon experience of the practitioner, along with the interpretation of written symptoms. Sensor technology can be used as a tool to assist with routine point of care diagnosis of conditions that arise from tear abnormalities.

The role of tears as a protective barrier between the eye and the atmosphere is important in maintaining the functionality of the eye. Tears remove any particles that come into contact with the surface of the eye before they can do damage

or scratch the eye. The eye is flooded with tears so that particles are moved out of the eye, stopping any damage that could be caused<sup>151</sup>.

Tear analytes are important constituents of tears, as they define the characteristics of the tear, and its ability to carry out its functions in the intended manner. If any tear analyte is out of the normal range, it could cause a number of eye-related diseases or disorders<sup>145</sup>. If, for example, the levels of potassium and sodium ions are out of the normal range, they are indicative of the condition, dry eye. Dry eye can be caused by insufficient tear production, or by abnormal tear composition, resulting in increased evaporation of the tear. Tear abnormalities can be problematic for contact lens wear, as they not only cause discomfort for the patient, but can also result in the contact lens sticking to the eye as it dries out when the wearer suffers from dry eye. Another example of tear abnormalities causing problems to contact lens wearers is higher than normal levels of protein or calcium, resulting in white spots on the contact lenses, which reduce patients' visibility<sup>152</sup>.

Tear diagnostic techniques can be used not just for the diagnosis of tear abnormalities and diseases, but to aid contact lens fitting. For instance, if a patient has higher than normal levels of calcium, appropriate contact lenses can be prescribed in order to avoid the formation of white spots on the lens. This would help reduce the number of visits to the optician, as it would provide data in order for a suitable lens to be fitted in the first place. Furthermore, the use of diagnostic techniques could assist in the recommendation of suitable contact lens care solution based on the wearers tear analysis. In addition to the contact lens fitting and care solution recommendation, tear diagnostic techniques could also provide information to manufacturers about the problems arising from the use of particular contact lenses in a percentage of the wearers that have been using the contact lens. This would help companies gain a deeper understanding about the link between contact lens materials, care solutions and the eye.

A useful way to look at the contact lens matrix is as a fishing net, which catches not only the large molecules like proteins, but also the tear and the tear analytes that are dissolved in tears. Therefore, contact lenses are an ideal

vehicle for the collection of tears for *ex-vivo* assay, as a contact lens can be placed in the eye until the tear has replaced the packing solution; the lens could then be removed and put into contact with a probe designed to measure a particular tear analyte.

Contact lenses have been exploited as a method of analysis of the tear analytes and other components via techniques such as HPLC and electrophoresis. In both cases, the lens undergoes some form of extraction in order to remove the target molecules into an aqueous solution, which is then subsequently analysed<sup>153,154</sup>. This analysis requires equipment normally found in a laboratory, which is usually off-site. Therefore, the contact lens needs to be stored and transported, usually frozen to prevent degradation of the target molecules, as well as migration out of the contact lens of the target molecule. Ideally, analysis of a target molecule should occur as soon as possible after the collection of the sample.

Osmometry has recently been employed as a method of looking at conditions of the eye, in particular for the diagnosis of dry eye. Nevertheless, it has been used in conjunction with other diagnostic methods, such as tear break-up times, McMonnies dry eye survey primary symptoms ( a questionnaire designed to use patient symptoms, and score the severity of the symptom, to diagnose dry eye) and ocular surface staining<sup>155</sup>. Another application of tear osmometry is the use of the Tearlaboratory<sup>TM</sup> Osmolarity System to assess the effectiveness of the treatment of dry eye<sup>137</sup>. Whilst this has been proven as a useful tool, it only measures a function of all the tear components together, without looking at individual components that are associated with dry eye.

Techniques such as osmolarity do not look at individual tear components, and therefore are not useful for measuring particular components that are associated with a particular condition. The technique described herein is unique in its approach because it uses existing transferable technologies, and combines them in a new way in order to produce a method of analysis of individual components in *ex-vivo* lenses. This technique can be used in routine



optometric practice and thus give immediate results, removing the need to send samples away for analysis.

Patients with dry eye show a higher than normal concentration of potassium in tears. The sensor membrane for the detection of potassium in tears collected in from *ex-vivo* lenses must be hydrophilic enough to draw the tears from the contact lens into the sensor membrane. Entrapment of the chemotropic agent within the membrane must not reduce its functionality.

### ***7.6.2 Applications in the water industry***

The measurement and detection of dissolved metal ions in water is important for the water industry and the environmental departments. Some dissolved metal ions can lead to water tasting bad, or to health problems. Aluminium in water has been link to Alzheimer's disease<sup>90</sup>. Other metal ions in water are acceptable in certain levels, but once they exceed that limit they can be poisonous. The sensor system developed could be used to measure the levels of dissolved metal ions at remote locations, or in the feed lines for water processing facilities. A system such as this could be useful in preventing issues derived from inadequate monitoring of a water processing facility. Personnel working in such facilities are not always qualified to carry out the necessary tests to determine if there are contaminants or certain ions present in higher than permitted levels. Therefore, the plant would have to be shut down until the qualified person is able to carry out the necessary testing, before any corrective action could be carried out and normal operations begin again. The use of a system like the one developed hereby could be used to detect specific ions, so that the plant can be shut down accordingly and corrective actions can be taken without the need to call a qualified person out to do the necessary testing. This would reduce the time that the facility is not operating.

### **7.6.3 Applications in wound healing monitoring**

Wounds can be categorised into two broad types, healing and non-healing<sup>159</sup>, and the respective treatments differ. Currently, medical personnel decide when and which dressings to use on a wound, based on experience and on how a wound looks. This type of determination is purely qualitative. By applying the sensing system developed herein it becomes possible to measure the metal ions present in the wound fluid by embedding the probes used in the developed system into a wound dressing. The sensor system could then be connected to the probe and a reading can be taken. This would allow the medical personnel to make a decision based on the actual levels of metal ions that are indicative of a healing wound. The person would then be able to know whether the wound dressing needs replacing, without having to disturb the wound and consequently the healing process. Additionally, the ability to determine quantitatively the wound healing stage enables for a specific type of dressing to be used to aid the healing process.

### **7.7 Issues of result reproducibility**

One of the main challenges facing the development of spectroscopic techniques, such as the sensor technology developed in the work conducted and discussed in this thesis, is the issue of repeatability of results within an acceptable limit. In the tests conducted, the results always showed a correlation between increasing signal loss and increasing levels of the target species. However, the results differed in the values at which signal loss occurred for a given coating and target species.

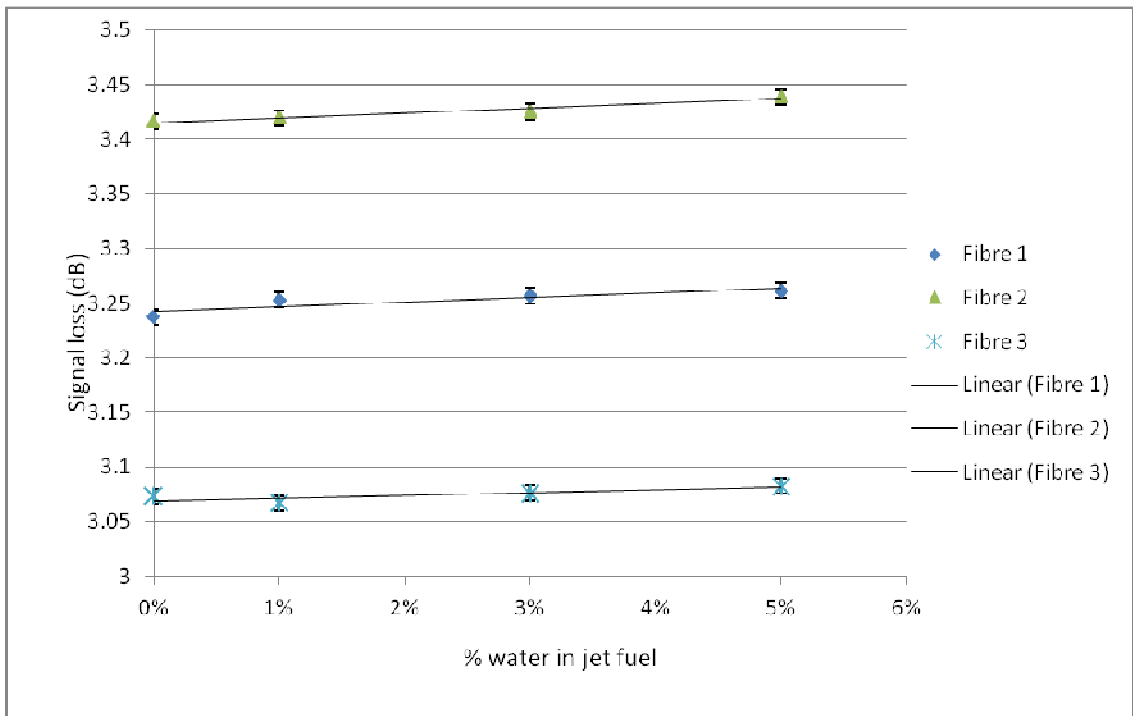


**Figure 82.** Three “U” bend PMMA probes coated with hydrogel DH9 exposed to jet fuel containing various levels of water to show the difference in signal loss between fibres.

For example, when using a “U” bend PMMA fibre optic probe coated with DH9 coating for the detection of water in jet fuel, the signal loss range differs from fibre to fibre. As shown in figure 82, the trend observed for signal loss generated from three different “U” bend PMMA fibre probes coated in DH9 is an increase with increasing levels of water. However, the range at which these signal losses are detected is different for each fibre. For a sensor system to be successful, the difference between readings at the same level of water must be minimal.

There are several factors that affect the signal loss generated by a fibre optic sensor system of this type. Firstly is the fabrication of the fibre optic cable “U” bend probe. The PMMA fibre optic cable was obtained from Lasirvis on a spool. A “U” bend PMMA probe is prepared following the method discussed in 3.3.1. Herein lies the problem inherent in this type of fabrication. As the probe is bent around a metal rod by hand, the “U” bend in each fibre is not the same. This causes the path length that light has to travel to be different from fibre to fibre.

Any spectroscopic technique that uses light requires the path length the light travels to be the same. The second issue arising from this method of production is the polishing of the cleaved ends of the fibre. Polishing of the cleaved fibre ends is done by hand using polishing sheets and a metal disc with a hole in the centre, to ensure that there is no angle polished onto the end of the fibre. The quality of the polished fibre end determines how much light is transmitted across any connection. This, however, is extremely difficult to achieve without a method of looking at the fibres with sufficient magnification, or a method for determining the integrity of the fibres. Another factor affecting the repeatability of the experimentation is the coating of the hydrogel onto the surface of the fibre optic probe cable. If the coating is not uniformly spread over the same area from probe to probe, this leads to variations in the signal loss due to the contribution of the hydrogel to the generated signal loss. Coating techniques like spin coating produce uniform thin film coatings on flat surfaces<sup>99</sup>. The surface of the fibre core is round, making coating techniques such as spray coating to be more appropriate in achieving uniformity. Dip coating, the technique employed to coat the fibre optic sensor probes fabricated in the laboratory, often lead to the formation of droplets on the surface of the fibre core. Several dips were used to try to achieve a coating that was as even as possible. Finally, the light source used in any spectroscopic technique is assumed to remain at a constant intensity throughout its operational lifetime. The calculations that are carried out are based on the intensity of the light source being constant rather than variable. In reality, the light source's intensity will decay over time. As such, the LED used as the light source for these experiments dimmed over time. This was not visible to the naked eye, however the effects were observed as there was no return signal due to the reduced amount of light emitted into the fibre optic cable. When this occurred, the light source needed to be replaced.

In an attempt to overcome the largest issue of the reproducibility of the bend in the PMMA "U" bend probes, the end stop probe design was employed. This probe type did not require any bending, just accurate cutting of the length of fibre optic cable used each time. As the PMMA cable supplied came in spools, this meant that it had a natural curvature, which was not desirable. Therefore,

the use of glass fibre optic cable was decided as an alternative route to obtain straight “end stop” fibre optic probes.

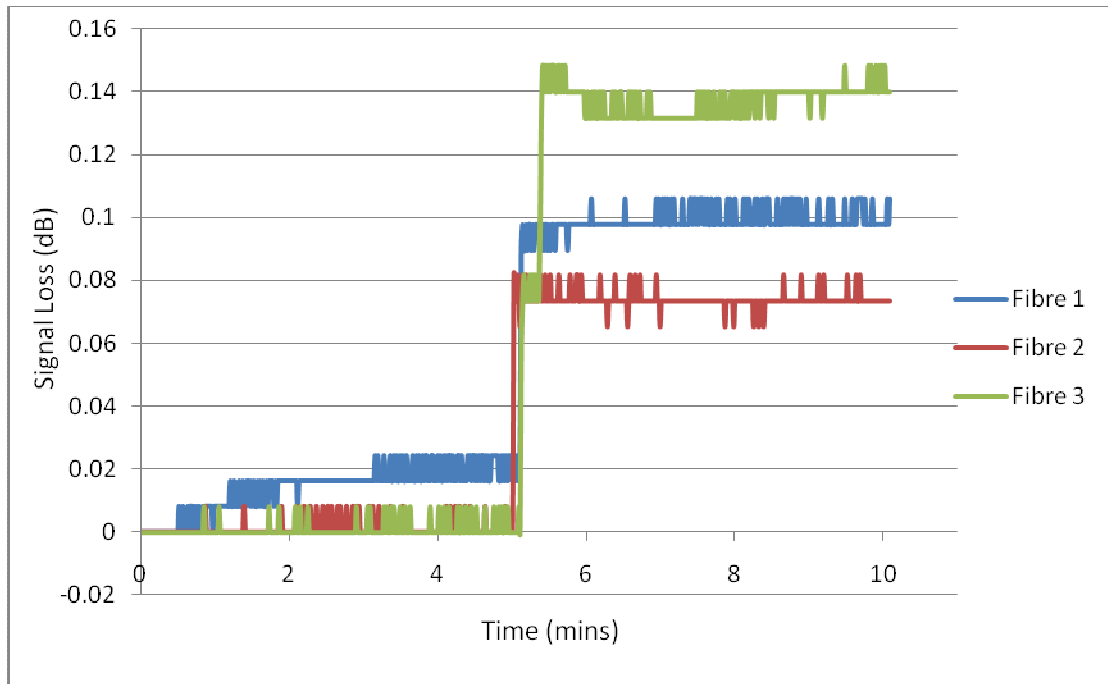


**Figure 83.** Three “end stop” glass probes exposed to air, and dry jet fuel to show the difference in signal loss between fibres.

As can be seen in figure 83, the signal loss generated from an uncoated glass “end stop” probe follows the same pattern from fibre to fibre; however the signal loss generated for the probe in air and water gave different signal loss values between probes. With the removal of the bend from the probe, this difference highlights the importance of the polishing of the cleaved ends of the fibre optic cable, as the difference in the polishing quality results in a difference in signal losses.

The issues of reproducibility of the system fall into two main categories. Firstly is the thickness of the hydrogel coating onto the fibre optic cable probes. Such an issue can be overcome with the use of a more sophisticated coating technique, such as an aerosol employed to disperse the coating solution onto the fibre optic cable probe. This would ensure an even thickness of the hydrogel coating. The second category is the fabrication of the fibre optic

probes. This issue is not as easily solved, as it requires detailed knowledge, honed skills and specialist equipment to produce fibre optic probes of the exact same optical properties. Unfortunately, the CASE sponsor company for this project, EvanesCo Ltd, closed down half way through the project. This meant that the source of the expert knowledge and skill required for the developed sensor system was not available to help tackle these issues.

## **Chapter 8. Summary and Conclusions**

## **8.1 Development of the system: experimental aspects**

### **8.1.1 Refractive index changes and water sensing**

Early experimentation with the developed sensor revealed that the system did not conform to the ideal evanescent wave model. Addition of water to the hydrogel coating, lowering its RI, should have caused a signal loss decrease. Instead, the observed signal loss increased. The pattern was observed in all the conducted experiments. This effect is possibly due to the RI of the test samples not being uniform – that is either the coating or the distribution of absorbed water is non-uniform. Another possibility is, as the predicted signal loss is based on the evanescent wave model, that the sensor system developed may not conform to this theoretical model. Whatever the reason, the results were consistent and illustrate the gap that sometimes exists between physics theory and chemical practice.

One of the issues faced during this project was the reproducibility of the value of signal loss for a target species at a given concentration. From fibre to fibre, a pattern of increasing signal loss was observed, as the concentration of the target species was increased, but the values of the signal loss at a concentration were different for each fibre. This is due to the issues faced when producing the fibre optic probes by hand in the laboratory environment. Inevitably, this lead to variations in the path length, due to non-uniformity of the fibres in terms of the cutting and bending, in the case of the “U” bend fibre and the quality of the polished ends of the probes for all probe variations. The manufacturer regards this as a consistent problem that would be overcome in a production environment where reproducibility of process would be required.

Monomers that depend upon refractive index change for the detection of water showed a relationship of increasing signal loss with increasing concentration of water in jet fuel. As hydrogels are able to be rehydrated many times, the coated fibre optic probes were able to be used many times to take sample readings. This robustness of the hydrogel coating means that these probes could have a possible application in in-line sensing, i.e. measuring the water content of hydrocarbon media being pumped through a pipe.



Hydrogel coatings were designed and synthesized during this work to meet particular design criteria. For example, DH8 included 2,2,2, trifluoro-ethylacrylate to lower the RI of the resulting hydrogel; DH5 was designed to be a hydrogel of high hydrophilicity by the inclusion of NaAMPs; DH6 was designed to be an extremely hydrophilic hydrogel, sensitive to very low levels of moisture. Inevitably problems were encountered when trying to apply chemical design principles to specific polymer coatings. DH6 was originally based on acrylamidoglycolic acid as the hydrophilic component but it had to be redesigned, as the structural integrity of DH6 was poor. This led to DH9, which was synthesized with higher levels of hydroxyl cross-linking sites (for subsequent functionalisation by N-methylol acrylamide) by increasing the amount of hydroxyethyl acrylamide monomer and reducing the amount of acrylamidoglycolic acid used. This compromise was typical of the structural manipulation that took place as coatings evolved.

When the gross signal loss for three coatings referred to above, namely DH5, DH8 and DH9, were compared, the signal loss patterns were very similar in the range that they covered. However, the baseline signal loss – the point from which the subsequent change in signal occurred – was significantly different. This was dependent upon the initial RI of the hydrogel. Thus, with the hydrophilic hydrogel coatings DH5 and DH9, signal loss readings fell in the ranges 4.314 dB to 4.366 dB, and 4.604 dB to 4.655 dB, respectively. They are based on non-fluorinated monomers. DH8 on the other hand, which contained the fluorinated monomer 2,2,2, trifluoro ethylacrylate as a means of lowering the RI of the coating, had a signal loss range that fell between 2.746 dB and 2.770 dB, which was significantly lower. This highlighted the importance of the monomer choice in the design of sensor coatings and specifically showed the importance of both the RI of the parent coating and the change in RI brought about by water ingress. The synthesis of hydrogel coatings is very much an example of design for purpose.

The entrapment of chemotropic agents to enhance the sensing capabilities of the RI responsive hydrogels showed a similar relationship in producing increased signal loss as the concentration of water increased. Cobalt salt

chemotropic agents relied on the coordination of water molecules around the cobalt ion. pH indicators, crystal violet and methyl orange, were also used as chemotropic agents for the detection of water. The parent coating used in this part of the work was DH9, which contains the highly hydrophilic sulfonate groups as a means of maximising water uptake. This enhances the power of water sensing in media such as jet fuel that desirably only contain very low levels of water. As the sulfonic acid group has a very low  $pK_a$ , matching it with an indicator, with a colour change at low pH such as crystal violet, makes an effective supplement to simple refractive index change. The presence of small amounts of water liberates  $H^+$  ions from the sulfonate groups. As such, the coating thus becomes acidic, which then leads to protonation of the pH indicator. The underlying principle – which is exploited with both the pH indicators and coordinating chemotropic agents – is that a colour change is observed in the presence of the analyte (e.g. water), which in turn causes light to be lost from the system.

### **8.1.2 Inorganic analytes and chemotropic sensing**

Using chemotropic agents with an associated colour change in the presence of a target species has the potential to be expanded to dual sensing. The use of a white light source and the detection of the change in intensity of light at certain wavelengths leads to the possibility of coating two or more coatings onto the surface of a fibre optic cables core, provided that the wavelengths of the colour changes do not overlap.

Always accepting the care and difficulty involved in making reproducible sensing probes (i.e. fibre and coating) on a laboratory scale, the use of chemotropic agents in conjunction with purpose-designed hydrogel coatings appears to have significant potential. This was demonstrated with the development of a prototype point of care potassium sensor for which there is a known clinical need, particularly in optometry and ophthalmology.

In summary, several strands of technology have been brought together to enable inexpensive fibre optic sensors to be produced. The versatility of probe configuration design, coupled with the ability to design a range of sensor coatings able to take advantage of the combined optics and electronics platform, mean that a wide range of potential analytes can be targeted. Point of care medical applications are particularly attractive, especially in the case of tear film analysis, because of difficulties with the size and storage of samples. The fact that a freshly removed contact lens carries information not just about normal tear components but also plasma-derived species through vascular leakage is a considerable bonus. However, the major point is that such a system would enable key tear analytes to be assayed in the clinic, rather than the laboratory.

Through the work conducted in this research, a promising sensor technology has been explored showing the potential to become a fully operational sensor system once several areas have been addressed, namely in the fabrication of the fibre optic cable probes and the coating technique used to apply the coating to the surface of the fibre optic cable core. These are important issues because design optimisation and product reproducibility would need to be addressed for a mass-produced system to become a reality, but the principles are clearly illustrated in the prototype system.

## **8.2 Future Work**

There are several opportunities for future work that could further research into hydrogel coatings for fibre optic sensing.

Further work on reproducibility of the sensing system requires the standardisation of the fabrication of the fibre optic probes used and the application of the hydrogel coating at the point of the core to be used as the sensing tip. Essentially, it will be necessary to produce fibre optic cable probes of the same path length and coatings of uniform thickness and area. The synthesis of more controlled sequence-distributed hydrogels is desirable, to ensure homogeneity and reproducibility of the materials. This would avoid

possible problems in the coating leading to localised signal loss generation. Alternatively, investigation into a calibration method could overcome some of the issues of repeatability. Ideally a simple calibration method would make this a more versatile sensor system in terms of portability.

The potassium sensor could be extended to include both calcium and magnesium, which are now recognised as early markers of meibomium gland disease.

Water-borne metals present in water supplies are an important target area. Research is needed into the possible contaminating and interfering effects of non-target metal ion species and fouling agents that would be present in a real life application of the system and interfere with the performance of the sensor system.

Finally, further understanding of the reasons why this sensor system does not conform to the ideal evanescent wave model would be desirable.

## **Chapter 9. References**

1. This image was originally published in La Nature 2<sup>nd</sup> half year. Colladon, D., La Fontaine Colladon, p325, Copyright La Nature, 1884. Permission granted by the Musée d'histoire des sciences de Genève to reproduce this image.
2. Chu, P. L., Recent Development of a Polymer Optical Fibre and its Applications. In Pal, B. P. Editor, Guided Wave Optical Components and Devices. Elsevier Academic Press, 2006, Burlington, MA. p27-40
3. Knight, J. C., Birks, P., Russell, St. J., Atkin, D. M., All-silica single-mode optical fibre with photonic crystal cladding. *Optics Lett.*, (1996), **21**, 19, 1457-1459.
4. Monroe, T., Richardson, D. Holey optical fibre: Fundamental properties and device applications. C. R. Physique **2003**, *4*, 175-186
5. This image was published in C. R. Physique, *4*, Monroe, T., Richardson, D. Holey optical fibre: Fundamental properties and device applications. P176, Copyright Elsevier. 2003.
6. Hecht, J., City of Light: The Story of Fibre Optics, Oxford University Press, 1999, New York. p14
7. Koike, Y., Progress of Plastic Optical Fibre Technology. Proc. ECOC' 15<sup>th</sup>-19<sup>th</sup> Sept 1996, paper MoB.3.1, 1.41, (1996).
8. Okoshi, O., Optical Fibres. Academic Press, 1982, New York. p 36-37
9. Hecht, J., City of Light: The Story of Fibre Optics, Oxford University Press, 1999, New York. p172.
10. Iizuka, K., Elements of Photonics volume 2: For Fiber and Integrated Optics. John Wiley & Sons, Inc. 2002, New York p1084.
11. Hecht, J., Understanding Lasers: An Entry-Level Guide. 2<sup>nd</sup> Ed. John Wiley & Sons Inc. 1993, New York p4.
12. Dutton, H., Understanding Optical Communications [Online ebook]. IBM Redbooks 1998 p79 URL:  
<http://library.aston.ac.uk/search~S9?/Xunderstanding+optical+communications&searchscope=9&SORT=DZ/Xunderstanding+optical+communications&searchscope=9&SORT=DZ&extended=0&SUBKEY=understanding%20optical%20communications/1.8.8.B/856~b1276433&FF=Xunderstanding+optical+communications&searchscope=9&SORT=DZ&1.1.1.0> Accessed November 10, 2010
13. Brandrup, J., Immergut, E. H., Grulke, E.A., Editors Polymer Handbook 4<sup>th</sup> Edition. Wiley & Sons, Inc. **1999**, New York, pages V/89, V/53, V/93.
14. Hecht, J., City of Light: The Story of Fibre Optics, Oxford University Press, **1999**, New York. p24-25
15. This image was published in [http://en.wikipedia.org/wiki/File:TIR\\_in\\_PMMA.jpg](http://en.wikipedia.org/wiki/File:TIR_in_PMMA.jpg) accessed 20/04/11
16. Iizuka, K., Elements of Photonics, Volume I: In Free Space and Special Media. John Wiley & Sons, Inc. **2002**, New York p130-131.

17. This image was published in Guided Wave Optical Components and Devices. Chu, P. L., Recent Development of a Polymer Optical Fibre and its Applications. p30. Copyright Elsevier **2006**
18. This image was published in Guided Wave Optical Components and Devices. Chu, P. L., Recent Development of a Polymer Optical Fibre and its Applications. p30. Copyright Elsevier **2006**
19. Dutton, H., Understanding Optical Communications [Online ebook]. IBM Redbooks **1998** p39-41 URL:  
<http://library.aston.ac.uk/search~S9?/Xunderstanding+optical+communications&searchscope=9&SORT=DZ/Xunderstanding+optical+communications&searchscope=9&SORT=DZ&extended=0&SUBKEY=understanding%20optical%20communications/1,8,8,B/l856~b1276433&FF=Xunderstanding+optical+communications&searchscope=9&SORT=DZ&1,1,,1,0> Accessed November 10, 2010
20. Luo, F. Jingyuan, L. Ma, N. Morse, T. A fibre optic microbend sensor for distributed sensing application in the structural strain monitoring. Sensors and Actuators, **1999**, 75, 41-44.
21. This image was published in Sensors and Actuators, 75, Luo, F. Jingyuan, L. Ma, N. Morse, T. A fibre optic microbend sensor for distributed sensing application in the structural strain monitoring. p41-42. Copyright Elsevier **1999**.
22. Roy, S. Fibre optic sensor for determining adulteration of petrol and diesel by kerosene. Sensors and Actuators, **1999**, 55, 212-216
23. This image was published in Sensors and Actuators, 55. Roy, S. Fibre optic sensor for determining adulteration of petrol and diesel by kerosene. p213, Copyright Elsevier **1999**.
24. This image was published in Sensors and Actuators, 55. Roy, S. Fibre optic sensor for determining adulteration of petrol and diesel by kerosene. p213, Copyright Elsevier **1999**.
25. Iizuka, K., Elements of Photonics volume 2: For Fiber and Integrated Optics. John Wiley & Sons, Inc. 2002, New York p747
26. Dutton, H., Understanding Optical Communications [Online ebook]. IBM Redbooks **1998** p211-213 URL:  
<http://library.aston.ac.uk/search~S9?/Xunderstanding+optical+communications&searchscope=9&SORT=DZ/Xunderstanding+optical+communications&searchscope=9&SORT=DZ&extended=0&SUBKEY=understanding%20optical%20communications/1,8,8,B/l856~b1276433&FF=Xunderstanding+optical+communications&searchscope=9&SORT=DZ&1,1,,1,0> Accessed November 10, **2010**
27. Trpkovski, S. Wade, S. A. Baxter, G. W. Collins, S. F. Dual temperature and strain sensor using a combined fibre Bragg grating and fluorescence intensity ratio technique in Er<sup>3+</sup>-doped fibre. Rev. Sci. Instrum., **2003**, 74, 5, 2880-2885

28. This image was published in *Rev. Sci. Instrum.*, **74**, 5, Trpkovski, S. Wade, S. A. Baxter, G. W. Collins, S. F. Dual temperature and strain sensor using a combined fibre Bragg grating and fluorescence intensity ratio technique in Er<sup>3+</sup>-doped fibre. p2883, , Copyright Elsevier **2003**.
29. This image was published in *Rev. Sci. Instrum.*, **74**, 5, Trpkovski, S. Wade, S. A. Baxter, G. W. Collins, S. F. Dual temperature and strain sensor using a combined fibre Bragg grating and fluorescence intensity ratio technique in Er<sup>3+</sup>-doped fibre. p2883, , Copyright Elsevier **2003**.
30. Wu, S., Cheng, W., Qiu, Y., Li, Z., Shuang, S., Dong, C., Fibre Optic pH sensor based on mode-filtered light detection. *Sensors and Actuators B: Chemical.*, **2010**, *144*, 255-259
31. This image was published in *Sensors and Actuators B: Chemical.* **144**, Wu, S., Cheng, W., Qiu, Y., Li, Z., Shuang, S., Dong, C., Fibre Optic pH sensor based on mode-filtered light detection. p257, Copyright Elsevier **2010**.
32. Estella, J. Vincente, P. Echeverria, J. Garrido, J. A fibre-optic humidity sensor on a porous silica xerogel film as the sensing element. *Sensors and Actuators B.* **2010**, *149*, 122-128.
33. This image was published in *Sensors and Actuators B.* **149**, Estella, J. Vincente, P. Echeverria, J. Garrido, J. A fibre-optic humidity sensor on a porous silica xerogel film as the sensing element. p124. Copyright Elsevier **2010**.
34. Nolan, D. A., Blaszyk, P. E., *Optical Fibres* In Udd, E., Editor *Fibre Optic Sensors: An introduction for Engineers and Scientists.* John Wiley & Sons **2006** Hoboken, New Jersey p31- 35
35. Udd, E., *Light Sources*, In Udd, E., Editor. *Fibre Optic Sensors: An introduction for Engineers and Scientists.* John Wiley & Sons **2006** Hoboken, New Jersey p47
36. Davies, M. L., Tighe, B. J., The potential of hydrogel polymers in sensor applications. *Selective Electrode Rev.*, **1991**, *13*, 159-226
37. Roorda, W. E., Boddé, H. E., de Boer, A. G., Junginger, H. E., Synthetic hydrogels as drug delivery systems, *Pharmacy World & Science.*, **1986**, *8*,(3), 165-189
38. Nicolson, P. C., Vogt, J., Soft contact lens polymers: an evolution. *Biomaterials*, **2001**, *22*, 3273-3283.
39. Tighe, B., *Contact Lens Materials*, In Stone, J., Phillips, A. J., Editors, *Contact Lenses* 2. 2<sup>nd</sup> Edition, Butterworths, **1981**, London. p392-399.
40. Tighe, B. *Contact Lens Materials*, In Phillips, A. J., Speedwell, L. Editors *Contact Lenses* 5<sup>th</sup> Edition. Butterworth-Heinemann **2007**, Edinburgh; New York p59-78.
41. Park, K., Park. H., *Smart Hydrogels*, In *Polymeric Materials Encyclopedia*, Salamone J. C., Editor-in-Chief. Vol 10 Q-S. **1996** CRC Press Inc. New York. p7785-7791
42. Hoffman, A. S., *Hydrogels for biomedical applications.* *Advanced Drug Delivery Reviews*, **2002**, *54*, (1), 3-12



43. Schrenkhammer, P., Wolfbeis, O. S., Fully reversible biosensors for uric acid using oxygen transduction. *Biosensors and Bioelectronics*, **2008**, *24*, 994-999.
44. Raimundo Jr, I. M., Narayanaswamy, R., Evaluation of Nafion-Crystal Violet films for the construction of an optical relative humidity sensor. *Analyst*, **1999**, *124*, 1623-1627.
45. Costa, S. C. S., Gester, R. M., Guimaraes, J. R., Amazonas, J. G., Del Nero, J., Silva, S. B. C., Galembeck, A., The entrapment of organic dyes into sol-gel matrix: Experimental results and modelling for photonic application. *Optical Materials*, **2008**, *30*, 1432-1439.
46. Habib Jiwan, J. L., Soumillion J.-Ph., A halogen anion sensor based on the hydrophobic entrapment of a fluorescent probe in silica sol-gel thin films. *Journal of Non-Crystalline Solids*, **1997**, *220*, 316-322
47. Goldfinch, M. J., Lowe, C. R., A solid-phase optoelectronic sensor for serum albumin, *Anal. Biochem.* **1988**, *60*, 76-81
48. Tighe, B., Contact Lens Materials, In Stone, J., Phillips, A. J., Editors, *Contact Lenses 2. 2<sup>nd</sup> Edition*, Butterworths, 1981, London. p393.
49. Yao, S., Chen, X., Nie, L., Fibre Optic Sensor with Bio-Membrane Supported Immobilized Morin for Aluminium Determination. *Mikrochim. Acta*, **1990**, *1*, 299-304.
50. This image was published in *Contact Lenses 5<sup>th</sup> Edition*. Tighe, B. *Contact Lens Materials*, p7, Copyright Butterworth-Heinemann **2007**.
51. Koffas, T., Opdahl, A., Marmo, C., Somorjai, G. A., Effect of Equilibrium Bulk Water Content on the Humidity-Dependent Surface Mechanical Properties of Hydrophilic Contact Lenses Studied by Atomic Force Microscopy. *Langmuir*, **2003**, *19*, 3453-3400.
52. This image was published in *Contact Lenses 5<sup>th</sup> Edition*. Tighe, B. *Contact Lens Materials*, p74, Copyright Butterworth-Heinemann **2007**.
53. Tighe, B. *Contact Lens Materials*, In Phillips, A. J., Speedwell, L. Editors *Contact Lenses 5<sup>th</sup> Edition*. Butterworth-Heinemann **2007**, Edinburgh; New York p74.
54. Stephen, D. K., Beuerman, R. W., Structure and Function of the cornea, In Kaufman, H. E., Barron, B. A., Mc Donald, M. B., Editors *The Cornea 2<sup>nd</sup> Edition*. Butterworth-Heinemann **1998**, Oxford p3-50.
55. Ju, H. K., Kim, S. Y., Kim, S. J., Lee, Y. M., pH/Temperature-Responsive Semi-IPN hydrogels Composed of Alginate and Poly(N-isopropylacrylamide). *Applied Polymer Science*. **2002**, *83*, 1128-1139.
56. Park, K., Park. H., Smart Hydrogels, In *Polymeric Materials Encyclopedia*, Salamone J. C., Editor-in-Chief. Vol 10 Q-S. **1996** CRC Press Inc. New York. p7785
57. Young, R. J., Lovell, P. A., *Introduction to polymers 2<sup>nd</sup> edition* **1996**, London. p3-4
58. Kojima, T. Sakauchi, M. Yamauchi, K-I. Urata, Y. Swelling of Poly (methyl methacrylate-co-poly(oxytetramethylene) dimethacrylate)s. *Macromolecules*. **1990**, *23*, 4990.
59. McMurray, J., *Organic Chemistry 6<sup>th</sup> Edition*. Thompson Brooks/Cole. **2004**, Belmont, CA.

60. Cowie, J. M. G., Arrighi, V., *Polymers: Chemistry and physics of modern materials* 3<sup>rd</sup> Edition. CRC Press, **2008**, Boca Raton, FL. P58-63
61. Walling, C., *Free radicals in solution*. John Wiley & Sons, **1957**, New York, p169-170.
62. Kitano, S., Koyama, Y., Kataoka, K., Okano, T., Sakurai, Y., A novel drug delivery system utilizing a glucose responsive polymer complex between poly(vinyl alcohol) and poly (*N*-vinyl-2-pyrrolidone) with a phenylboronic acid moiety. *J Controlled. Rel.* **1992**, *16*, (1-3) 161-170
63. Morris, J.E. Hoffman, A.S. Fisher, R.R. Affinity precipitation of proteins by polyligands. *Biotech. Bioeng.* **1993**, *41*, 991-997
64. Hooper, H. H. Baker, J. P. Blanch, H. W. Prausnitz,. Swelling equilibria for positively ionized polyacrylamide hydrogels. *Macromolecules*, **1990**, *23*, (4), 1096-1104.
65. Kinoshita, T. Kakiuchi, T. Takizawa, A. Tsujita, Y. Solute Permeability Enhancement at a Specific pH by an Amphiphili Copolypeptide Membrane. *Macromolecules*. **1990**, *23*, (5), 1389-1394
66. Baker, J. P. Stephens, D. R. Blanch, H. W. Prausnitz, Swelling equilibria for acrylamide-based polyampholyte hydrogels. *Macromolecules*, **1992**, *25*, (7) 1955-1958.
67. Katono, H. Sanui, K. Ogata, N. Okano, T. Sakurai, Y. Drug Release OFF Behavior and Deswelling Kinetics of Thermo-Responsive IPNs Composed of Poly(acrylamide-co-butyl methacrylate) and Poly(acrylic acid) *Polym J.* **1991**, *23*, (10) 1179-1189.
68. Badiger, M. V., Rajamohanam, P. R., Kulkarni, M. G., Ganapathy, S., Mashelkar R. A., Proton MASS-NMR: a new tool to study thermoreversible transition in hydrogels. *Macromolecules*, **1991**, *24*, (1), 106-111.
69. Feil, H. Bae, Y. H. Feijen, J. Kim, S. W. Effect of comonomer hydrophilicity and ionization on the lower critical solution temperature of *N*-isopropylacrylamide copolymers. *Macromolecules* **1993**, *26*, (10), 2496-2500.
70. Ishihara, K. Kobayashi, M. Shionohara, I. Control of Insulin Permeation through a Polymer Membrane with Responsive Function for Glucose. *Makromol. Chem. Rapid Commun.* **1983**, *4*, 327-331
71. Klumb, J. A., Horbett, T. A., The effect of hydronium ion transport on the transient behaviour of glucose sensitive membranes. *J. Controlled Rel.* **1993**, *27*, 95-114.
72. De Rossi, D. Susuki, M. Osada, Y. Morasso, P. Pseudomuscular Gel Actuators for Advanced Robotics *J. Intell Mater. Syst. Struct.* **1992**, *3*, 75-95.
73. Marchetti, M., Cussler, E. L., Hydrogels as Ultrafiltration Devices, *Sep. Purif. Methods.* **1989**, *18*, 177-192.
74. Gekrke, S.H. Andrews, G.P. Cussler, E.L. Chemical aspects of gel extraction. *Chem. Eng. Sci.***1986**, *41*, 2153-2160.
75. Vasheghani-Farahani, E. Cooper, D.G. Vera, J.H., Weber, M.E. Concentration of large biomolecules with hydrogels. *Chem. Eng. Sci.***1992**, *47*, 31-40.
76. Park, T. G. Hoffman, A. S. Immobilization and characterization of  $\beta$ -galactosidase in thermally reversible hydrogel beads *Biomed. Mater. Res.* **1990**, *24*, 21-38.

77. Zhang, X, Yang, Y., Chung, T., Ma, K., Preparation and Characterization of Fast Response Macroporous Poly(*N*-isopropylacrylamide) Hydrogels. *Langmuir*, **2001**, *17*, 6094-6099.
78. Wang, B., Zhang, J., Cheng, G., Dong, S., Amperometric enzyme electrode for the determination of hydrogen peroxide based on sol–gel/hydrogel composite film ,*Analytica Chimica Acta* **2000**, *407*, 111-118.
79. Davies, M. L., Murphy, S. M., Hamilton, C. J., Tighe, B. J., Polymer membranes in clinical sensor applications. III. Hydrogels as refractive matrix membranes in fibre optic sensors *Biomaterials*, **1992**, *13*, (14) 991-999.
80. Gehrke, S. H., Harsh, D. C., Environmentally responsive gels. In *Polymeric Materials Encyclopedia*, Salamone J. C., Editor-in-Chief. Vol 3 D-E. **1996** CRC Press Inc. New York. p2093-2102
81. Herman, M. F., Editor *Encyclopedia of polymer science and technology* 3<sup>rd</sup> edition. Wiley-Interscience **2007**, New York, Chichester p1124.
82. Crank, J., *The Mathematics of Diffusion* 2<sup>nd</sup> Edition. Oxford **1976**, London, p1-2
83. Bloomfield, M. M., *Chemistry and the Living Organism* 5<sup>th</sup> Edition. John Wiley & Sons, Inc. **1992**, New York, p315-318
84. Atkins, P., de Paula, J., *Elements of Physical Chemistry* 5<sup>th</sup> Edition. Oxford, **2009**, Oxford, p255-258.
85. Osada, Y., Ross-Murphy, S.B., *Intelligent Gels*, *Sci, Am*, **1993**, *285*, (5) , 82-88
86. Shibayama, M., Spatial inhomogeneity and dynamic fluctuations of polymer gels. *Macromol. Chem. Phys.* **1998**, *199*, 1-30.
87. Ouellette A L., Li J J., Cooper J E, Ricco A J and. Kovacs G T A, Evolving point-of-care diagnostics using up-converting phosphor bioanalytical systems, *Anal. Chem.*, **2009**, *81*, 3216–3221.
88. Winder A F, Laboratory screening for metabolic eye disease: a review., *J R Soc Med.* **1981**, August; *74* (8): 610–615.
89. Young, D. A., Miller, A. H., Coburn Jr, J. F., Method and apparatus for detection free water in hydrocarbon fuels. US Pat. 3,873,271 **1975**
90. Martyn, C. N., Osmond, C., Edwardson, J. A., Barker, D. J. P., Harris, E. C., Lacey, R. F. Geographical relation between Alzheimer's disease and aluminium in drinking water. *The Lancet*, **1989**, *333*, (8629), 61-62.
91. Wohlfahrt, Ch.: *2 Pure Liquids: Data*. Madelung, O. (ed.). Springer Materials - The Landolt-Börnstein Database (<http://www.springermaterials.com>). DOI: 10.1007/10047452\_2
92. Fakhree, A. A. A., Delgado, D., Martinez, F., Jouyban, A., The importance of Dielectric Constant for Drug Solubility Prediction in Binary Solvent Mixtures: Electrolytes and Zwitterions in Water and Ethanol, *AAPS PharmSci Tech* , **2010**, *11*, (4), 1726-1729.

93. McMurray, J., Organic Chemistry 7<sup>th</sup> Edition. Thompson Brooks/Cole. **2004**, Belmont, CA, p422-433.
94. Pasquale, A. J., Long, T. E., Determination of Monomer Reactivity Ratios Using *In situ* FTIR Spectroscopy for Maleic Anhydride/Norbornene-Free-Radical Copolymerization. Journal of Applied Polymer Science, **2004**, 92, (5), 3240-3246.
95. Lichtenhan, J. D., Otonari, Y. A., Carr, M. J., Linear Hybrid Polymer Building Blocks: Methacrylate-Functionalized Polyhedral Oligomeric Silsesquioxane Monomers and Polymers. Macromolecules **1995**, 28, 8435-8437
96. McMurray, J., Organic Chemistry 7<sup>th</sup> Edition. Thompson Brooks/Cole. **2004**, Belmont, CA, p882-898.
97. Liu, Y, Fan, X., Wei, B., Si, Q., Chen, W., Sun, L., pH-responsive amphiphilic hydrogel networks with IPN structure: A strategy for controlled drug release. International Journal of Pharmaceutics, **2006**, 308, (1-2), 205-209.
98. Moore, D. R., Wuensch, D. L., Multimode fibre optic coupler and method for making. US Patent 4,772,085 **1988**.
99. Lawrence, C. J., The mechanics of spin coating of polymer films, Phys. Fluids, **1988**, 31,(10), 2786-2796.
100. Takahashi, Y., Matsuoka, Y., Dip-coating of TiO<sub>2</sub> films using a sol derived from Ti (O-*i*-Pr)<sub>4</sub>-diethanolamine-H<sub>2</sub>O-*i*-PrOH system, Journal of Materials Science, **1988**, 23, 2259-2266.
101. Broka, K., Ekdunge, P., Oxygen and hydrogen permeation properties and water uptake of Nafion® 117 membrane and recast film for PEM fuel cell. Journal of Applied Electrochemistry, **1997**, 27, (2), 117-123.
102. Godin, I., Wylie, C., Heasman, J., Genital ridges exert long-range effects on mouse primordial germ cell numbers and direction of migration in culture, Development, **1990**, 108, 357-363.
103. Housecroft, C. E., Sharpe, A. G., Inorganic Chemistry. Prentice Hall, **2001**, Essex. p170-184.
104. Housecroft, C. E., Sharpe, A. G., Inorganic Chemistry. Prentice Hall, **2001**, Essex. p159-167
105. Housecroft, C. E., Sharpe, A. G., Inorganic Chemistry. Prentice Hall, **2001**, Essex. P152-154.
106. Tarsa, P. B., Lehmann, K. K., Cavity Ring-Down Biosensing, In Ligler, F. S., Taitt, C. R., Editors. Optical Biosensors: Today and Tomorrow 2<sup>nd</sup> Edition. Elsevier **2008**. Amsterdam: Boston, p403-418.
107. McMurray, J., Organic Chemistry 6<sup>th</sup> Edition. Thompson Brooks/Cole. **2004**, Belmont, CA, p325-326.
108. Okay, O., Durmaz, S., Charge density dependence of elastic modulus of strong polyelectrolyte hydrogels. Polymer, **2002**, 43, 1215-1221.

109. Kliment, K., Vacik, J., Ott, Z., Majkus, V., Stoy, V., Stol, M., Wichterle, O., Carriers for biologically active substances. US Patent 3,551,556 **1970**.
110. This image was published in Contact Lenses 2<sup>nd</sup> Edition, Tighe, B., Contact Lens Materials, p394. Copyright Butterworths **1981**.
111. Jianqi, F. Lixia, G. PVA/PAA thermo-crosslinking hydrogel fibre: preparation and pH-sensitive properties in electrolyte solution. European Polymer Journal, **2002**, 38, 1653-1658
112. This image was published in European Polymer Journal, 38, Jianqi, F. Lixia, G. PVA/PAA thermo-crosslinking hydrogel fibre: preparation and pH-sensitive properties in electrolyte solution. p1656. Copyright Elsevier 2002.
113. McMurray, J., Organic Chemistry 6<sup>th</sup> Edition. Thompson Brooks/Cole. **2004**, Belmont, CA, p43-50.
114. McMurray, J., Organic Chemistry 6<sup>th</sup> Edition. Thompson Brooks/Cole. **2004**, Belmont, CA, p613-615.
115. Rayss, J., Sudolski, G., Ion adsorption in the porous sol-gel silica layer in the fibre optic pH sensor. Sensors and Actuators B: Chemical, **2002**, 87, (3), 397-405
116. Von Lerber, T., Sigrist, M. W., Cavity-ring-down principle for fibre-optic resonators: experimental realization of bending loss and evanescent-field sensing. Applied Optics, **2002**, 41, (8), 3567-3575.
117. Kosterev, A. A., Malinovsky, A. L., Tittel, F. K., Gmachl, C., Capasso, F., Sivco, D. L., Baillargeon, J. N., Hutchinson, A. L., Cho, A. Y., Cavity Ringdown Spectroscopic Detection of Nitric Oxide with a Continuous-Wave Quantum-Cascade Laser. Applied Optics, **2001**, 40, (30), 5522-5529.
118. Dutton, H., Understanding Optical Communications [Online ebook]. IBM Redbooks **1998** p91-93 URL: <http://library.aston.ac.uk/search~S9?/Xunderstanding+optical+communications&searchscope=9&SORT=DZ/Xunderstanding+optical+communications&searchscope=9&SORT=DZ&extended=0&SUBKEY=understanding%20optical%20communications/1,8,8,B/I856~b1276433&FF=Xunderstanding+optical+communications&searchscope=9&SORT=DZ&1,1,,1,0> Accessed November 10, **2010**
119. Dutton, H., Understanding Optical Communications [Online ebook]. IBM Redbooks **1998** p275-285 URL: <http://library.aston.ac.uk/search~S9?/Xunderstanding+optical+communications&searchscope=9&SORT=DZ/Xunderstanding+optical+communications&searchscope=9&SORT=DZ&extended=0&SUBKEY=understanding%20optical%20communications/1,8,8,B/I856~b1276433&FF=Xunderstanding+optical+communications&searchscope=9&SORT=DZ&1,1,,1,0> Accessed November 10, 2010
120. Ohashi, T., Yamaki, M., Pandav, C. S., Karmarkar, M. G., Irie, M., Simple Microplate Method for Determination of Urinary Iodine. Clinical Chemistry, **2000**, 46, (4), 529-536.

121. Pino, S., Fnag, S., Braverman, L.E., Ammonium persulfate: a safe alternative oxidizing reagent for measuring urinary iodine. *Clinical Chemistry*, **1996**, *42*, (2), 239-243.
122. Wichterle, O., Lim, D., Hydrophilic gels for biological use, *Nature*, **1960**, *185*, 117-118.
123. Ferry, J. D., *Viscoelastic Properties of Polymers*. Wiley **1980**, New York p529-530
124. Russell, A. P., Fletcher, K. S., Optical sensor for the determination of moisture. *Analytica Chimica Acta*, **1985**, *170*, 209-216.
125. Lamb, J. D., Izatt, R. M., Christensen, J. J., Stability constants of cation-macrocyclic complexes and their effect on facilitated membrane transport rates. In Izatt, R. M., Christensen, J. J., Editors. *Progress in macrocyclic chemistry*, Volume 2, Wiley-Interscience, **1981**, New York, p41-90
126. Brandrup, J., Immergut, E. H., Grulk, E. A., Editors *Polymer Handbook* 4<sup>th</sup> Edition. Wiley, **1999**, Chichester, pVI/203-VI/204.
127. This image was published in *Contact Lenses* 2, 2<sup>nd</sup> Edition, Tighe, B., *Contact Lens Materials*, p393. Copyright Butterworths **1981**.
128. Ng, C. O., *Synthetic hydrogels in contact lens applications*. PhD Thesis. University of Aston in Birmingham. 1974.
129. Khuri, R. N., Device for determination of tear constituents, United States Patent 5352411 **1994**.
130. Anderson, G. P., Taitt, C. R., Evanescent wave fibre optic biosensors. In Ligler, F. S., Taitt, C. R., Editors. *Optical Biosensors: Today and Tomorrow* 2<sup>nd</sup> Edition. Elsevier **2008**. Amsterdam: Boston, p83-138.
131. Housecroft, C. E., Sharpe, A. G., *Inorganic Chemistry*. Prentice Hall, **2001**, Essex. p437-450.
132. Atkins, P., de Paula, J., *Elements of Physical Chemistry* 7<sup>th</sup> Edition. Oxford, **2009**, Oxford, p240-245.
133. Air Accidents Investigation Branch, Interim Report – Boeing 777–236ER, G-YMMM, Crown Copyright. Published Sept 2008  
[http://www.aaib.gov.uk/sites/aaib/publications/interim\\_reports/boeing\\_777\\_236er\\_g\\_y\\_mmm.cfm](http://www.aaib.gov.uk/sites/aaib/publications/interim_reports/boeing_777_236er_g_y_mmm.cfm) accessed 10/04/2011
134. Gammon, J., *Aviation Quality Control Procedures*: 3<sup>rd</sup> Edition. ASTM International **2004** West Conshohocken, p28
135. Holly, F. J., Refojo, M. F., Wettability of Hydrogels I. Poly(2-Hydroxyethyl Methacrylate) *J. Biomed. Matter. Res.* **1975**, *9*, 315-326.
136. Chirila, T. V., Chen, Y., Griffin, B. J., Constable, I. J., Hydrophilic sponges based on 2-hydroxyethyl methacrylate. I. Effect of monomer mixture composition on the pore size. *Polymer International*. **1993**, *32*, (3), 221-232.
137. Ouellette, A. L., Li, J. J., Cooper, J. E., Ricco, A. J., Kovacs, G. T. A., Evolving point-of-care diagnostics using up-converting phosphor bioanalytical systems, *Anal. Chem.*, **2009**, *81*, 3216–3221.

138. Benelli. U, Nardi. M, Posarelli. C, Albert. TG. Tear osmolarity measurement using the TearLaboratory Osmolarity System in the assessment of dry eye treatment effectiveness. *Contact Lens and Anterior Eye*. **2010**, 33, (2), 61-67.
139. Gilbard, J. P., Human tear film electrolyte concentrations in health and dry-eye disease. *International Ophthalmology Clinics*, **1994**, 34, 27-36.
140. Kratz, A., Ferraro, M., Sluss, P. M., Lewandrowski, K. B., Ellender, S. M., Peters, C. C., Kratz, A., Ferraro, M., et al. "Case records of the Massachusetts General Hospital. Weekly clinicopathological exercises. Laboratory reference values". *The New England journal of medicine*, **2004**, 351, (15), 1548–1563.
141. Ettinger, P. O., Regan, T. J., Oldewurtel, H. A., Hyperkalemia, cardiac conduction, and the electrocardiogram: A review. *American Heart Journal*, **1974**, 88, (3), 360-371
142. Gennari, J. F., Hypokalemia. *The New England Journal of Medicine*. **1998**, 339, (7) 451-458.
143. Thaysen, J. H., Thorn, N. A., Excretion of urea, sodium, potassium and chloride in human tears, *Amer. J. Physiol* **1954**, 178, 160-164.
144. Avisar, R., Savir, H., Sidi, Y., Pinkhas, J., Tear Calcium and magnesium levels of normal subjects and patients with hypocalcemia or hypercalcemia, *Invest. Ophthalmol.*, **1977**, 16, 1150-1151.
145. Johnson, M., Murphy, P., Changes in the tear film and ocular surface from dry eye syndrome. *Progress in Retinal and Eye Research* **2004**, 23, 449–474.
146. Lewa, H., Yuna, Y. S., Leeb, S. Y., Electrolytes and electrophoretic studies of tear proteins in tears of patients with nasolacrimal duct obstruction, , *Ophthalmologica* **2005**, 219, 142-146.
147. Speight, J. G., *Langes handbook of chemistry* 16<sup>th</sup> Edition, McGraw-Hill, **1972**, New York, p145
148. Miller, R. B., Tear concentrations of sodium and potassium during adaptation to contact lenses: 11. Potassium observations. *Am J Ophthalmol*, **1970**, 47, 773-779,
149. Uotila, M. H., Soble, R. E., Savory, J., Measurement of tear calcium levels, *Invest. Ophthalmol.*, **1972**, 11, 258-259
150. Jungreis, E., *Spot test analysis. Clinical, Environmental, Forensic, and Geochemical Applications*. 2<sup>nd</sup> Edition. Wiley-Interscience, **1997**, New York, p90-91.
151. Selinger. D, Selinger. R, Reed. W. Resistance to infection of the external eye: The role of tears. *Survey of Ophthalmology*. **1989**, 24, (1), 33-38.
152. Hart. D, Tidsale. R, Sack. R. Origin and composition of lipid deposits on soft contact lenses. *Ophthalmology*. **1986**, 93, (4), 495-503.
153. Keith. D, Hong. B, Christensen. M. A novel procedure for the extraction of protein deposits from soft hydrophilic contact lenses for analysis. *Current Eye Research*. **1997**, 16, (5), 503-510.
154. Leahy. C, Mandell. R, Lin. S. Initial in Vivo Tear Protein Deposition on Individual Hydrogel Contact Lenses. *Optometry and Vision Science*. **1990**, 67, (7), 504-511.

155. Albiets. J. Prevalence of Dry Eye Subtypes in Clinical Optometry Practice. *Optometry and Vision Science*, **2000**, 77, (7), 357-363.
156. Lee, K. Y., Mooney, D. J., Hydrogels for Tissue Engineering *Chemical Reviews*, **2001**, 101, (7), 1869-1879.
157. Connolly D. J., Gresham, W. F., Fluorocarbon vinyl ether polymers. US Patent 3,282,875, **1966**.
158. Liao, X., Wang, Y., Zhou, S. Q., High refractive index hydrogels prepared from polymers and copolymers of N-benzyl-N-methylacrylamide. US Pat. 5,717,049 **1998**.
159. Diegelmann, R. F., Evans, M. C., Wound healing: an overview of acute, fibrotic and delayed healing. *Frontiers in Bioscience*, **2004**, 9, 283-289.